

## Supplementary information

### **Unprecedented cyclization catalyzed by a cytochrome P450 in benzastatin biosynthesis**

Hayama Tsutsumi<sup>1</sup>, Yohei Katsuyama<sup>1,2,\*</sup>, Miho Izumikawa<sup>3,+</sup>, Motoki Takagi<sup>3</sup>, Manabu Fujie<sup>4</sup>, Noriyuki Satoh<sup>4</sup>, Kazuo Shin-ya<sup>5</sup> and Yasuo Ohnishi<sup>1,2,\*</sup>

<sup>1</sup>Department of Biotechnology, Graduate School of Agricultural and Life Sciences, The University of Tokyo, 1-1-1 Yayoi, Bunkyo-ku, Tokyo 113-8657, Japan

<sup>2</sup>Collaborative Research Institute for Innovative Microbiology, The University of Tokyo, 1-1-1 Yayoi, Bunkyo-ku, Tokyo 113-8657, Japan

<sup>3</sup>Japan Biological Informatics Consortium (JBIC), 2-4-7 Aomi, Koto-ku, Tokyo 135-0064, Japan

<sup>4</sup>Okinawa Institute of Science and Technology Graduate University, 1919-1 Tancha, Onna-son, Kunigami-gun, Okinawa 904-0495, Japan

<sup>5</sup>National Institute of Advanced Industrial Science and Technology (AIST), 2-4-7 Aomi, Koto-ku, Tokyo 135-0064, Japan

<sup>+</sup>Deceased on 23 December 2015

\*Corresponding authors:

ayasuo@mail.ecc.u-tokyo.ac.jp (Yasuo Ohnishi)

aykatsu@mail.ecc.u-tokyo.ac.jp (Yohei Katsuyama)

## Table of contents

## MATERIALS and METHODS

### SUPPLEMENTARY TABLES

**Supplementary Table 1.** Deduced functions of ORFs in the *bez* gene cluster.

**Supplementary Tables 2–7.** NMR data.

**Supplementary Table 8.** Optical rotation of benzastatin E and JBIR-67 (**5a**).

**Supplementary Table 9.** Primers used in this study.

**Supplementary Table 10.** Plasmids constructed in this study.

### SUPPLEMENTARY FIGURES

**Supplementary Figure 1.** Plasmid constructed for heterologous expression of benzastatin biosynthesis genes in *S. lividans*.

**Supplementary Figure 2.** Tandem mass spectra of virantmycin (**6d**) and *O*-demethylvirantmycin (**6c**).

**Supplementary Figure 3.** Tandem mass spectra of benzastatin K (**7a**) and methylbenzastatin K (**7b**).

**Supplementary Figure 4.** Complementation of the *ΔbezE*, *ΔbezG* and *ΔbezJ* strains by each gene on a chromosome integration vector.

**Supplementary Figure 5.** *In vitro* analysis of non-enzymatic degradation of **6d**.

**Supplementary Figure 6.** Tandem mass spectra of 7-hydroxyl benzastatin D (**6'd**) and its isomer (**6'd\***).

**Supplementary Figure 7.** SDS-PAGE of recombinant proteins used in this study.

**Supplementary Figure 8.** *In vitro* analysis of BezA and BezC.

**Supplementary Figure 9.** *In vitro* analysis of BezF.

**Supplementary Figure 10.** Feeding of PHABA to the *ΔbezJ* strain.

**Supplementary Figure 11.** *In vitro* analysis of BezG.

**Supplementary Figure 12.** Spectroscopic analysis of BezE.

**Supplementary Figure 13.** *In vitro* analysis of JBIR-67 (**5a**) formation by BezE.

**Supplementary Figure 14.** Feeding of 7-hydroxyl benzastatin J (**2a**), 7-hydroxyl benzastatin B (**2b**), and 7-hydroxyl *O*-demethylbenzastatin A (**2c**) to *S. lividans* strains harboring pTYM2k-*bezEGJ*, pTYM-*bezA-JΔbezA*, and pTYM-*bezA-JΔbezC*,

respectively.

**Supplementary Figure 15.** Putative benzastatin biosynthetic gene clusters discovered by genome scanning.

**Supplementary Figure 16.** Sequence alignment and phylogenetic analysis of BezE and P450s.

**Supplementary Figure 17.** Schematic representation of aziridine ring opening.

**Supplementary Figure 18.**  $^1\text{H}$  NMR ( $\text{CD}_3\text{OD}$ ) spectrum for **2a**.

**Supplementary Figure 19.**  $^{13}\text{C}$  NMR ( $\text{CD}_3\text{OD}$ ) spectrum for **2a**.

**Supplementary Figure 20.** COSY spectrum for **2a**.

**Supplementary Figure 21.** HMBC spectrum for **2a**.

**Supplementary Figure 22.** HMQC spectrum for **2a**.

**Supplementary Figure 23.** NOESY spectrum for **2a**.

**Supplementary Figure 24.**  $^1\text{H}$  NMR ( $\text{CD}_3\text{OD}$ ) spectrum for **2b**.

**Supplementary Figure 25.**  $^{13}\text{C}$  NMR ( $\text{CD}_3\text{OD}$ ) spectrum for **2b**.

**Supplementary Figure 26.** COSY spectrum for **2b**.

**Supplementary Figure 27.** HMBC spectrum for **2b**.

**Supplementary Figure 28.** HMQC spectrum for **2b**.

**Supplementary Figure 29.** NOESY spectrum for **2b**.

**Supplementary Figure 30.**  $^1\text{H}$  NMR ( $\text{CD}_3\text{OD}$ ) spectrum for **2c**.

**Supplementary Figure 31.**  $^{13}\text{C}$  NMR ( $\text{CD}_3\text{OD}$ ) spectrum for **2c**.

**Supplementary Figure 32.** COSY spectrum for **2c**.

**Supplementary Figure 33.** HMBC spectrum for **2c**.

**Supplementary Figure 34.** HMQC spectrum for **2c**.

**Supplementary Figure 35.** NOESY spectrum for **2c**.

**Supplementary Figure 36.**  $^1\text{H}$  NMR ( $\text{CD}_3\text{OD}$ ) spectrum for **5b**.

**Supplementary Figure 37.**  $^1\text{H}$  NMR ( $\text{CDCl}_3$ ) spectrum for **5b**.

**Supplementary Figure 38.**  $^{13}\text{C}$  NMR ( $\text{CD}_3\text{OD}$ ) spectrum for **5b**.

**Supplementary Figure 39.** COSY spectrum for **5b**.

**Supplementary Figure 40.** HMBC spectrum for **5b**.

**Supplementary Figure 41.** HMQC spectrum for **5b**.

**Supplementary Figure 42.** NOESY spectrum for **5b**.

**Supplementary Figure 43.**  $^1\text{H}$  NMR ( $\text{CD}_3\text{OD}$ ) spectrum for **6'c**.

**Supplementary Figure 44.**  $^{13}\text{C}$  NMR ( $\text{CD}_3\text{OD}$ ) spectrum for **6'c**.

**Supplementary Figure 45.** COSY spectrum for **6'c**.  
**Supplementary Figure 46.** HMBC spectrum for **6'c**.  
**Supplementary Figure 47.** HMQC spectrum for **6'c**.  
**Supplementary Figure 48.** NOESY spectrum for **6'c**.  
**Supplementary Figure 49.**  $^1\text{H}$  NMR ( $\text{CD}_3\text{OD}$ ) spectrum for **7a**.  
**Supplementary Figure 50.**  $^{13}\text{C}$  NMR ( $\text{CD}_3\text{OD}$ ) spectrum for **7a**.  
**Supplementary Figure 51.** COSY spectrum for **7a**.  
**Supplementary Figure 52.** HMBC spectrum for **7a**.  
**Supplementary Figure 53.** HMQC spectrum for **7a**.  
**Supplementary Figure 54.** NOESY spectrum for **7a**.

#### **SUPPLEMENTARY REFERENCES**



## MATERIALS and METHODS

### Materials and media.

Solvents and chemicals were purchased from Wako Chemicals (Tokyo, Japan), Kanto Chemical Corporation (Tokyo, Japan), Sigma-Aldrich (St. Louis, Missouri, USA), or Nacalai Tesque (Kyoto, Japan), unless noted otherwise. Oligonucleotide primers were purchased from Fasmac Corporation (Kanagawa, Japan), Sigma-Aldrich, or Hokkaido System Science Corporation (Hokkaido, Japan) and are listed in [Supplementary Table 9](#). Artificial DNAs were purchased from Thermo Fisher Scientific (Waltham, Massachusetts, USA). Restriction enzymes were purchased from Takara Bio (Shiga, Japan). LC-ESIMS analysis was performed with an Agilent 1100 series HPLC System (Agilent Technologies, Santa Clara, California, USA) and the high-capacity trap plus system (Bruker Daltonics, Billerica, Massachusetts, USA) equipped with a COSMOCORE 2.6C<sub>18</sub> packed column (2.1 × 150 mm, Nacalai Tesque), unless noted otherwise. NMR spectra were recorded on a JEOL JNM-ECA500II spectrometer (JEOL, Tokyo, Japan) operating at 500 MHz for <sup>1</sup>H and 125 MHz for <sup>13</sup>C. DNA manipulation was performed according to standard protocols. HRMS data were obtained using a 6550 iFunnel Q-TOF-MS (Agilent Technologies).

ISP2 medium was prepared by dissolving yeast extract (0.4%), malt extract (1.0%), and glucose (0.4%) in water. SMM medium was prepared by dissolving glucose (0.9%), asparagine (0.9%), (NH<sub>4</sub>)<sub>2</sub>SO<sub>4</sub> (0.2%), Trizma (Tris base) (0.24%), NaCl (0.1%), K<sub>2</sub>SO<sub>4</sub> (0.05%), MgSO<sub>4</sub>·7H<sub>2</sub>O (0.02%), CaCl<sub>2</sub> (0.01%), KH<sub>2</sub>PO<sub>4</sub> (0.0034%), and 1% trace element solution in water. The pH of these media was adjusted to 7.2 before autoclaving. Terrific broth medium was prepared by dissolving yeast extract (2.4%), bacto tryptone (1.2%), glycerol (0.4% [v/v]), KH<sub>2</sub>PO<sub>4</sub> (0.23%), and K<sub>2</sub>HPO<sub>4</sub> (1.25%) in water. TSB medium was prepared by dissolving tryptic soy broth (3%) in water. YEME medium was prepared by dissolving yeast extract (0.3%), peptone (0.5%), malt extract (0.3%), glucose (1.0%), sucrose (34%), glycine (0.5%), and MgCl<sub>2</sub> (0.048%) in water. All media were autoclaved prior to inoculation.

### Genome sequencing.

Genome sequencing was performed using Roche 454 GS FLX Titanium chemistry. The shotgun and paired-end reads were assembled using the Newbler

software package (a *de novo* sequence assembly software).

### **Construction of heterologous expression plasmids.**

The plasmids constructed in this study are listed in [Supplementary Table 10](#). The thiostrepton-inducible promoter (*tipA* promoter, abbreviated to  $P_{tipA}$ ) derived from pIJ6021<sup>1</sup> was used for the expression of *bez* genes.

pTONA-*bezA-J* is a plasmid which was previously constructed for the heterologous expression of *bez* gene cluster, which contains  $P_{tipA}$ -*bezD-J*,  $P_{tipA}$ -*bezA*,  $P_{tipA}$ -*bezB*, and  $P_{tipA}$ -*bezC* on pTONA5.<sup>2,3</sup> This plasmid was digested with PshBI and XbaI and the insert DNA fragment was cloned into the NdeI and XbaI sites of pTYM19gt<sup>4</sup>, resulting in pTYM-*bezA-J* ([Supplementary Figure 1](#)).

Each heterologous expression plasmid lacking one of the *bez* genes was constructed from pTYM-*bezA-J* using a general method described below. A chloramphenicol resistance gene flanked with SpeI sites, as well as 44 bp homology arms to enable homologous recombination with a target gene, was amplified by PCR using chloramphenicol resistance gene as a template. The core region of a *bez* gene was substituted with a chloramphenicol resistance gene using the amplified DNA fragment and the Red/ET recombination system<sup>5</sup> with GB05-dir (Gene Bridge, Heidelberg, Germany). After recombination, the chloramphenicol resistance gene was removed by SpeI digestion followed by self-ligation. A heterologous expression plasmid lacking *bezC* could not be obtained by this method; therefore, it was constructed by substituting a region containing  $P_{tipA}$ -*bezA*,  $P_{tipA}$ -*bezB*, and  $P_{tipA}$ -*bezC* with a DNA fragment containing  $P_{tipA}$ -*bezA* and  $P_{tipA}$ -*bezB*, as follows. A DNA fragment containing  $P_{tipA}$ -*bezA* was amplified by PCR using pTYM-*bezA-J* as a template and cloned into the NheI and XbaI sites of pTYM-*bezA-J*, resulting in pTYM-*bezA-J*Δ*bezBC*. A DNA fragment containing  $P_{tipA}$ -*bezB* was amplified by PCR using pTYM-*bezA-J* as a template. The amplified DNA fragment was cloned into the XbaI site of pTYM-*bezA-J*Δ*bezBC*, resulting in pTYM-*bezA-J*Δ*bezC*. Correct construction of desired plasmids was confirmed by restriction enzyme analysis. Each plasmid was then introduced into *S. lividans* and integrated into the chromosome.

### **Analysis of metabolites produced by *S. lividans* harboring a heterologous expression plasmid.**

ISP2 medium (100 ml) containing 5 µg/ml thiostrepton was inoculated with *S. lividans* harboring one of the heterologous expression plasmids and incubated at 30°C for 4 days. All cells were harvested by centrifugation and transferred into SMM medium (100 ml) containing 5 µg/ml thiostrepton and further incubated at 30°C for 2 days. Then, 5 ml of the fermentation broth was mixed with 0.2 ml of brine and 5 ml of ethyl acetate. After centrifugation, the organic layer was collected and evaporated to dryness under reduced pressure. The residual materials were dissolved in methanol (20 µl) and applied to LC-ESIMS analysis. The compounds were eluted with a linear gradient of water-acetonitrile containing 0.1% formic acid (2%-100% acetonitrile) as a mobile phase at 0.3 ml/min (**Figure 3**).

#### **Isolation and structural elucidation of compounds.**

Compounds **2a**, **2b**, **2c**, **5b**, **6'c**, and **7a** were characterized by NMR (**Supplementary Tables 2-7** and **Supplementary Figures 18-54**). Because yields of **6c** and **7b** were very low, these compounds were characterized by comparing their tandem mass spectra with those of **6d** and **7a**, respectively (**Supplementary Figures 2** and **3**). Compounds **5a**, **6d**, and **6'd** were characterized by comparing their retention times, UV and mass spectra with authentic samples.

#### *7-Hydroxyl benzastatin J (2a)*

ISP2 medium (200 ml) was inoculated with *S. lividans* harboring pTYM-bezA-JΔbezE and incubated at 30°C for 5 days. The whole culture was transferred to ISP2 medium (8 l) containing 5 µg/ml thiostrepton and further incubated at 30°C for 4 days. Amberlite FPX66 resin (160 g, ORGANO Corporation, Tokyo, Japan) was added to the culture to absorb low molecular-weight compounds. The mixture of resin and cells was harvested by filtration and compounds were extracted from the resin and cells with methanol. The organic layer was evaporated *in vacuo*. The residual materials were applied to a normal-phase medium pressure liquid chromatography system (MPLC, Shoko Scientific, Kanagawa, Japan) equipped with a silica column (Purif-Pack, Shoko Scientific), and compounds were eluted using a linear gradient of chloroform-methanol (0%–100% methanol) as a mobile phase. The fractions containing benzastatin derivatives were concentrated and further purified by reverse-phase high performance liquid chromatography (HPLC) using an Octa Decyl

Silyl (ODS) column (5C<sub>18</sub>-AR-II, 10 × 250 mm, Nacalai Tesque). Compounds were eluted using a linear gradient of water-methanol containing 0.1% formic acid (50%–100% methanol) as a mobile phase at 3.0 ml/min. Compounds were further purified by HPLC using a  $\pi$ -NAP column (10 × 250 mm, Nacalai Tesque) and eluted using a linear gradient of water-methanol containing 0.1% formic acid (50%–100% methanol) as a mobile phase at 3.0 ml/min. Compound **2a** was purified by reverse-phase HPLC using a Cholestero column (4.6 × 250 mm, Nacalai Tesque) and eluted using a linear gradient of water-methanol containing 0.1% formic acid (50%–100% methanol) as a mobile phase at 1.0 ml/min. The yield of **2a** was 0.8 mg. HR-ESI-MS:  $m/z$  274.1854 [M+H]<sup>+</sup>; calculated for [M (C<sub>17</sub>H<sub>23</sub>NO<sub>2</sub>)+H]<sup>+</sup>, 274.1802.

#### 7-Hydroxyl benzastatin B (**2b**)

ISP2 medium (2 l) was inoculated with *S. lividans* harboring pTYM-*bezA-JΔbezJ* and incubated at 30°C for 2 days. The whole cultured cells were transferred to SMM medium (2 l) containing 5 μg/ml thiostrepton and further incubated at 30°C for 3 days. Amberlite FPX66 resin (40 g) was added to absorb low molecular-weight compounds. The mixture of resin and cells was harvested by filtration and the compounds extracted from the resin and cells with methanol. The organic layer was evaporated to dryness *in vacuo*. The residual materials were applied to a normal-phase MPLC system equipped with the silica column, and eluted with a linear gradient of chloroform-methanol (0%–100% methanol) as a mobile phase. Fractions containing benzastatin derivatives were evaporated to dryness and applied to an LH20 column (GE Healthcare, Little Chalfont, United Kingdom) and the compounds were eluted with methanol. Compound **2b** was further purified by reverse-phase HPLC using the ODS column. The compound was eluted with a linear gradient of water-methanol containing 0.1% formic acid (50%–100% methanol) as a mobile phase at 3.0 ml/min. Compound **2b** was further purified by reverse-phase HPLC using the  $\pi$ -NAP column. The compound was eluted with a linear gradient of water-methanol containing 0.1% formic acid (50%–100% methanol) at 3.0 ml/min. The yield of **2b** was 0.7 mg. HR-ESI-MS:  $m/z$  288.2009 [M+H]<sup>+</sup>; calculated for [M (C<sub>18</sub>H<sub>25</sub>NO<sub>2</sub>)+H]<sup>+</sup>, 288.1958.

#### 7-Hydroxyl O-demethylbenzastatin A (**2c**)

ISP2 medium (100 ml) was inoculated with *S. lividans* harboring

pTYM-*bezA-JΔbezJ* and incubated at 30°C for 2 days. The whole culture was transferred to ISP2 medium (4 l) containing 5 µg/ml thiostrepton and further incubated at 30°C for 4 days. Amberlite FPX66 resin (160 g) was added to absorb low molecular-weight compounds. Compound **2c** was purified using the method described for the purification of **2b**. The yield of **2c** was 0.7 mg. HR-ESI-MS:  $m/z$  304.1928  $[M+H]^+$ ; calculated for  $[M(C_{18}H_{25}NO_3)+H]^+$ , 304.1907.

#### *7-Hydroxyl benzastatin F (5b)*

ISP2 medium (100 ml) was inoculated with *S. lividans* harboring pTYM-*bezA-JΔbezC* and incubated at 30°C for 4 days. A portion of the culture (50 ml) was transferred to ISP2 medium (4 l) containing 5 µg/ml thiostrepton. The culture was further incubated at 30°C for 3 days. Amberlite FPX66 resin (80 g) was added to absorb low molecular-weight compounds. Compound **5b** was purified using the method described for the purification of **2b**. The yield of **5b** was 0.5 mg. HR-ESI-MS:  $m/z$  304.1943  $[M+H]^+$ ; calculated for  $[M(C_{18}H_{25}NO_3)+H]^+$ , 304.1907.

#### *7-Hydroxyl O-demethylbenzastatin D (6'c)*

ISP2 medium (100 ml) was inoculated with *S. lividans* harboring pTYM-*bezA-JΔbezB* and incubated at 30°C for 4 days. A portion of the culture (50 ml) was transferred to ISP2 medium (4 l) containing 5 µg/ml thiostrepton and further incubated at 30°C for 3 days. Compound **6'c** was purified using the method described for the purification of **2b**. The yield of **6'c** was 0.8 mg. HR-ESI-MS:  $m/z$  320.1881  $[M+H]^+$ ; calculated for  $[M(C_{18}H_{25}NO_4)+H]^+$ , 320.1856.

#### *Benzastatin K (7a)*

ISP2 medium (1 l) was inoculated with *S. lividans* harboring pTYM-*bezA-JΔbezE* and incubated at 30°C for 5 days. All cells were harvested by centrifugation and transferred into SMM medium (1 l) containing 5 µg/ml thiostrepton and further incubated at 30°C for 2 days. Compound **7a** was purified using the method described for the purification of **2a**. The yield of **7a** was 1.0 mg. HR-ESI-MS:  $m/z$  272.1681  $[M+H]^+$ ; calculated for  $[M(C_{17}H_{21}NO_2)+H]^+$ , 272.1645.

**Complementation of the *S. lividans*  $\Delta bezE$ ,  $\Delta bezG$ , and  $\Delta bezJ$  strains by each gene**

**on a chromosome integration vector.**

First, pHKO4 was constructed as follows. A small DNA fragment was amplified by PCR using pTONA5<sup>2</sup> as a template. The amplified DNA fragment was cloned into the SacI and EcoRV sites of pTONA5, resulting in pHKO1. By this procedure, the SacI and EcoRV fragment including *melC* was removed from pTONA5. A DNA fragment containing *P<sub>tipA</sub>* and multi cloning site was amplified from pIJ6021<sup>1</sup> by PCR. The DNA fragment was digested with PshBI and NdeI (an NdeI site is included in the multi cloning site of the amplified DNA), and the DNA fragment containing *P<sub>tipA</sub>* was cloned into the PshBI and NdeI sites of pHKO1, resulting in pHKO4.

*bezE*, *bezG*, and *bezJ* were individually amplified by PCR using genomic DNA of *Streptomyces* sp. RI18 as a template. Each of the amplified fragments was cloned into pHKO4, resulting in pHKO4-*bezE*, pHKO4-*bezG*, and pHKO4-*bezJ*. The *P<sub>tipA</sub>-bezE* was amplified by PCR using pHKO4-*bezE* as a template, and cloned into the PshBI and XbaI sites of pTYM2k harboring the BT1 integrase gene, resulting in pTYM2k-*bezE*. Similarly, the *P<sub>tipA</sub>-bezG* and *P<sub>tipA</sub>-bezJ* were amplified by PCR using pHKO4-*bezG* and pHKO4-*bezJ*, respectively, as a template, and cloned into the XbaI and HindIII sites of pTYM2k, resulting in pTYM2k-*bezG* and pTYM2k-*bezJ*, respectively. Finally, pTYM2k-*bezE*, pTYM2k-*bezG*, and pTYM2k-*bezJ* were then integrated into the chromosome of *S. lividans* harboring pTYM-*bezA-JΔbezE*, pTYM-*bezA-JΔbezG*, and pTYM-*bezA-JΔbezJ*, respectively, for complementation test ([Supplementary Figure 4](#)).

#### ***In vitro* analysis of non-enzymatic degradation of **6d**.**

Quantification of ergothioneine in *Streptomyces* sp. RI18 was performed using the method described by Fahey and Newton<sup>6</sup>, which revealed that intracellular concentration of ergothioneine in *Streptomyces* sp. RI18 as  $9.48 \pm 0.33$  mg/l ( $\sim 41$   $\mu$ M). This was six times larger than the amount of **6d** ( $2.52 \pm 0.25$  mg/l:  $\sim 7.2$   $\mu$ M) in *Streptomyces* sp. RI18. *In vitro* synthesis of **6'e** was performed in a solution containing 50 mM HEPES buffer (pH 7.4), 100  $\mu$ M **6d**, and 200  $\mu$ M ergothioneine (Funakoshi, Tokyo, Japan). The solution was incubated at 27°C for 1 h and water was removed by evaporation under reduced pressure. The residual materials were dissolved in methanol (20  $\mu$ l) and applied to LC-ESIMS analysis ([Supplementary Figures 5 and 6](#)).

**Purification of recombinant BezA, BezC, BezE, BezG, BezJ, CamA, and CamB proteins and preparation of crude BezF solution.**

*bezA*, *bezC*, *bezF*, and *bezJ* were individually amplified by PCR using genomic DNA of *Streptomyces* sp. RI18 as a template. The amplified *bezA* fragment was cloned into the NdeI and BamHI sites of pColdI, resulting in pColdI-*bezA*. The amplified *bezC* fragment was cloned into the SacI and XbaI sites of pColdI, resulting in pColdI-*bezC*. The amplified *bezF* fragment was cloned into the NdeI and EcoRI sites of pHKO4, resulting in pHKO4-*bezF*. The amplified *bezJ* fragment was cloned into the NdeI and BamHI sites of pET16b, resulting in pET16b-*bezJ*. *bezE* was amplified using a synthetic DNA template, in which *bezE* codons were optimized for expression in *E. coli*. The amplified *bezE* fragment was cloned into the NdeI and XhoI sites of pET26b, resulting in pET26b-*bezE*. *bezG* was amplified using genomic DNA of *S. niveus* as a template and cloned into the NdeI and XhoI sites of pET16b, resulting in pET16b-*bezG*.

*E. coli* BL21(DE3) harboring pColdI-*bezA* or pET16b-*bezG* was pre-cultured overnight in Luria-Bertani (LB) broth containing 100 µg/ml ampicillin at 37°C. The obtained culture was transferred into terrific broth containing 100 µg/ml ampicillin and incubated at 37°C until OD<sub>600</sub> reached 0.4. The cells were cooled on ice and gene expression was induced by addition of 0.1 mM isopropyl β-D-thiogalactopyranoside. The culture was further incubated at 15°C for 24 h. The cells were harvested by centrifugation and resuspended in lysis buffer (20 mM Tris, 200 mM NaCl, and 20% [v/v] glycerol; pH 8.0). The cells were lysed with sonication and cell debris was removed by centrifugation. The resulting supernatant was mixed with His-Accept (Clontech, Mountain View, California), and the resin was subsequently collected and washed with lysis buffers containing 20 and 50 mM imidazole. Recombinant BezA, BezG, and BezJ, which have an N-terminally-fused histidine tag, were stepwisely eluted with lysis buffers containing 100, 250 and 500 mM imidazole. The fractions containing recombinant proteins were collected, and imidazole in the elutant was removed by dialysis.

*E. coli* BL21(DE3) harboring pColdI-*bezC* was pre-cultured overnight in LB broth containing 100 µg/ml ampicillin at 37°C. The obtained culture was transferred into terrific broth containing 100 µg/ml ampicillin, 80 mg/L 5-aminolevulinic acid and 0.1 mM Fe(NH<sub>4</sub>)<sub>2</sub>(SO<sub>4</sub>)<sub>2</sub> and incubated at 37°C until OD<sub>600</sub> reached 0.4. Then, expression of *bezC* was induced and recombinant BezC having an N-terminally-fused



histidine tag was purified using the same method as described above.

*E. coli* BL21(DE3) harboring pET26b-*bezE* was pre-cultured overnight in LB broth containing 50 µg/ml kanamycin at 37°C. The obtained culture was transferred into terrific broth containing 50 µg/ml kanamycin, 80 mg/L 5-aminolevulinic acid, and 0.1 mM Fe(NH<sub>4</sub>)<sub>2</sub>(SO<sub>4</sub>)<sub>2</sub> and incubated at 37°C until OD<sub>600</sub> reached 0.4. Then, expression of *bezE* was induced and recombinant BezE having an *N*-terminally-fused histidine tag was purified using the same method as described above.

*E. coli* BL21(DE3) harboring pET28b-*camA* or pET28b-*camB* was pre-cultured overnight in LB broth containing 50 µg/ml kanamycin at 37°C. The obtained culture was transferred into LB medium containing 50 µg/ml kanamycin and incubated at 37°C until OD<sub>600</sub> reached 0.6. Then, expression of *camA* or *camB* was induced and recombinant CamA and CamB, which have an *N*-terminally-fused histidine tag, were purified using the same method as described above.

*S. lividans* harboring pHKO4-*bezF* was pre-cultured in TSB medium containing 50 µg/ml kanamycin at 30°C for 3 days. The culture was transferred into YEME medium and incubated at 30°C. After 2 days, 5 µg/ml thiostrepton was added to induce P<sub>tipA</sub>. The culture was further incubated at 30°C for 3 days. The cells were harvested by centrifugation and resuspended in lysis buffer (20 mM Tris, 200 mM NaCl, and 20% [v/v] glycerol; pH 8.0). The cells were lysed with sonication and cell debris was removed by centrifugation. The resulting supernatant was centrifuged by 100,000 × *g* for 1 h at 4°C. The BezF-containing cell membrane pellet was resuspended and incubated in lysis buffer containing 0.1% CHAPS at 4°C for 30 min to solubilize the membrane fraction. The debris was removed by centrifugation at 20,000 × *g*. The supernatant containing solubilized BezF was used for *in vitro* assay.

The amount and purity of each recombinant protein were analyzed by SDS-PAGE ([Supplementary Figure 7](#)).

### ***In vitro* analysis of BezA, BezC, and BezF.**

For the examination of methylation of **2a** by BezA, the reaction mixture (100 µl) contained 1 mM MgCl<sub>2</sub>, 10 µM **2a**, 80 µM SAM, and 1 µM BezA in 50 mM Tris-HCl (pH 7.4). For the examination of hydroxylation of **2b** by BezC, the reaction mixture (100 µl) contained 1 mM MgCl<sub>2</sub>, 10 µM **2b**, 1 mM NADH, 8 µM CamA, 20 µM CamB, and 1 µM BezC in 50 mM Tris-HCl (pH 7.4). After incubation at 30°C for 1



h, the compounds were extracted with ethyl acetate and the organic layer was evaporated to dryness under reduced pressure. The residual materials were dissolved in methanol (20  $\mu$ l) and applied to LC-ESIMS analysis. The compounds were eluted with a linear gradient of water-acetonitrile containing 0.1% formic acid (2%-100% acetonitrile) as a mobile phase at 0.3 ml/min (**Supplementary Figure 8a** and **b**).

For the examination of methylation of GPP (**1a**) by BezA, reaction mixture (100  $\mu$ l) contained 1 mM MgCl<sub>2</sub>, 30  $\mu$ M GPP, 80  $\mu$ M *S*-adenosyl-L-methionine (SAM), and 1  $\mu$ M BezA in 50 mM Tris-HCl (pH 7.4). To detect accumulation of *S*-adenosyl-L-homocysteine (SAH), it was concentrated and dissolved in methanol (20  $\mu$ l) and applied to LC-ESIMS analysis equipped with COSMOSIL 5PYE column (2.0  $\times$  150 mm, Nacalai Tesque). The compounds were eluted with a linear gradient of water-acetonitrile containing 0.1% formic acid (2%-100 % acetonitrile) as a mobile phase at 0.4 ml/min (**Supplementary Figure 8c**). For the examination of sequential methylation and hydroxylation of GPP (**1a**) by BezA and BezC, reaction mixture (100  $\mu$ l) contained 1 mM MgCl<sub>2</sub>, 30  $\mu$ M GPP, 80  $\mu$ M SAM, 1 mM NADH, 8  $\mu$ M CamA, 20  $\mu$ M CamB, 1  $\mu$ M BezA, and 1  $\mu$ M BezC in 50 mM Tris-HCl (pH 7.4). After incubation at 30°C for 1 h, enzymes were removed using Microcon® Centrifugal Filters (Molecular weight cut-off 10,000 Da, Merck, Darmstadt, Germany). Then, BezF and PABA were added to the filtrate. The mixture was further incubated overnight at 30°C. The compounds were extracted with ethyl acetate and the organic layer was evaporated to dryness under reduced pressure. The residual materials were dissolved in methanol (20  $\mu$ l) and applied to LC-ESIMS analysis (**Figure 4**).

#### **Synthesis of *p*-hydroxyaminobenzoic acid (PHABA).**

*p*-Hydroxyaminobenzoic acid (PHABA) was synthesized according to the previously published procedure<sup>7</sup> and purified by reverse-phase HPLC equipped with the ODS column. Compounds were eluted using a linear gradient of water-methanol containing 0.1% formic acid (5%–100% methanol) as a mobile phase at 3.0 ml/min. The synthesized compound was characterized by comparing the <sup>1</sup>H NMR spectrum with previously reported data. <sup>1</sup>H NMR (DMSO-*d*<sub>6</sub>, 500 MHz) 12.2 (s, 1H), 8.83 (s, 1H), 8.55 (s, 1H), 7.71 (d, *J* = 8.6 Hz, 1H), 6.78 (d, *J* = 8.7 Hz, 1H).

#### **Feeding experiment of PHABA.**

*S. lividans* harboring pTYM-*bezA-JΔbezJ* was pre-cultured in ISP2 medium (5 ml) containing 5 µg/ml thiostrepton at 30°C for 2 days. All cells were harvested by centrifugation and transferred into SMM medium (5 ml) containing 5 µg/ml thiostrepton and PHABA (100 µM). The culture was further incubated at 30°C for 3 days. Then, the fermentation broth (5 ml) was mixed with brine (0.2 ml) and ethyl acetate (5 ml). After centrifugation, the organic layer was collected and evaporated to dryness under reduced pressure. The residual materials were dissolved in methanol (20 µl) and applied to LC-ESIMS analysis ([Supplementary Figure 10](#)).

#### ***In vitro* analysis of BezG.**

The reaction mixture (100 µl) containing 0.5 µM BezG, 100 µM PHABA (or PABA), 100 µM acetyl-CoA, and 50 mM Tris-HCl buffer (pH7.4) was incubated at 30°C for 10 min. The reaction mixture was concentrated under reduced pressure. The residual materials were dissolved in methanol (20 µl) and applied to LC-ESIMS analysis equipped with a COSMOSIL 5PYE column. The compounds were eluted with a linear gradient of water-acetonitrile containing 0.1% formic acid (2%-100 % acetonitrile) as a mobile phase at 0.4 ml/min ([Supplementary Figure 11](#)).

#### ***In vitro* analysis of BezE.**

For the examination of cyclization of **4a** by BezE, the reaction mixture (100 µl) contained 1 µM BezE, 3 µM BezG, 10 µl BezF, 30 µM GPP (**1a**), 100 µM PHABA, 100 µM acetyl-CoA, and 1 mM MgCl<sub>2</sub> in 50 mM Tris-HCl buffer (pH7.4). After incubation at 30°C for 1 h, compounds were extracted with ethyl acetate. After centrifugation, the organic layer was collected and evaporated to dryness under reduced pressure. The residual materials were dissolved in methanol (20 µl) and applied to LC-ESIMS analysis ([Figure 5a](#) and [b](#)).

To determine the origin of hydroxyl group of JBIR-67 (**5a**), the following two reactions were carried out. First, the reaction mixture (100 µl) containing 1 µM BezE, 1 µM BezG, 5 µl BezF, 30 µM GPP (**1a**), 100 µM PHABA, 100 µM acetyl-CoA, 1 mM MgCl<sub>2</sub>, 50 µl H<sub>2</sub><sup>18</sup>O (50% [v/v], Sigma-Aldrich), and 50 mM Tris-HCl buffer (pH7.4) was incubated at 30°C for 1 h. Second, the reaction mixture (100 µl) containing 1 µM BezE, 1 µM BezG, 10 µl BezF, 30 µM GPP (**1a**), 100 µM PHABA, 100 µM acetyl-CoA, 1 mM MgCl<sub>2</sub>, and 50 mM Tris-HCl buffer (pH7.4) was incubated at 30°C for 1 h under

the presence of  $^{18}\text{O}_2$ . This reaction was carried out in a recovery flask sealed hermetically with a butyl rubber plug as described below. First, a reaction mixture without all the enzymes was placed inside the flask. Then, the air was removed from the flask using a vacuum pump.  $^{18}\text{O}_2$  (Taiyo Nippon Sanso corporation, Tokyo, Japan) was introduced into the flask using a balloon filled with  $^{18}\text{O}_2$ . This procedure was repeated three times to remove atmospheric molecular oxygen completely. After the substitution of the air with  $^{18}\text{O}_2$ , all the enzymes in a small amount of buffer were added to the reaction mixture in the flask using a syringe. After these reactions using  $\text{H}_2^{18}\text{O}$  and  $^{18}\text{O}_2$ , compounds were extracted with ethyl acetate. After centrifugation, the organic layer was collected and evaporated to dryness under reduced pressure. The residual materials were dissolved in methanol (20  $\mu\text{l}$ ) and applied to LC-ESIMS analysis (**Figure 5h** and **i**).

For further investigation of the cyclization reaction, time course reaction of BezE was carried out. The reaction mixture (100  $\mu\text{l}$ ) containing 1  $\mu\text{M}$  BezE, 1  $\mu\text{M}$  BezG, 10  $\mu\text{l}$  BezF, 30  $\mu\text{M}$  GPP (**1a**), 100  $\mu\text{M}$  PHABA, 100  $\mu\text{M}$  acetyl-CoA, 1 mM  $\text{MgCl}_2$ , and 50 mM Tris-HCl buffer (pH7.4) was incubated at 30°C for 2 h (**Supplementary Figure 12a**).

To examine the effect of the addition of redox partner, CamA and CamB were added to the reaction mixture. The reaction mixture (100  $\mu\text{l}$ ) containing 1  $\mu\text{M}$  BezE, 1  $\mu\text{M}$  BezG, 10  $\mu\text{l}$  BezF, 30  $\mu\text{M}$  GPP (**1a**), 8  $\mu\text{M}$  CamA, 20  $\mu\text{M}$  CamB, 100  $\mu\text{M}$  PHABA, 100  $\mu\text{M}$  acetyl-CoA, 1 mM NADH, 1 mM  $\text{MgCl}_2$ , and 50 mM Tris-HCl buffer (pH7.4) was incubated at 30°C for 10 min. The compounds were extracted with ethyl acetate. After centrifugation, the organic layer was collected and evaporated to dryness under reduced pressure. The residual materials were dissolved in methanol (20  $\mu\text{l}$ ) and applied to LC-ESIMS analysis (**Supplementary Figure 12b**).

For the examination of cyclization of **4b** by BezE, the reaction mixture (100  $\mu\text{l}$ ) contained 1  $\mu\text{M}$  BezA, 30  $\mu\text{M}$  GPP (**1a**), and 1 mM  $\text{MgCl}_2$  in 50 mM Tris-HCl buffer (pH7.4). After incubation at 30°C for 1 h, 1  $\mu\text{M}$  BezE, 3  $\mu\text{M}$  BezG, 5  $\mu\text{l}$  BezF, 100  $\mu\text{M}$  acetyl-CoA, and 100  $\mu\text{M}$  PHABA were added. The mixture was further incubated overnight at 30°C. The compounds were extracted with ethyl acetate and brine, and the organic layer was evaporated to dryness under reduced pressure. The residual materials were dissolved in methanol (20  $\mu\text{l}$ ) and applied to LC-ESIMS analysis (**Figure 5c** and **d**).

For the examination of cyclization of **4c** by BezE, the reaction mixture (100  $\mu$ l) contained 1  $\mu$ M BezA, 1  $\mu$ M BezC, 8  $\mu$ M CamA, 20  $\mu$ M CamB, 30  $\mu$ M GPP (**1a**), 1 mM NADH, and 1 mM MgCl<sub>2</sub> in 50 mM Tris-HCl buffer (pH7.4). After incubation at 30°C for 1 h, 1  $\mu$ M BezE, 3  $\mu$ M BezG, 5  $\mu$ l BezF, 100  $\mu$ M acetyl-CoA and 100  $\mu$ M PHABA were added. The mixture was further incubated overnight at 30°C. The compounds were extracted with ethyl acetate and brine, and the organic layer was evaporated to dryness under reduced pressure. The residual materials were dissolved in methanol (20  $\mu$ l) and applied to LC-ESIMS analysis (**Figure 5e** and **f**).

#### ***In vitro* analysis using hemin instead of BezE**

To confirm the importance of scaffold of BezE for the cyclization activity, hemin was used to synthesize **5a** *in vitro* instead of BezE. The reaction mixture (100  $\mu$ l) containing 100  $\mu$ M hemin, 1  $\mu$ M BezG, 10  $\mu$ l BezF, 30  $\mu$ M GPP (**1a**), 100  $\mu$ M PHABA, 100  $\mu$ M acetyl-CoA, 1 mM MgCl<sub>2</sub>, and 50 mM Tris-HCl buffer (pH7.4) was incubated at 30°C for 1 h. The compounds were extracted with ethyl acetate, and the organic layer was evaporated to dryness under reduced pressure. The residual materials were dissolved in methanol (20  $\mu$ l) and applied to LC-ESIMS analysis (**Supplementary Figure 12c**).

#### **UV-Vis spectroscopic analysis of BezC and BezE.**

UV-visible spectra were measured by using a spectrophotometer (UV-1850, SHIMADZU, Kyoto, Japan) with a 1-cm path length quartz cuvette. The excess amount of sodium hydrosulfide was added into the BezC and BezE solution in lysis buffer (20 mM Tris, 200 mM NaCl, and 20% [v/v] glycerol; pH 8.0). Then, carbon monoxide (CO) gas was bubbled for 1 min. UV-Vis spectra of each solution was measured, and the CO differential spectrum was obtained using sodium hydrosulfide-added solution as a reference (**Supplementary Figures 8d** and **12a**).

#### **Substrate-binding analysis of BezE.**

UV-visible spectra were measured by using a spectrophotometer (SpectraMax M2 Microplate Reader, Molecular Devices Japan, Tokyo, Japan) with a 1-cm path length 96-well plate. BezE was in lysis buffer (20 mM Tris, 200 mM NaCl, and 20% [v/v] glycerol; pH 8.0). Each substrate analog (**2a**, **2b**, or **2c**) was added into the BezE

solution (final concentration 10, 5, 2.5, 1.25 and 0.625  $\mu$ M). Each sample was incubated for 2 min and UV-Visible spectrum was measured using the BezE solution with no substrate analog as a reference (**Supplementary Figure 12b**). For determination of the dissociation constant ( $K_d$ ) with each substrate analog, the difference in absorbance of each spectrum at 414 nm (the bottom) and 434 nm (the peak) was calculated in triplicate, and the average was plotted against the substrate analog concentration. The  $K_d$  value was calculated by fitting the data with a hyperbolic curve (**Supplementary Figure 12c**).

**Feeding of 7-hydroxyl benzastatin J (2a), 7-hydroxyl benzastatin B (2b), and 7-hydroxyl O-demethylbenzastatin A (2c) to *S. lividans* strains harboring pTYM2k-bezEGJ, pTYM-bezA-J $\Delta$ bezA, and pTYM-bezA-J $\Delta$ bezC, respectively.**

P<sub>tipA</sub>-bezJ was amplified by PCR using pHKO4-bezJ as a template, and cloned into the SpeI and HindIII sites of pTYM2k-bezG, resulting in pTYM2k-bezGJ. pTYM2k-bezGJ was digested with XbaI and HindIII and the P<sub>tipA</sub>-bezG-P<sub>tipA</sub>-bezJ fragment was cloned into the XbaI and HindIII sites of pTYM2k-bezE, resulting in pTYM2k-bezEGJ. This plasmid was then integrated into the chromosome of *S. lividans*. *S. lividans* harboring pTYM2k-bezEGJ was inoculated in ISP2 medium (5 ml) containing 50  $\mu$ g/ml kanamycin and 5  $\mu$ g/ml thiostrepton at 30°C for 7 days. All cells were harvested by centrifugation and transferred into SMM medium (5 ml) containing 50  $\mu$ g/ml kanamycin, 5  $\mu$ g/ml thiostrepton, and 10  $\mu$ M 7-hydroxyl benzastatin J (2a) and further incubated at 30°C for 3 days. Then, the fermentation broth (5 ml) was mixed with ethyl acetate (5 ml). After centrifugation, the organic layer was collected and evaporated to dryness under reduced pressure. The residual materials were dissolved in methanol (20  $\mu$ l) and applied to LC-ESIMS analysis (**Supplementary Figure 14a**).

*S. lividans* harboring pTYM-bezA-J $\Delta$ bezA and pTYM-bezA-J $\Delta$ bezC were inoculated in ISP2 medium (5 ml) containing 5  $\mu$ g/ml thiostrepton at 30 °C for 3 days. All cells were harvested by centrifugation and transferred into SMM medium (5 ml) containing 5  $\mu$ g/ml thiostrepton and 20  $\mu$ M 7-hydroxyl benzastatin B (2b) for *S. lividans* harboring pTYM-bezA-J $\Delta$ bezA or 7-hydroxyl O-demethylbenzastatin A (2c) for *S. lividans* harboring pTYM-bezA-J $\Delta$ bezC and further incubated at 30°C for 3 days. Then, the fermentation broth (5 ml) was mixed with ethyl acetate (5 ml). After centrifugation, the organic layer was collected and evaporated to dryness under reduced pressure. The residual materials were dissolved in methanol (20  $\mu$ l) and applied to

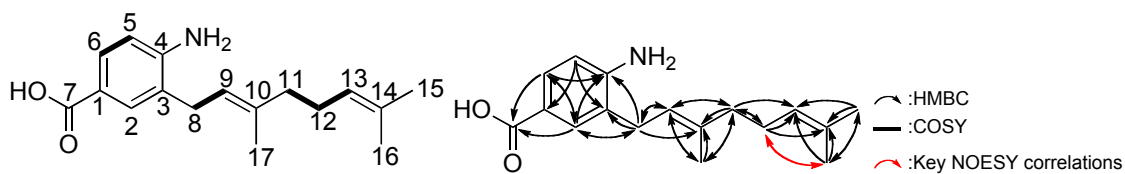
LC-ESIMS analysis ([Supplementary Figure 14b](#) and [c](#)).

## SUPPLEMENTARY TABLES

**Supplementary Table 1. Deduced functions of ORFs in the *bez* gene cluster.**

ORF	Amino acids	Proposed function	Protein homology	Amino acid identity
<i>bezA</i>	303	Methyltransferase	<i>Streptomyces</i> sp. Mg1, gamma-tocopherol methyltransferase, WP_008735520.1	118/277 (43%)
<i>bezB</i>	276	Methyltransferase	<i>Lechevalieria aerocolonigenes</i> , demethylrebeccamycin D-glucose O-methyltransferase, Q8KZ94.1	128/276 (48%)
<i>bezC</i>	447	Cytochrome P450 monooxygenase	<i>Actinopolyspora erythraea</i> , cytochrome P450, KGI81810.1	129/407 (32%)
<i>bezD</i>	374	Polyprenyl synthetase	<i>Streptomyces</i> sp. NRRL S-1448, polyprenyl diphosphate synthase, WP_030410847.1	134/353 (38%)
<i>bezE</i>	416	Cytochrome P450 monooxygenase	<i>Streptomyces</i> sp. Tü6071 ABB69759, cytochrome P450 CYP161B1, WP_007821186.1	168/388 (43%)
<i>bezF</i>	297	Prenyltransferase	<i>Streptomyces xiamenensis</i> , XimB, AGY49248.1	141/294 (48%)
<i>bezG</i>	282	N-Acetyltransferase	<i>Streptomyces murayamaensis</i> , putative arylamine N-acetyltransferase, AAO65324.1	125/269 (46%)
<i>bezH</i>	729	PABA synthase	<i>Streptomyces bingchengensis</i> , anthranilate synthase, WP_043489224.1	412/749 (55%)
<i>bezI</i>	332	PABA synthase	<i>Streptomyces bingchengensis</i> , class IV aminotransferase, WP_043489223.1	118/238 (50%)
<i>bezJ</i>	317	N-Oxygenase	<i>Streptomyces thioluteus</i> , N-oxygenase AurF, 2JCD_A	91/300 (30%)

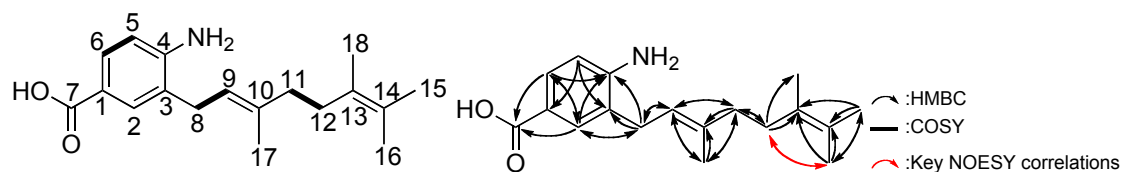
Supplementary Table 2.  $^1\text{H}$  and  $^{13}\text{C}$  NMR data for 7-hydroxyl benzastatin J (**2a**).



position	$^1\text{H}$	$^{13}\text{C}$
1		118.4
2	7.65 (s, 1H)	130.8
3		124.1
4		150.7
5	6.65 (d, 1H, $J = 8.5$ )	113.6
6	7.62 (d, 1H, $J = 8.7$ )	129.1
7		169.7
8	3.19 (d, 2H, $J = 7.0$ )	29.3
9	5.28 (t, 1H, $J = 6.8$ )	121.2
10		137.2
11	2.07 (t, 2H, $J = 6.5$ )	39.5
12	2.12 (dd, 2H, $J = 6.2, 7.7$ )	26.3
13	5.11 (t, 1H, $J = 6.8$ )	123.9
14		131.1
15	1.64 (s, 3H)	24.5
16	1.58 (s, 3H)	16.4
17	1.71 (s, 3H)	14.9

The  $^1\text{H}$  and  $^{13}\text{C}$  NMR spectra were recorded in  $\text{MeOH-}d_4$  and the solvent peak was used as an internal standard ( $\delta\text{C } 49.2$ ,  $\delta\text{H } 3.31$ ).

Supplementary Table 3.  $^1\text{H}$  and  $^{13}\text{C}$  NMR data for 7-hydroxyl benzastatin B (**2b**).

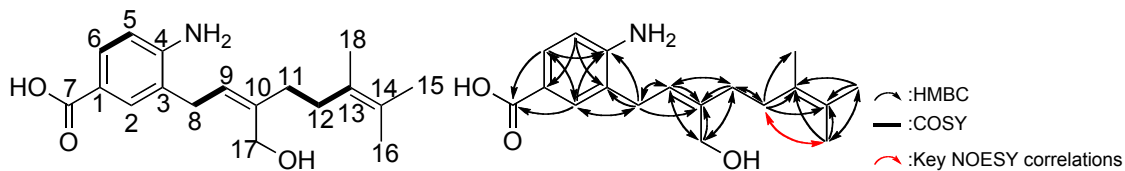


position	$^1\text{H}$	$^{13}\text{C}$
1		119.6
2	7.65 (d, 1H, $J = 2.0$ )	130.8
3		124.1
4		150.3
5	6.64 (d, 1H, $J = 8.0$ )	113.7
6	7.61 (dd, 1H, $J = 8.0, 2.0$ )	129.0
7		170.5
8	3.18 (d, 2H, $J = 7.0$ )	29.4
9	5.28 (t, 1H, $J = 6.6$ )	121.1
10		137.6
11	2.09 (m, 2H)	38.0
12	2.17 (m, 2H)	33.2
13		127.2
14		123.7
15	1.59 (s, 3H)	19.3
16	1.62 (s, 3H)	18.9
17	1.73 (s, 3H)	15.0
18	1.62 (s, 3H)	18.6

The  $^1\text{H}$  and  $^{13}\text{C}$  NMR spectra were recorded in  $\text{MeOH-}d_4$  and the solvent peak was used as an internal standard ( $\delta\text{C } 49.2$ ,  $\delta\text{H } 3.31$ ).



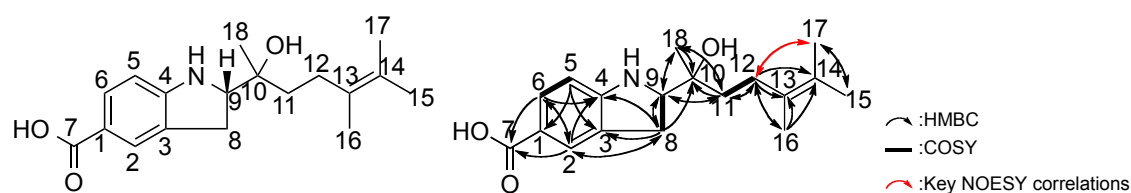
**Supplementary Table 4.  $^1\text{H}$  and  $^{13}\text{C}$  NMR data for 7-hydroxyl *O*-demethylbenzastatin A (**2c**).**



position	$^1\text{H}$	$^{13}\text{C}$
1		118.2
2	7.64 (s, 1H)	131.1
3		123.5
4		150.9
5	6.64 (d, 1H, $J = 8.8$ )	113.6
6	7.62 (d, 1H, $J = 9.7$ )	129.4
7		169.6
8	3.30 (d, 2H, $J = 8.1$ )	29.2
9	5.37 (t, 1H, $J = 7.4$ )	124.7
10		140.5
11	2.18 (s, 2H)	33.4
12	2.18 (s, 2H)	33.4
13		127.1
14		123.8
15	1.59 (s, 3H)	19.3
16	1.61 (s, 3H)	18.9
17	4.20 (s, 2H)	58.9
18	1.62 (s, 3H)	17.2

The  $^1\text{H}$  and  $^{13}\text{C}$  NMR spectra were recorded in  $\text{MeOH-}d_4$  and the solvent peak was used as an internal standard ( $\delta\text{C } 49.2$ ,  $\delta\text{H } 3.31$ ).

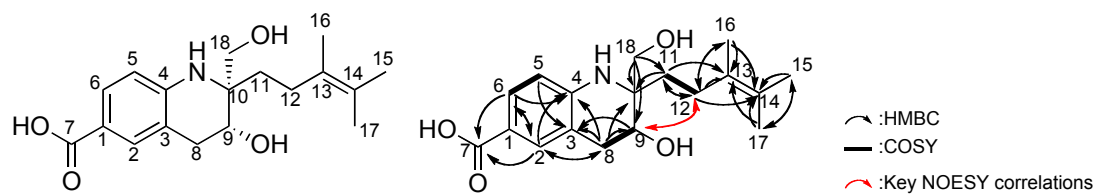
Supplementary Table 5. <sup>1</sup>H and <sup>13</sup>C NMR data for 7-hydroxyl benzastatin F (**5b**).



position	<sup>1</sup> H	<sup>13</sup> C
1		118.4
2	7.60 (s, 1H) [7.76 (s, 1H)] <sup>a</sup>	125.7
3		128.2
4		156.6
5	6.47 (d, 1H, <i>J</i> = 8.6) [6.58 (d, 1H, <i>J</i> = 8.1)] <sup>a</sup>	106.3
6	7.64 (d, 1H, <i>J</i> = 8.0) [7.81 (d, 1H, <i>J</i> = 7.6)] <sup>a</sup>	130.8
7		169.7
8	3.01 (d, 2H, <i>J</i> = 9.2) [3.05 (m, 2H)] <sup>a</sup>	29.7
9	3.90 (t, 1H, <i>J</i> = 9.2) [3.99 (t, 1H, <i>J</i> = 9.2)] <sup>a</sup>	67.4
10		73.3
11	1.48 (t, 2H, <i>J</i> = 9.1) [1.60 (m, 1H), 1.44 (m, 1H)] <sup>a</sup>	36.4
12	2.11 (m, 2H) [2.14 (ddd, 1H, <i>J</i> = 12, 12, 4.6, 2.07 (ddd, 1H, <i>J</i> = 12, 12, 4.6)] <sup>a</sup>	28.1
13		127.4
14		123.4
15	1.61 (s, 3H) [1.63 (s, 3H)] <sup>a</sup>	19.3
16	1.62 (s, 3H) [1.64 (s, 3H)] <sup>a</sup>	17.2
17	1.64 (s, 3H) [1.66 (s, 3H)] <sup>a</sup>	18.9
18	1.16 (s, 3H) [1.26 (s, 3H)] <sup>a</sup>	21.4

The <sup>1</sup>H and <sup>13</sup>C NMR spectra were recorded in MeOH-*d*<sub>4</sub> and the solvent peak was used as an internal standard (δC 49.2, δH 3.31). <sup>a</sup>The <sup>1</sup>H NMR data recorded in CDCl<sub>3</sub>

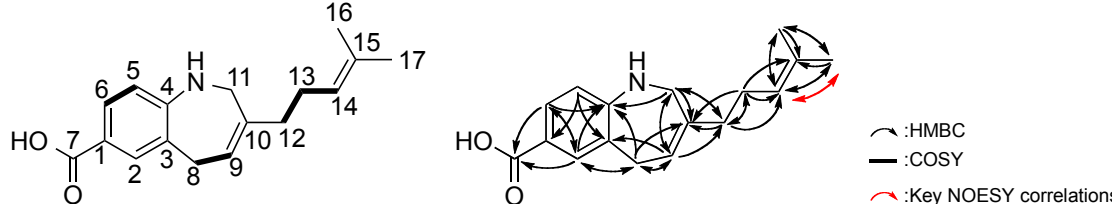
**Supplementary Table 6.  $^1\text{H}$  and  $^{13}\text{C}$  NMR data for 7-hydroxyl *O*-demethyl-benzastatin D (6'c).**



position	$^1\text{H}$	$^{13}\text{C}$
1		116.6
2	7.62 (s, 1H)	131.9
3		117.0
4		148.6
5	6.58 (d, 1H, $J = 8.3$ )	112.7
6	7.58 (d, 1H, $J = 7.7$ )	129.1
7		169.7
8	2.95 (dd, 1H, $J = 12, 4.7$ ) 2.80 (dd, 1H, $J = 10, 6.3$ )	32.6
9	3.85 (t, 1H, $J = 5.1$ )	66.2
10		57.5
11	1.53 (m, 2H)	32.3
12	2.14 (1H, m) 2.08 (1H, m)	27.2
13		127.4
14		123.5
15	1.59 (s, 3H)	19.4
16	1.59 (s, 3H)	17.3
17	1.59 (s, 3H)	18.8
18	3.55 (d, 1H, $J = 11$ ) 3.75 (d, 1H, $J = 11$ )	63.3

The  $^1\text{H}$  and  $^{13}\text{C}$  NMR spectra were recorded in  $\text{MeOH-}d_4$  and the solvent peak was used as an internal standard ( $\delta\text{C } 49.2$ ,  $\delta\text{H } 3.31$ ).

Supplementary Table 7.  $^1\text{H}$  and  $^{13}\text{C}$  NMR data for benzastatin K (**7a**).



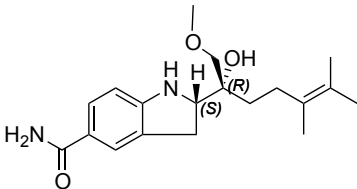
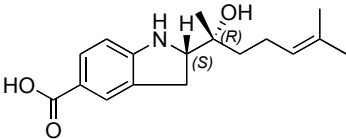
position	$^1\text{H}$	$^{13}\text{C}$
1		118.2
2	7.48 (s, 1H)	129.0
3		123.4
4		152.7
5	6.46 (d, 1H, $J = 8.5$ )	115.9
6	7.53 (d, 1H, $J = 8.4$ )	131.6
7		169.8
8	3.41 (d, 2H, $J = 6.4$ )	31.8
9	5.76 (t, 1H, $J = 6.6$ )	123.6
10		138.7
11	3.83 (s, 2H)	45.4
12	2.03 (t, 2H, $J = 7.3$ )	36.6
13	2.09 (q, 2H, $J = 7.1$ )	26.4
14	5.07 (t, 1H, $J = 6.3$ )	123.7
15		131.2
16	1.60 (s, 3H)	16.4
17	1.55 (s, 3H)	24.5

The  $^1\text{H}$  and  $^{13}\text{C}$  NMR spectra were recorded in  $\text{MeOH-}d_4$  and the solvent peak was used as an internal standard ( $\delta\text{C } 49.2$ ,  $\delta\text{H } 3.31$ ).

**Supplementary Table 8. Optical rotation of benzastatin E and JBIR-67 (5a).**

Because the reported specific rotation value of **5a** is close to that reported for benzastatin E, **5a** was concluded to have the same stereochemistry with this compound.

We think that absolute stereochemistry of **5b** should be the same with **5a**.

Name	Structure	Optical rotation	Reference number from the main text
Benzastatin E		$[\alpha]_D +21.3 \text{ } c \text{ } 0.10$ , MeOH	46 (Absolute stereochemistry was reported.)
JBIR-67 ( <b>5a</b> )		$[\alpha]_D +19.0 \text{ } c \text{ } 0.10$ , MeOH	23 (Only relative stereochemistry was reported.)

**Supplementary Table 9. Primers used in this study.**

No.	Name	Sequences (5' – 3')	Description
1	<i>ΔbezA_F</i>	<u>GATTACTCCGGTATGCGGCCAAGATCT</u> <u>GGGGCGCCGAACACCGG</u> <i>ACTAGTGGC</i> AGCATCACCCGACGCAC	Amplification of a chloramphenicol resistance gene to disrupt <i>bezA</i> on pTYM- <i>bezA-J</i> (nucleotide sequences of the upstream and downstream regions from <i>bezA</i> are indicated by underlining; a SpeI site is italicized)
2	<i>ΔbezA_R</i>	<u>TGCCATTCGGCGCCCAGCGCCTGGTT</u> <u>CGCCATCAGGGATATCCT</u> <i>ACTAGTATG</i> TGGATCCTACCAACCGG	
3	<i>ΔbezB_F</i>	<u>TGTGGGGTCCCAACATCCACTACGGCT</u> <u>ACTGGGAGAACGACGCC</u> <i>ACTAGTGGC</i> AGCATCACCCGACGCAC	Amplification of a chloramphenicol resistance gene to disrupt <i>bezB</i> on pTYM- <i>bezA-J</i> (nucleotide sequences of the upstream and downstream regions from <i>bezB</i> are indicated by underlining; a SpeI site is italicized)
4	<i>ΔbezB_R</i>	<u>GAGTCGGCCTTCTCCTCGCCGACCAG</u> <u>ATCGGACAGCTTGTCGCG</u> <i>ACTAGTATG</i> TGGATCCTACCAACCGG	
5	<i>ΔbezE_F</i>	<u>GCCGCTCGAACCCCGATCCGGAGGCC</u> <u>GCGGCGAAGGACAGCGGG</u> <i>ACTAGTGG</i> CAGCATCACCCGACGCAC	Amplification of a chloramphenicol resistance gene to disrupt <i>bezE</i> on pTYM- <i>bezA-J</i> (nucleotide sequences of the upstream and downstream regions from <i>bezE</i> are indicated by underlining; a SpeI site is italicized)
6	<i>ΔbezE_R</i>	<u>TCGCGCAGCCTCAGTTCCTCCGCGCC</u> <u>GACAGCCAGACGCAGGGT</u> <i>ACTAGTAT</i> GTGGATCCTACCAACCGG	
7	<i>ΔbezG_F</i>	<u>TGGGTTACCAGGGCGACGTGGCCCCG</u> <u>GACCTCGCCACGCTGCGG</u> <i>ACTAGTGGC</i> AGCATCACCCGACGCAC	Amplification of a chloramphenicol resistance gene to disrupt <i>bezG</i> on pTYM- <i>bezA-J</i> (nucleotide sequences of the upstream and downstream regions from <i>bezG</i> are indicated by underlining; a SpeI site is italicized)
8	<i>ΔbezG_R</i>	<u>CGGGAGGTCACCGGCTCCGCGGGACG</u> <u>TATTTCATGAGGGTGCT</u> <i>ACTAGTATGT</i> GGATCCTACCAACCGG	
9	<i>ΔbezJ_F</i>	<u>CGCAGCTGACGCGCCGCTGGGGGAAG</u> <u>CGGGTGGCCGTCAAGAAG</u> <i>ACTAGTGG</i> CAGCATCACCCGACGCAC	Amplification of a chloramphenicol resistance gene to disrupt <i>bezJ</i> on pTYM- <i>bezA-J</i> (nucleotide sequences of the upstream and downstream regions from <i>bezJ</i> are indicated by underlining; a SpeI site is italicized)
10	<i>ΔbezJ_R</i>	<u>AGGTCGTGGTCGATGCCAGGTCGTC</u> <u>GAGGAGGAGTCGCAACGG</u> <i>ACTAGTAT</i> GTGGATCCTACCAACCGG	

11	<i>tipA_F1</i>	AAGCTAGCGGGCTGAGGGAGCCGAC	Amplification of <i>tipA-bezA</i> or <i>tipA-bezB</i> fragment to disrupt <i>bezC</i> on pTYM- <i>bezA-J</i> (a NheI site is italicized)
12	<i>bezA_R1</i>	TTTCTAGATCACTTCCGCTCGAAGCG	Amplification of P <sub><i>tipA-bezA</i></sub> fragment to disrupt <i>bezC</i> on pTYM- <i>bezA-J</i> (an XbaI site is italicized)
13	<i>bezB_R1</i>	TTTCTAGATCACGCCCGACGGCGGTC	Amplification of P <sub><i>tipA-bezB</i></sub> fragment to disrupt <i>bezC</i> on pTYM- <i>bezA-J</i> (an XbaI site is italicized)
14	<i>tipA_F2</i>	AAATTAATGGGCTGAGGGAGCCGACG	Amplification of P <sub><i>tipA-bezE</i></sub> fragment to construct pTYM2k-P <sub><i>tipA-bezE</i></sub> (a PshBI site is italicized)
15	<i>tipA_F3</i>	TTTCTAGAGGGCTGAGGGAGCC	Amplification of P <sub><i>tipA-bezG</i></sub> fragment to construct pTYM2k-P <sub><i>tipA-bezG</i></sub> (an XbaI site is italicized)
16	<i>tipA_F4</i>	AAACTAGTGGGCTGAGGGAGCCGA	Amplification of P <sub><i>tipA-bezJ</i></sub> fragment to construct pTYM2k-P <sub><i>tipA-bezJ</i></sub> (a SpeI site is italicized)
17	<i>bezE_F1</i>	AACATATGTTGCCCTTCGAGCAGCCGA A	Amplification of <i>bezE</i> fragment to construct pHKO4- <i>bezE</i> (a NdeI site is italicized)
18	<i>bezE_R1</i>	TTTCTAGATCACACGTCACCGGAAGG	Amplification of <i>bezE</i> or P <sub><i>tipA-bezE</i></sub> fragment to construct pHKO4- <i>bezE</i> or pTYM2k-P <sub><i>tipA-bezE</i></sub> (an XbaI site is italicized)
19	<i>bezG_F1</i>	AACATATGAACGACGAACCGCGGG	Amplification of <i>bezG</i> fragment to construct pHKO4- <i>bezG</i> (a NdeI site is italicized)
20	<i>bezG_R1</i>	TTAAGCTTAA <u>ACTAGT</u> TCAGGGACCGT CCAAGGT	Amplification of <i>bezG</i> or P <sub><i>tipA-bezG</i></sub> fragment to construct pHKO4- <i>bezG</i> or pTYM2k-P <sub><i>tipA-bezG</i></sub> (a HindIII site is italicized and a SpeI site is indicated by underlining)
21	<i>bezJ_F</i>	AACATATGACCGTGGCACGTGAAGAG	Amplification of <i>bezJ</i> fragment to construct pHKO4- <i>bezJ</i> or pET16b- <i>bezJ</i> (a NdeI site is italicized)
22	<i>bezJ_R1</i>	TTAAGCTTTCATGGCCGGGTGGG	Amplification of P <sub><i>tipA-bezJ</i></sub> fragment to construct pTYM2k-P <sub><i>tipA-bezJ</i></sub> (a HindIII site is italicized)
23	<i>bezA_F2</i>	AACATATGTCGAATCTGGATGAACTTG C	Amplification of <i>bezA</i> to construct pColdI- <i>bezA</i> (a NdeI site is italicized)
24	<i>bezA_R2</i>	TTGGA CTGAGTCACTTCCGCTCGAA	Amplification of <i>bezA</i> to construct pColdI- <i>bezA</i> (an XhoI site is italicized)
25	<i>bezC_F</i>	AAGAGCTCATGTCTAGTTGGTTCTGGGC AA	Amplification of <i>bezC</i> to construct pColdI- <i>bezC</i> (a SacI site is italicized)

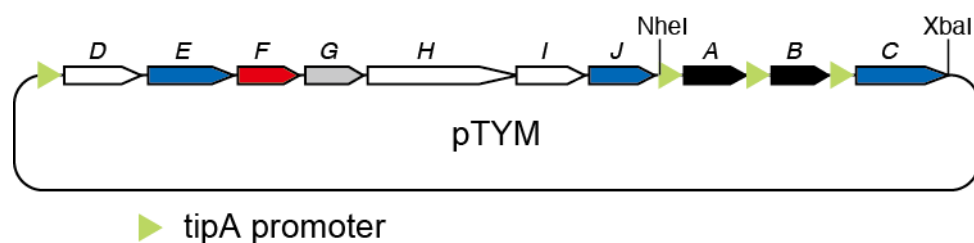
26	<i>bezC_R</i>	CGCGTCTAGACTATCTCTCCTGACCG CCGTCC	Amplification of <i>bezC</i> to construct pColdI- <i>bezC</i> (an XbaI site is italicized)
27	<i>bezE_F2</i>	AACATATGGGTGATAGCACCAGCGC	Amplification of <i>bezE</i> to construct pET26b- <i>bezE</i> (a NdeI site is italicized)
28	<i>bezE_R2</i>	TTCTCGAGCCAGGTAACCGGCAG	Amplification of <i>bezE</i> to construct pET26b- <i>bezE</i> (an XhoI site is italicized)
29	<i>bezF_F</i>	AACATATGGGCAGCAGCCATCATCATC ATCATCACATCGAGGGCCGCCATCTGC ACAAGATATCCA	Amplification of <i>bezF</i> to construct pHKO4- <i>bezF</i> (a NdeI site is italicized)
30	<i>bezF_R</i>	TTGAATTCTCATGTCAACTGCCC	Amplification of <i>bezF</i> to construct pHKO4- <i>bezF</i> (an XhoI site is italicized)
31	<i>bezG_F2</i>	AACATATGTGGCAGGGTAGCGGCGTC GACCTGGAC	Amplification of <i>bezG</i> to construct pET16b- <i>bezG</i> (a NdeI site is italicized)
32	<i>bezG_R2</i>	TTCTCGAGTCACGGACCGTCCAAG	Amplification of <i>bezG</i> to construct pET16b- <i>bezG</i> (an XhoI site is italicized)
33	<i>bezJ_R2</i>	TTGGATCCTCATGGCCGGGTGGGGCG G	Amplification of <i>bezJ</i> to construct pET16b- <i>bezJ</i> (a BamHI site is italicized)
34	pHKO1_F	AGGTTCGGCGATATCGCGAG	Amplification of a DNA fragment derived from pTONA5 (an EcoRV site is italicized)
35	pHKO1_R	CCAGAGCTCTCATCACTGACGAATCG AGGTC	Amplification of a DNA fragment derived from pTONA5 (a SacI site is italicized)
36	pHKO4_F	AAATTAATACTGCTGATCCGGTCAGCA G	Amplification of the <i>tipA</i> promoter and multi cloning site from pIJ6021 (a PshBI site is italicized)
37	pHKO4_R	TCTCACTCCGCTGAAACTGTTGAAAG	Amplification of the <i>tipA</i> promoter and multi cloning site from pIJ6021



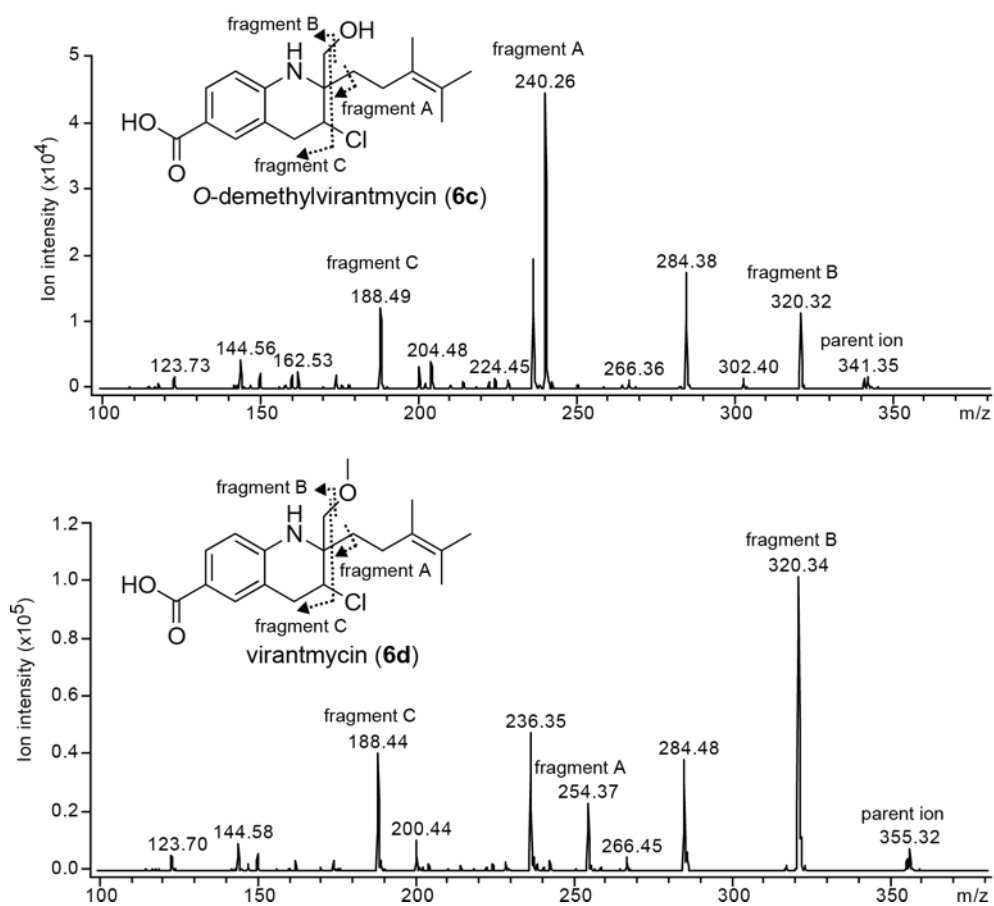
**Supplementary Table 10. Plasmids constructed in this study.**

Plasmid	Insert
pTYM- <i>bezA-J</i>	<i>P<sub>tipA</sub>-bezDEFGHIJ-P<sub>tipA</sub>-bezA-P<sub>tipA</sub>-bezB-P<sub>tipA</sub>-bezC</i>
pTYM- <i>bezA-JΔbezA</i>	<i>P<sub>tipA</sub>-bezDEFGHIJ-P<sub>tipA</sub>-bezB-P<sub>tipA</sub>-bezC</i>
pTYM- <i>bezA-JΔbezB</i>	<i>P<sub>tipA</sub>-bezDEFGHIJ-P<sub>tipA</sub>-bezA-P<sub>tipA</sub>-bezC</i>
pTYM- <i>bezA-JΔbezC</i>	<i>P<sub>tipA</sub>-bezDEFGHIJ-P<sub>tipA</sub>-bezA-P<sub>tipA</sub>-bezB</i>
pTYM- <i>bezA-JΔbezE</i>	<i>P<sub>tipA</sub>-bezDFGHIJ-P<sub>tipA</sub>-bezA-P<sub>tipA</sub>-bezB-P<sub>tipA</sub>-bezC</i>
pTYM- <i>bezA-JΔbezG</i>	<i>P<sub>tipA</sub>-bezDEFHIJ-P<sub>tipA</sub>-bezA-P<sub>tipA</sub>-bezB-P<sub>tipA</sub>-bezC</i>
pTYM- <i>bezA-JΔbezJ</i>	<i>P<sub>tipA</sub>-bezDEFGHI-P<sub>tipA</sub>-bezA-P<sub>tipA</sub>-bezB-P<sub>tipA</sub>-bezC</i>
pTYM2k- <i>P<sub>tipA</sub>-bezE</i>	<i>P<sub>tipA</sub>-bezE</i>
pTYM2k- <i>P<sub>tipA</sub>-bezG</i>	<i>P<sub>tipA</sub>-bezG</i>
pTYM2k- <i>P<sub>tipA</sub>-bezJ</i>	<i>P<sub>tipA</sub>-bezJ</i>
pColdI- <i>bezA</i>	<i>bezA</i>
pColdI- <i>bezC</i>	<i>bezC</i>
pET26b- <i>bezE</i>	<i>bezE</i>
pHKO4- <i>bezF</i>	<i>bezF</i>
pET16b- <i>bezG</i>	<i>bezG</i>
pET16b- <i>bezJ</i>	<i>bezJ</i>

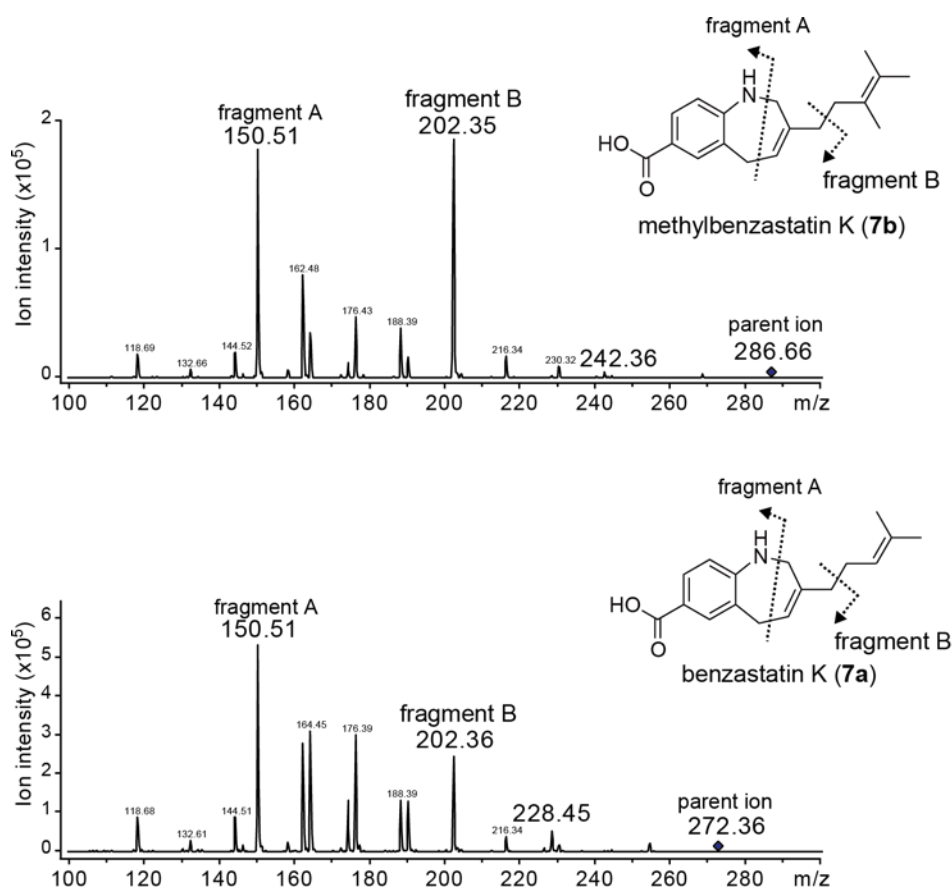
## SUPPLEMENTARY FIGURES



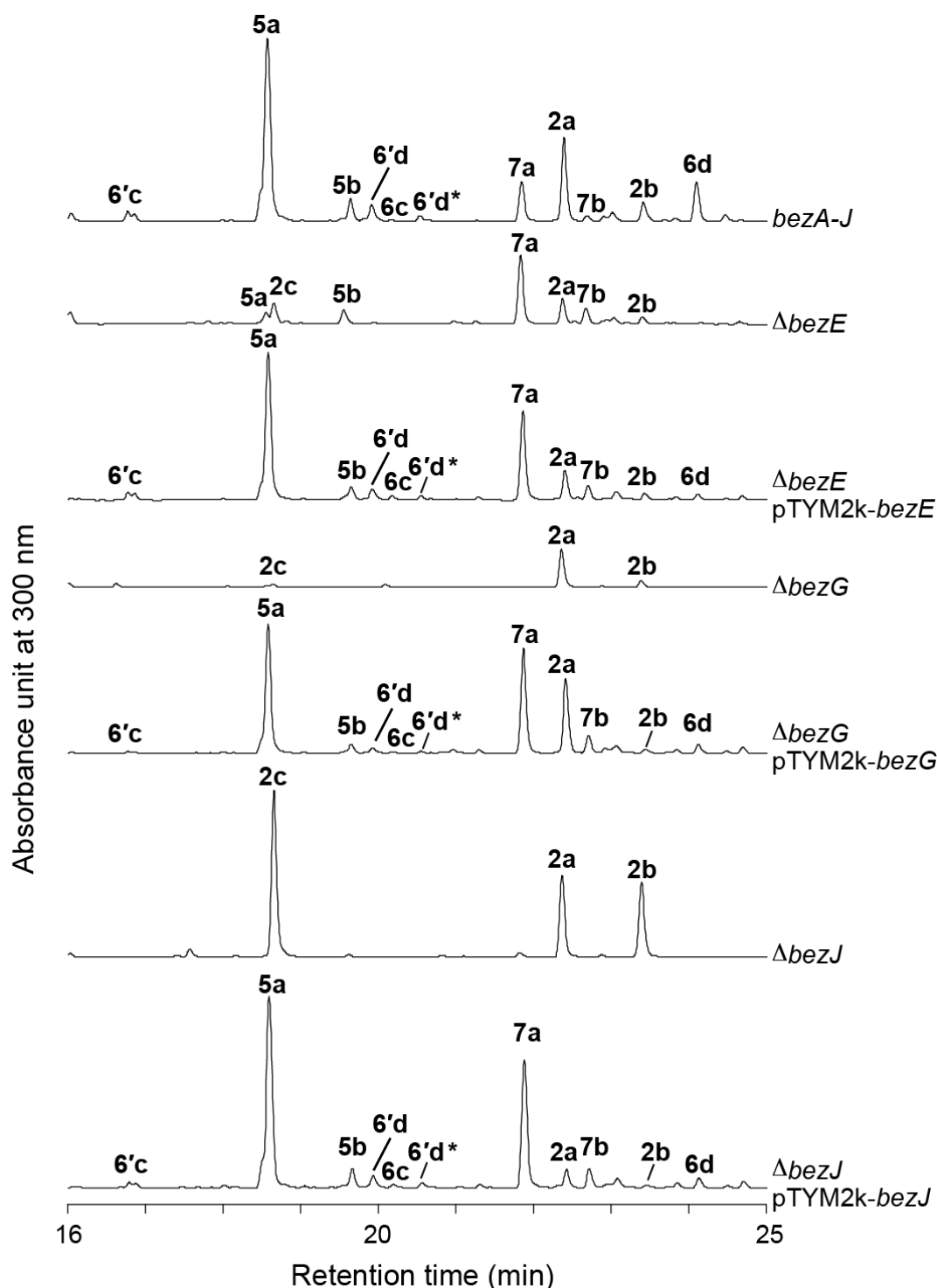
**Supplementary Figure 1. Plasmid constructed for heterologous expression of benzastatin biosynthesis genes in *S. lividans*.**



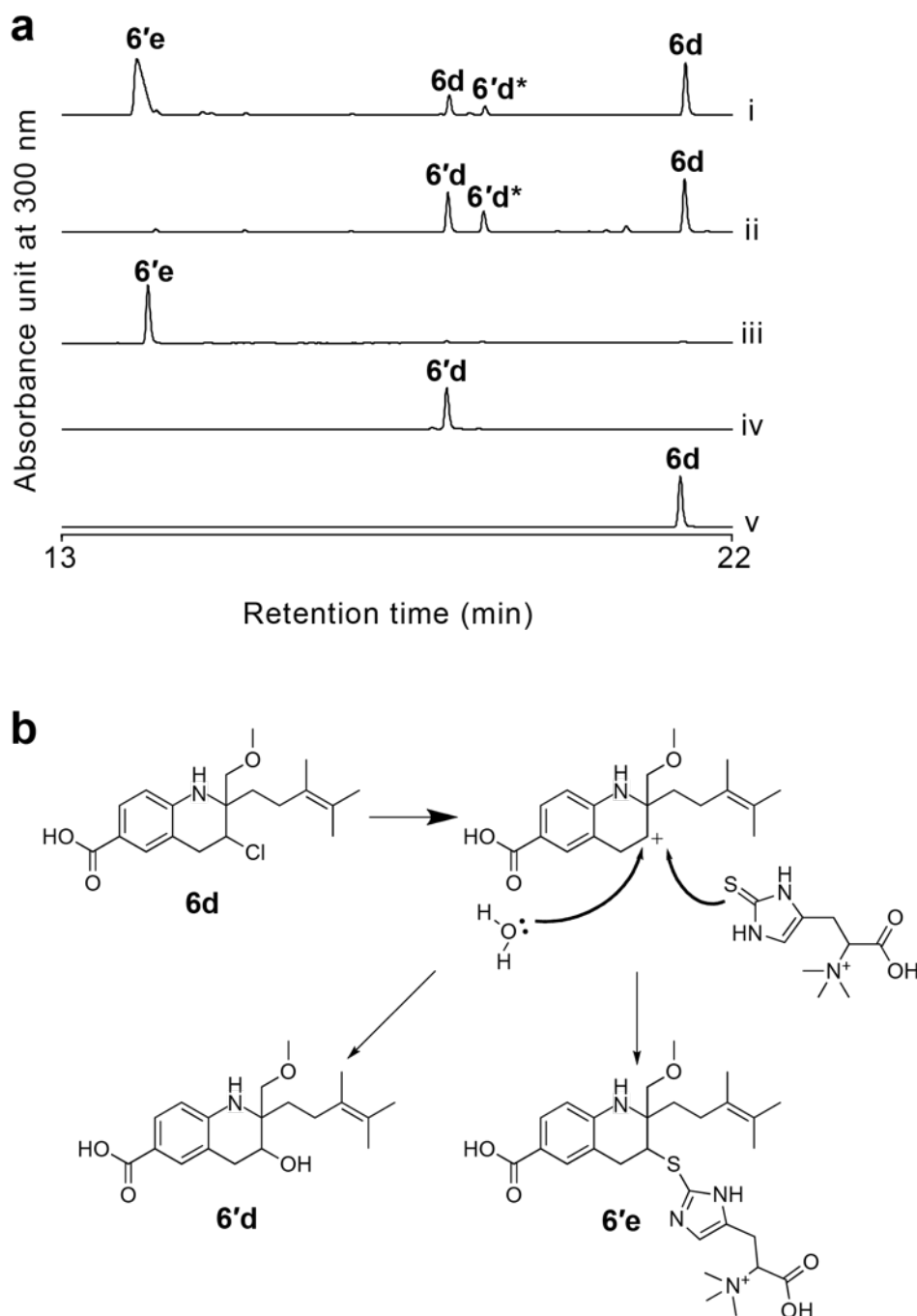
**Supplementary Figure 2. Tandem mass spectra of virantmycin (6d) and *O*-demethylvirantmycin (6c).** Compound 6c was characterized by comparing its tandem mass spectrum with that of 6d. Fragments A, B, and C were important to predict the structure of 6c.



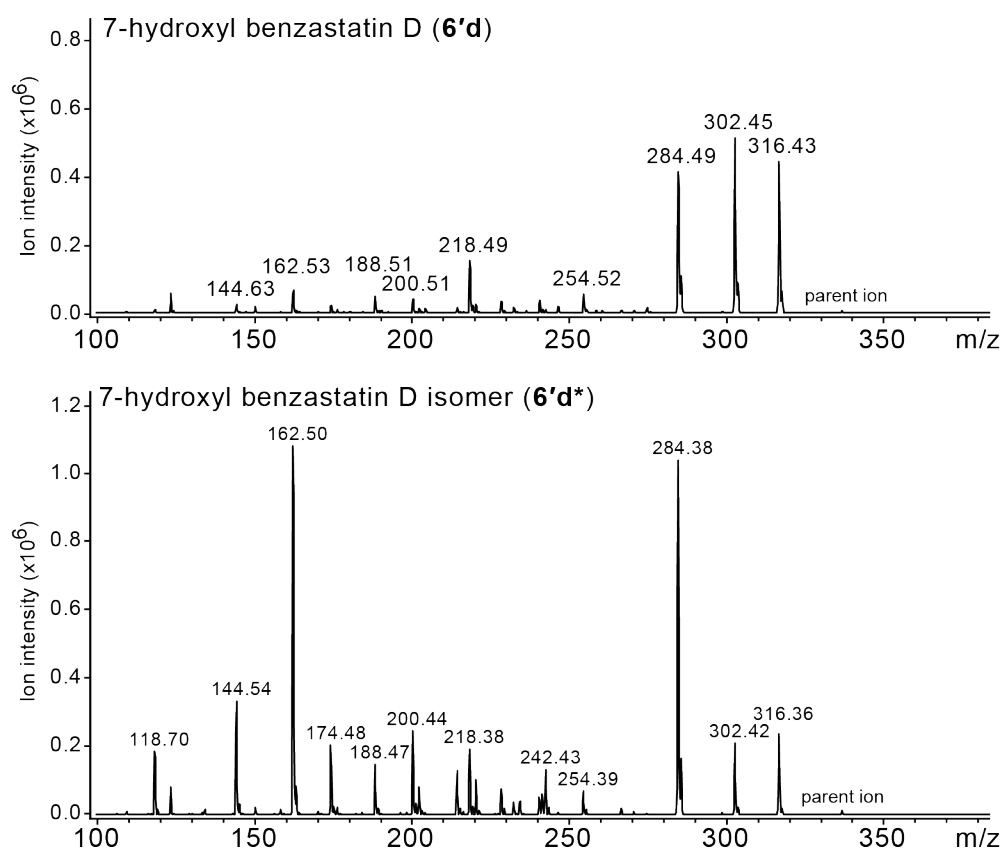
**Supplementary Figure 3. Tandem mass spectra of benzastatin K (7a) and methylbenzastatin K (7b).** The structure of 7b was characterized by comparing its tandem mass spectrum with that of 7a. Fragments A and B were important to predict the structure of 7b.



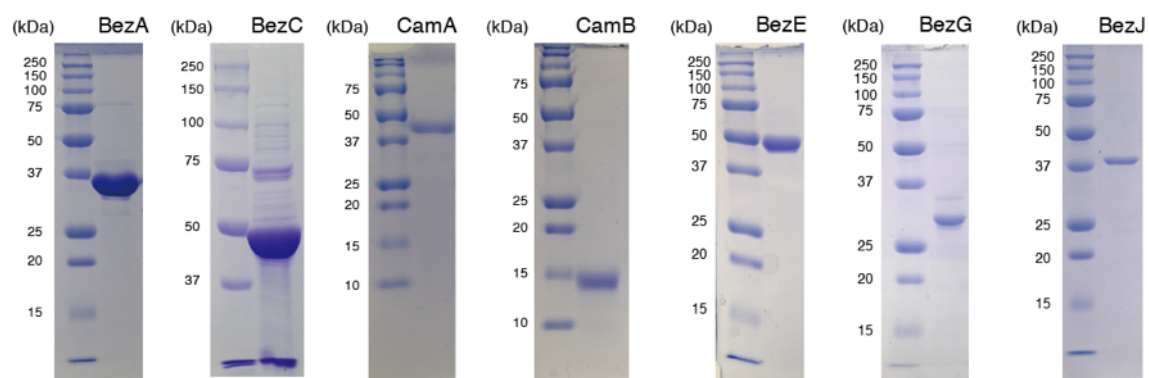
**Supplementary Figure 4. Complementation of the  $\Delta bezE$ ,  $\Delta bezG$ , and  $\Delta bezJ$  strains by each gene on a chromosome integration plasmid.** Because *bezE*, *bezG*, and *bezJ* are located at the immediate downstream of the *tipA* promoter in the respective complementation strains, the expression level of each gene introduced should be higher than that in the parent strain. We think this is the reason why the production profiles of the benzastatin derivatives are different between each complementation strain and the parent strain.



**Supplementary Figure 5. *In vitro* analysis of non-enzymatic degradation of **6d**.** (a) *In vitro* non-enzymatic synthesis of **6'e** from **6d** and ergothioneine. LC-MS analysis of the reaction mixtures containing **6d** with ergothioneine (i), **6d** without ergothioneine (ii). The reaction products were compared with authentic **6'e** (iii), authentic **6'd** (iv), and authentic **6d** (v). (b) Proposed mechanisms for non-enzymatic synthesis of **6e** and **6'd** from **6d**. Compound **6'd\*** is considered to be an isomer of **6'd** (see the legend of [Figure 3](#)). Degradation of **6d** seems to prefer  $S_N1$  reaction to  $S_N2$  reaction because of the steric hindrance by the dimethylpentenyl group at C-10, which yields more **6'd** than **6'd\***.

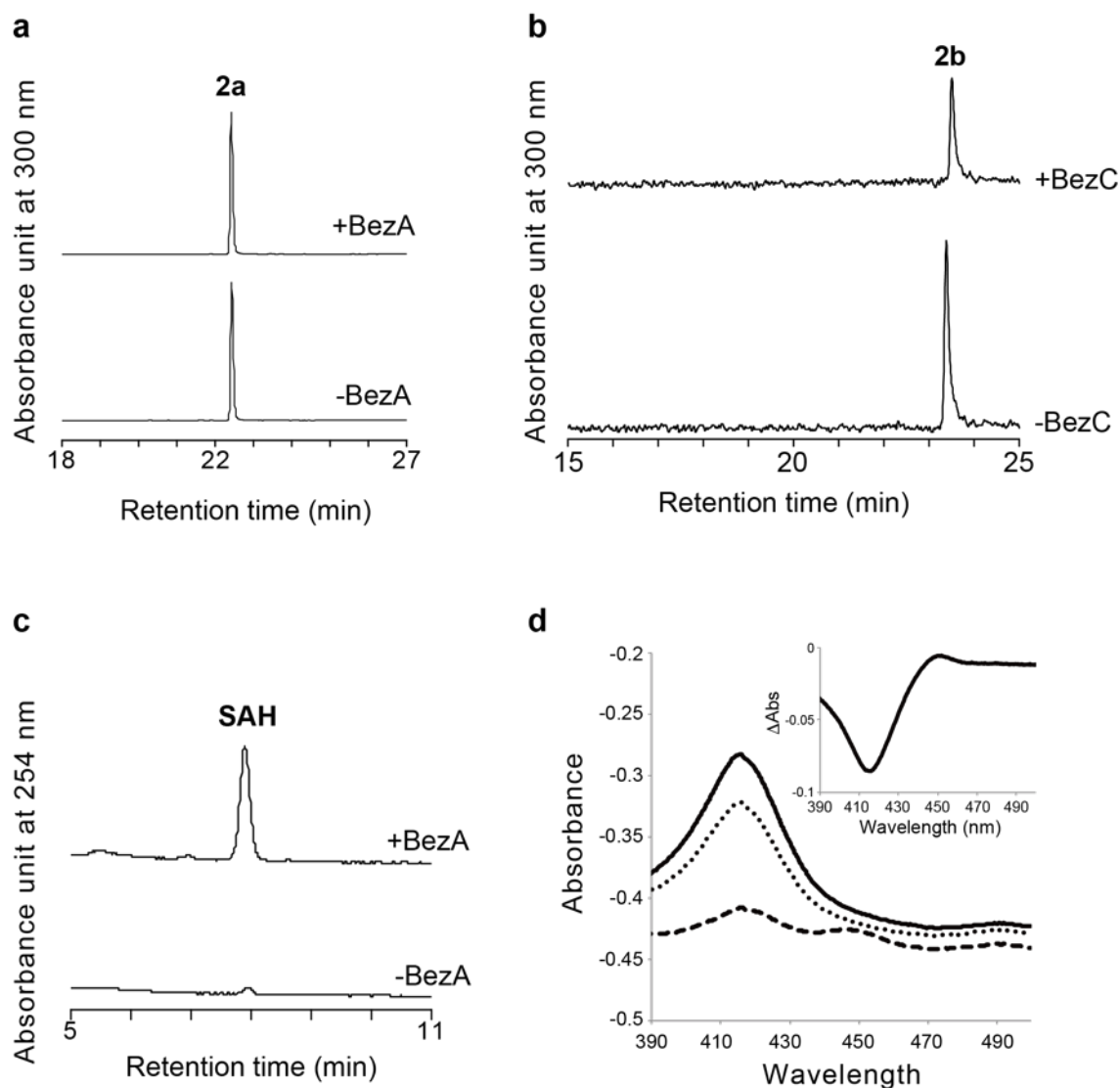


**Supplementary Figure 6. Tandem mass spectra of 7-hydroxyl benzastatin D (**6'd**) and its isomer (**6'd\***).** These two compounds showed similar fragmentation patterns. Therefore, **6'd\*** is likely to be an isomer of **6'd**, which possess different stereochemistry at position 9. This was also supported by the observation that both **6'd** and **6'd\*** were synthesized by hydrolysis of **6d** ([Supplementary Figure 5](#)).

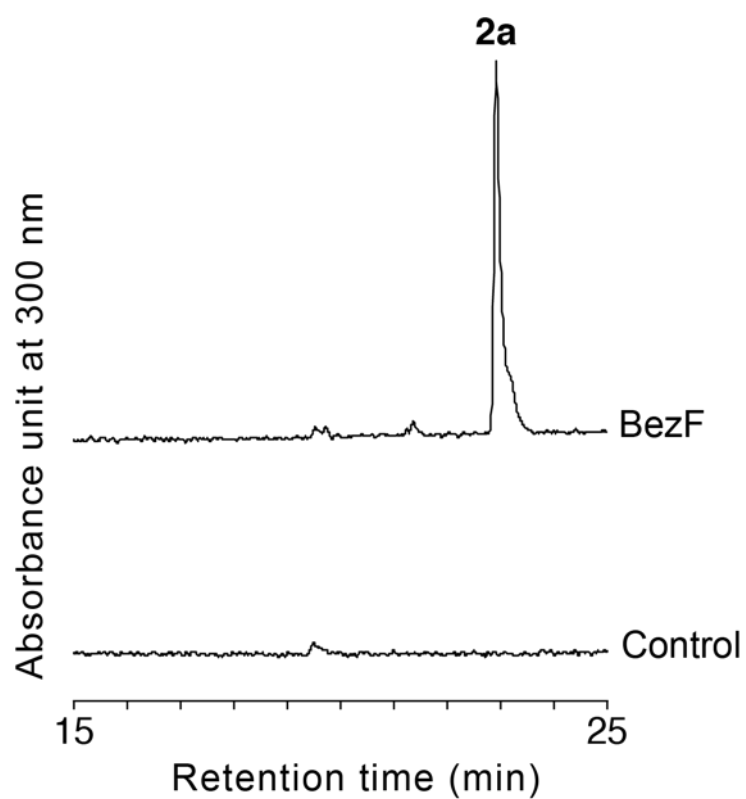


**Supplementary Figure 7. SDS-PAGE of recombinant proteins used in this study.** Theoretical molecular mass values (kDa) of recombinant proteins are Beza, 35.6; BezC, 51.9; CamA, 47.7; CamB, 13.7; BezE, 46.5; BezG, 32.6; BezJ, 38.3.

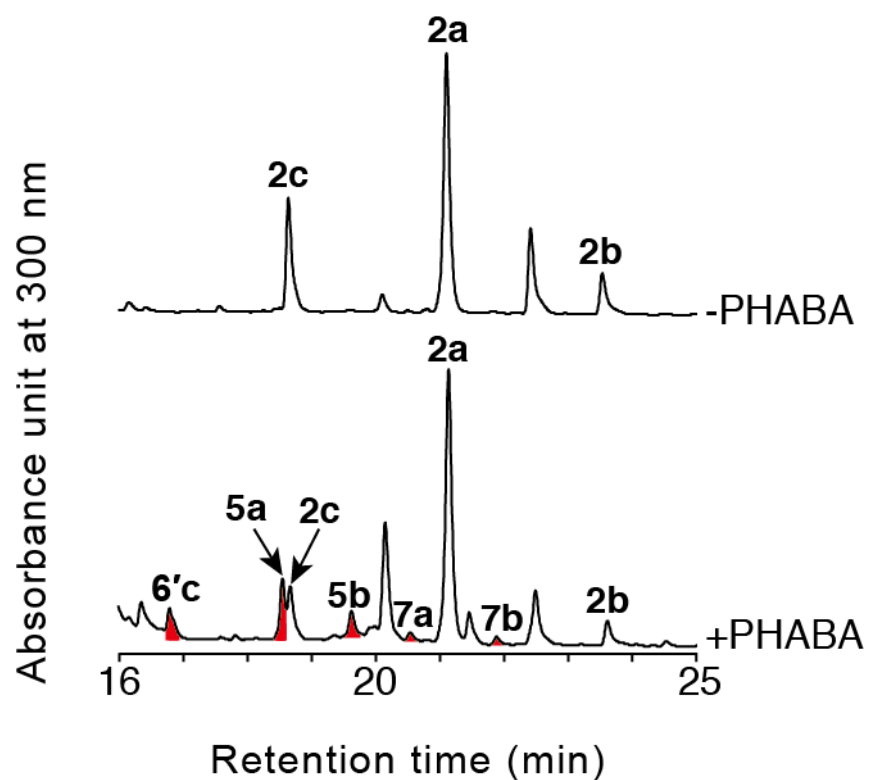




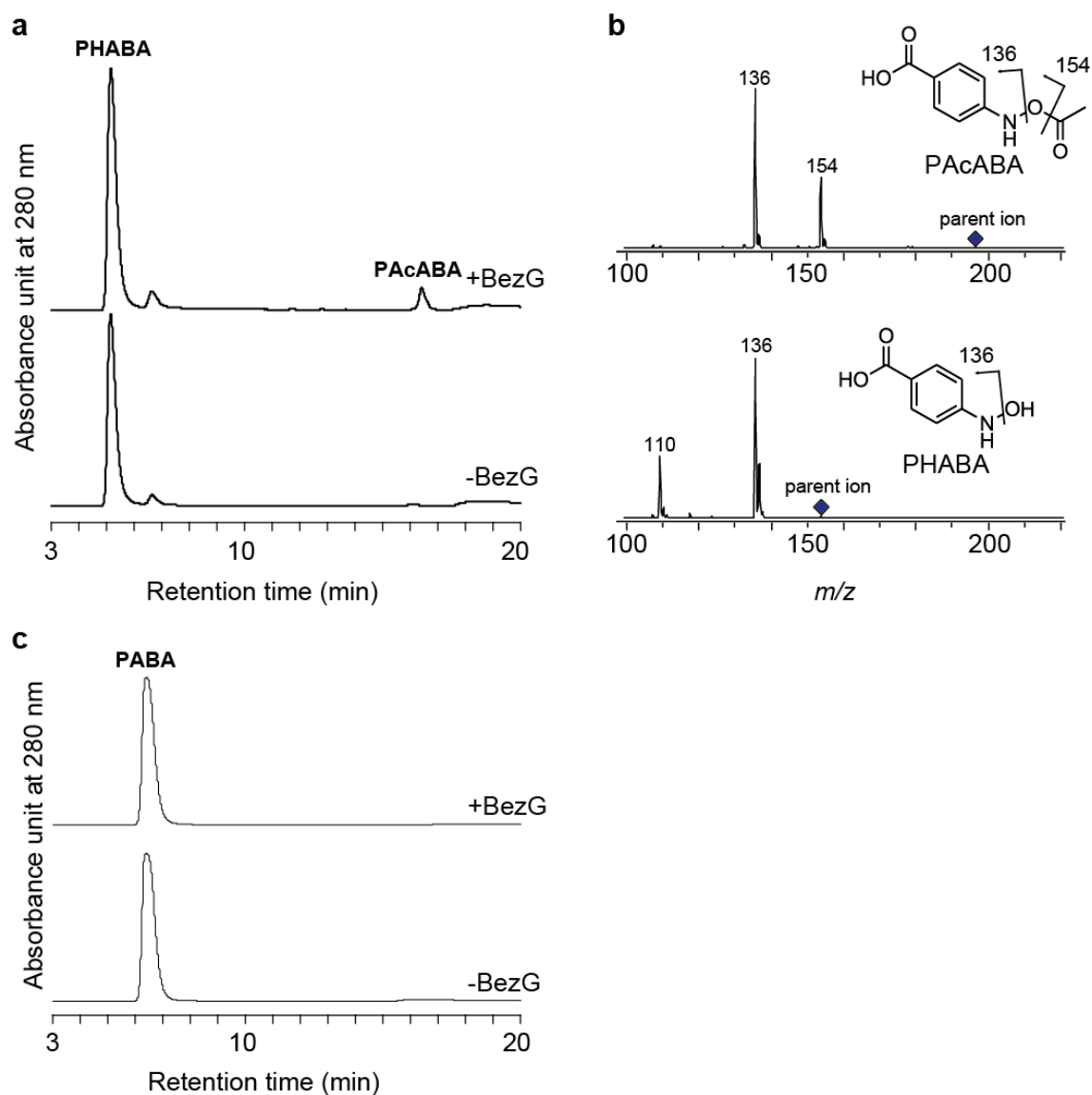
**Supplementary Figure 8. *In vitro* analysis of BezA and BezC.** (a) Incubation of BezA with **2a** resulted in no detectable product. (b) Incubation of BezC with **2b** in the presence of CamA, CamB, and NADH resulted in no detectable product. (c) Accumulation of *S*-adenosyl-L-homocysteine (SAH) was observed when BezA was incubated with GPP (**1a**) and SAM. (d) UV-visible spectra of recombinant BezC. Solid line, BezC; dotted line, BezC with sodium hydrosulfite; dashed line, BezC with sodium hydrosulfite and CO. *Inset*, CO differential spectrum of BezC: (BezC with sodium hydrosulfite and CO) minus (BezC with sodium hydrosulfite).



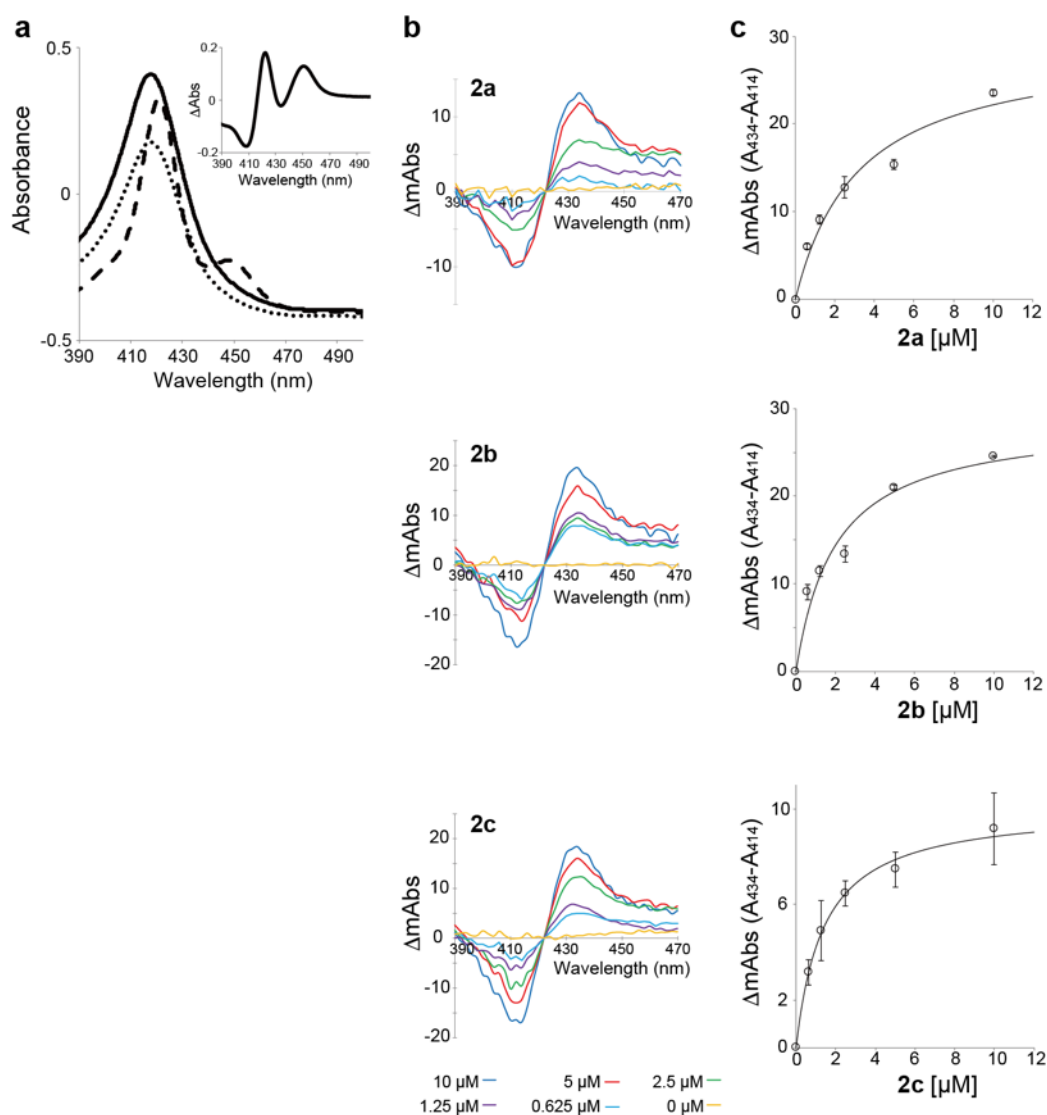
**Supplementary Figure 9. *In vitro* analysis of BezF.** When the crude BezF solution, which was prepared from the membrane fraction of *S. lividans* harboring pHKO4-bezF, was incubated with  $\text{Mg}^{2+}$ , PABA, and GPP (**1a**), formation of **2a** was observed. In contrast, formation of **2a** was not observed when solubilized membrane fraction of *S. lividans* harboring empty pHKO4 was used as a control.



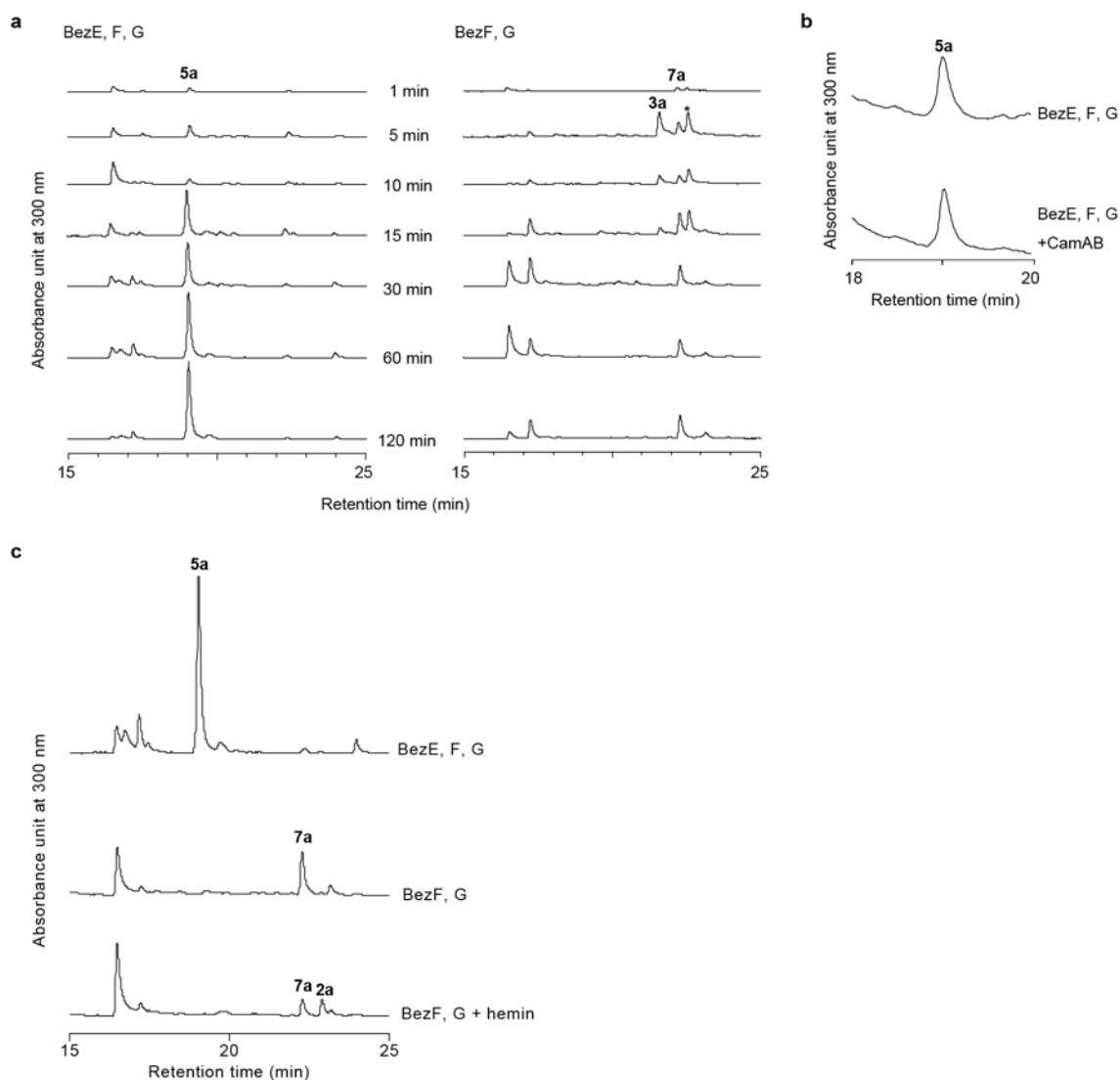
**Supplementary Figure 10. Feeding of PHABA to the  $\Delta bezJ$  strain.** In the presence of PHABA, production of cyclized benzastatins (shown in red) was observed in  $\Delta bezJ$  strain.



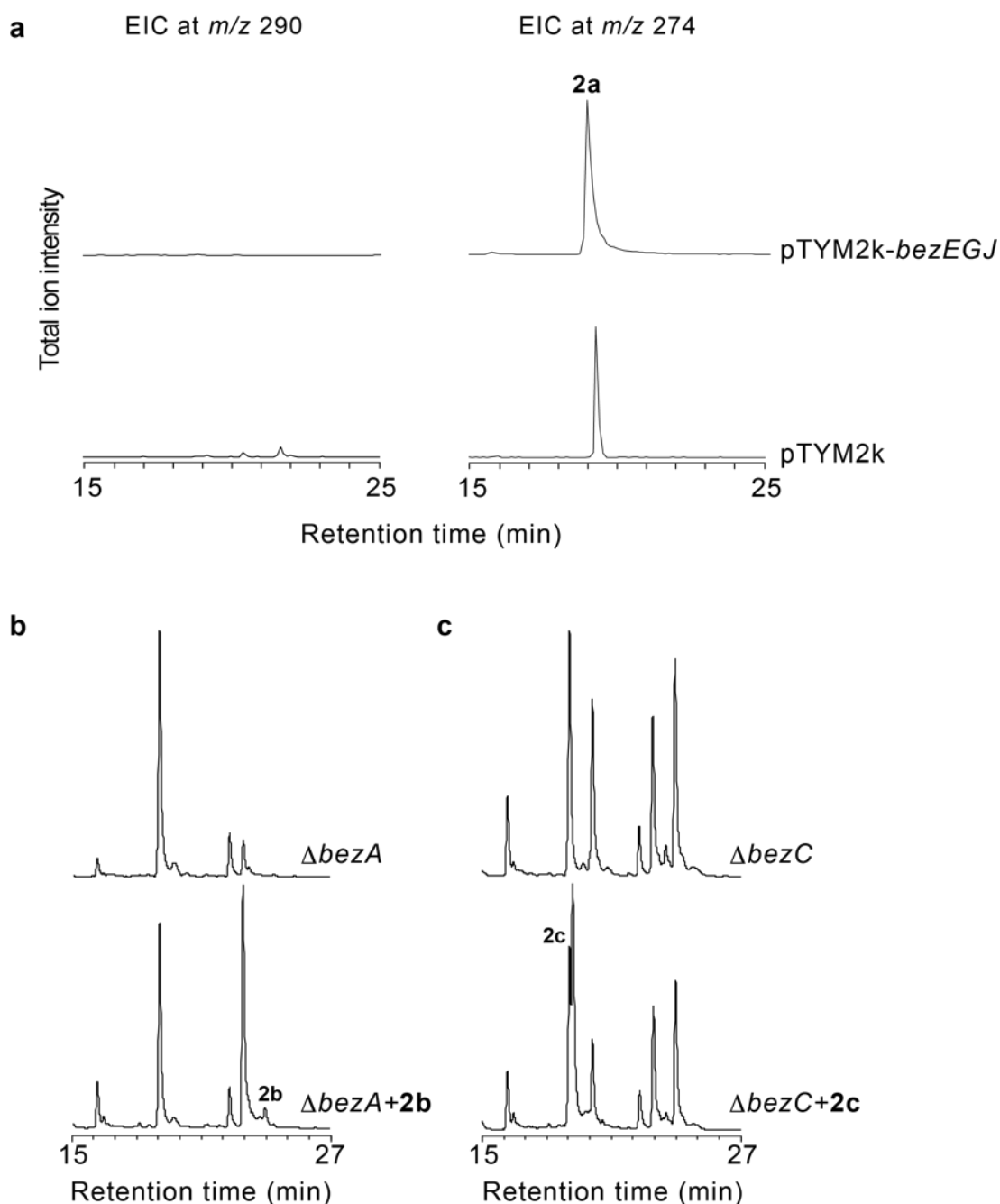
**Supplementary Figure 11. *In vitro* analysis of BezG.** (a) Formation of PAcABA was observed when BezG was incubated with PHABA and acetyl-CoA. (b) Tandem mass spectra of PAcABA and PHABA. (c) Acetylation reaction was not observed using PABA as a substrate.



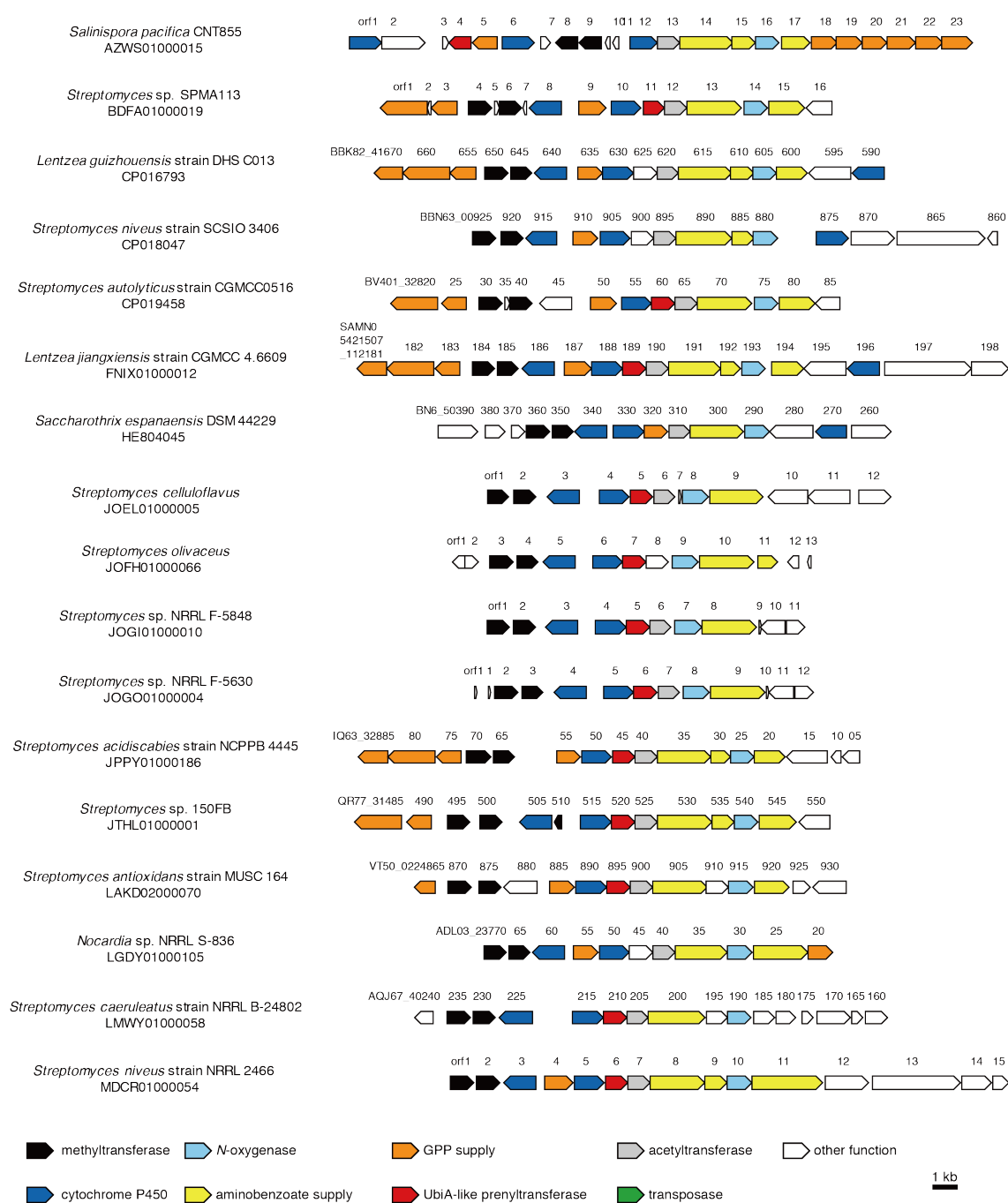
**Supplementary Figure 12. Spectroscopic analysis of BezE.** (a) UV-visible spectra of recombinant BezE. Solid line, BezE; dotted line, BezE with sodium hydrosulfite; dashed line, BezE with sodium hydrosulfite and CO. *Inset*, CO differential spectrum of BezE: (BezE with sodium hydrosulfite and CO) minus (BezE with sodium hydrosulfite). (b) and (c) Substrate-binding analysis of BezE. Type II spectra were observed (b). Difference in absorbance between 414 and 434 nm versus substrate concentration is plotted (c). For the analysis, **2a**, **2b**, and **2c** were used as substrate analogs.



**Supplementary Figure 13. *In vitro* analysis of JBIR-67 (**5a**) formation by BezE.** (a) Time course of the BezEFG and BezFG reactions. Compound **3a** was predicted to be geranylated PHABA by its mass spectrum (data not shown). The compound in the peak indicated by \* is unknown. (b) Addition of a redox partner (CamAB) to the BezEFG reaction. No effect on the rate of **5a** formation was observed. (c) Examination of whether an iron-containing porphyrin (hemin) plays the role of BezE. (i) BezEFG reaction as a positive control, (ii) BezFG reaction as a negative control, (iii) BezFG reaction in the presence of hemin. Hemin could not catalyze the formation of **5a**.

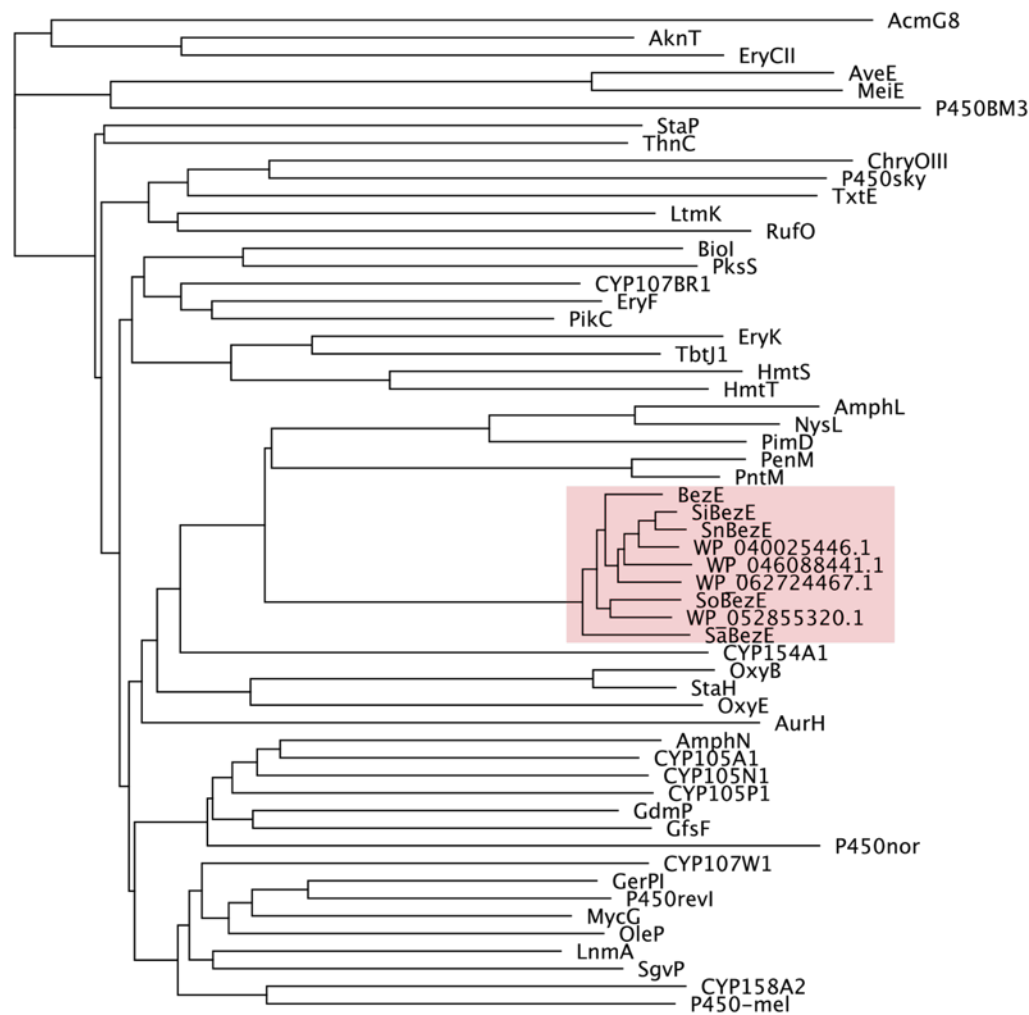


**Supplementary Figure 14. Feeding of 7-hydroxyl benzastatin J (**2a**), 7-hydroxyl benzastatin B (**2b**), and 7-hydroxyl *O*-demethylbenzastatin A (**2c**) to *S. lividans* strains harboring pTYM2k-*bezEGJ*, pTYM-*bezA-JΔbezA*, and pTYM-*bezA-JΔbezC*, respectively. (a) Extracted ion chromatograms of the ethylacetate extract of *S. lividans* strains harboring pTYM2k-*bezEGJ* and pTYM2k (empty vector) cultivated in the presence of exogenously added **2a**. **2a** can be detected on the extracted ion chromatograms at  $m/z$  290 and  $m/z$  274, respectively. **2a** was not converted to **5a**. (b and c) UV chromatograms of metabolites from *S. lividans* strains harboring pTYM-*bezA-JΔbezA* (b) and pTYM-*bezA-JΔbezC* (c). Feeding of **2b** and **2c** to the  $\Delta bezA$  and  $\Delta bezC$  mutants (lower chromatographs), respectively, did not lead to the formation of cyclized benzastatins.**

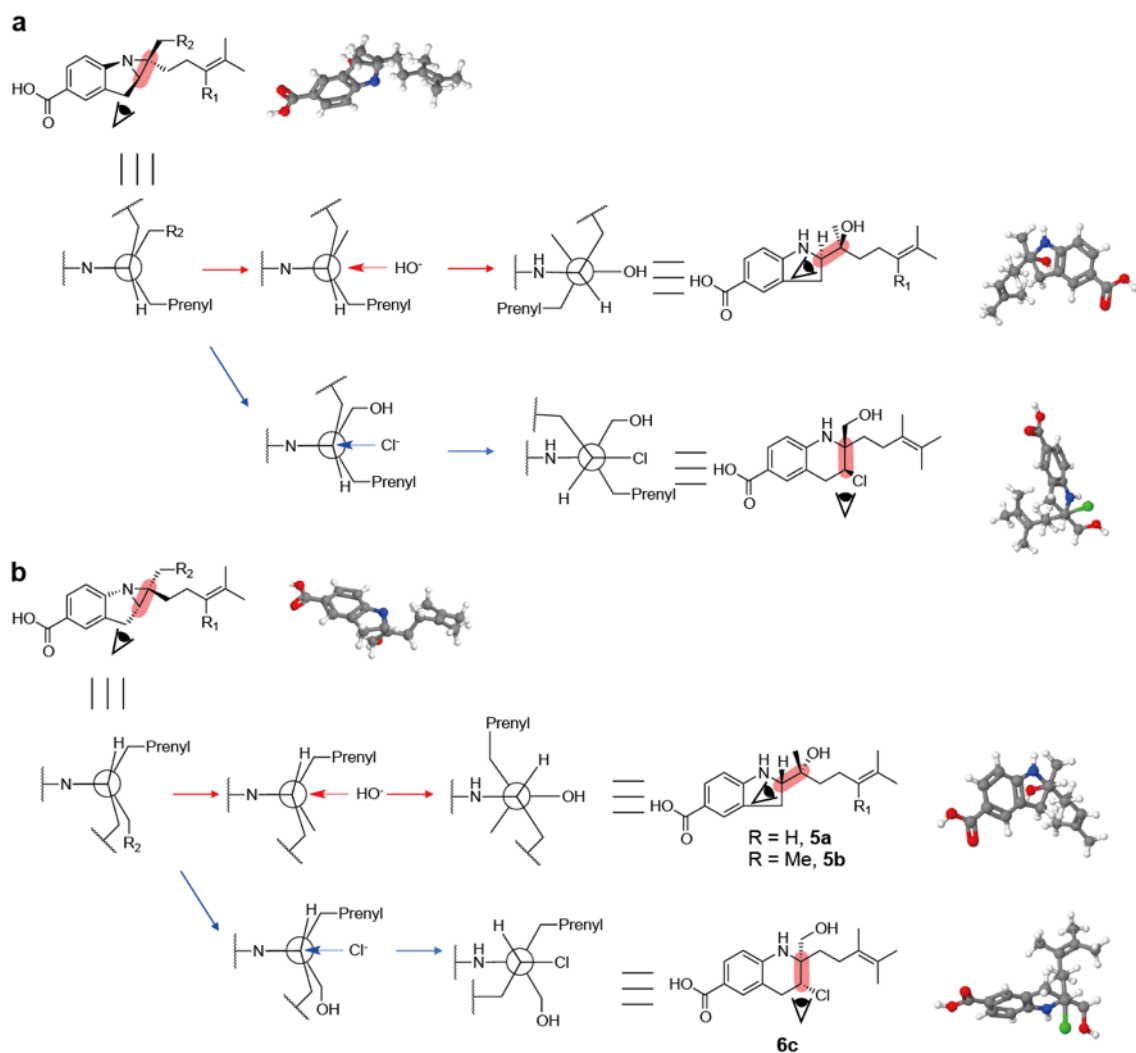


**Supplementary Figure 15. Putative benzastatin biosynthetic gene clusters discovered by genome scanning.**

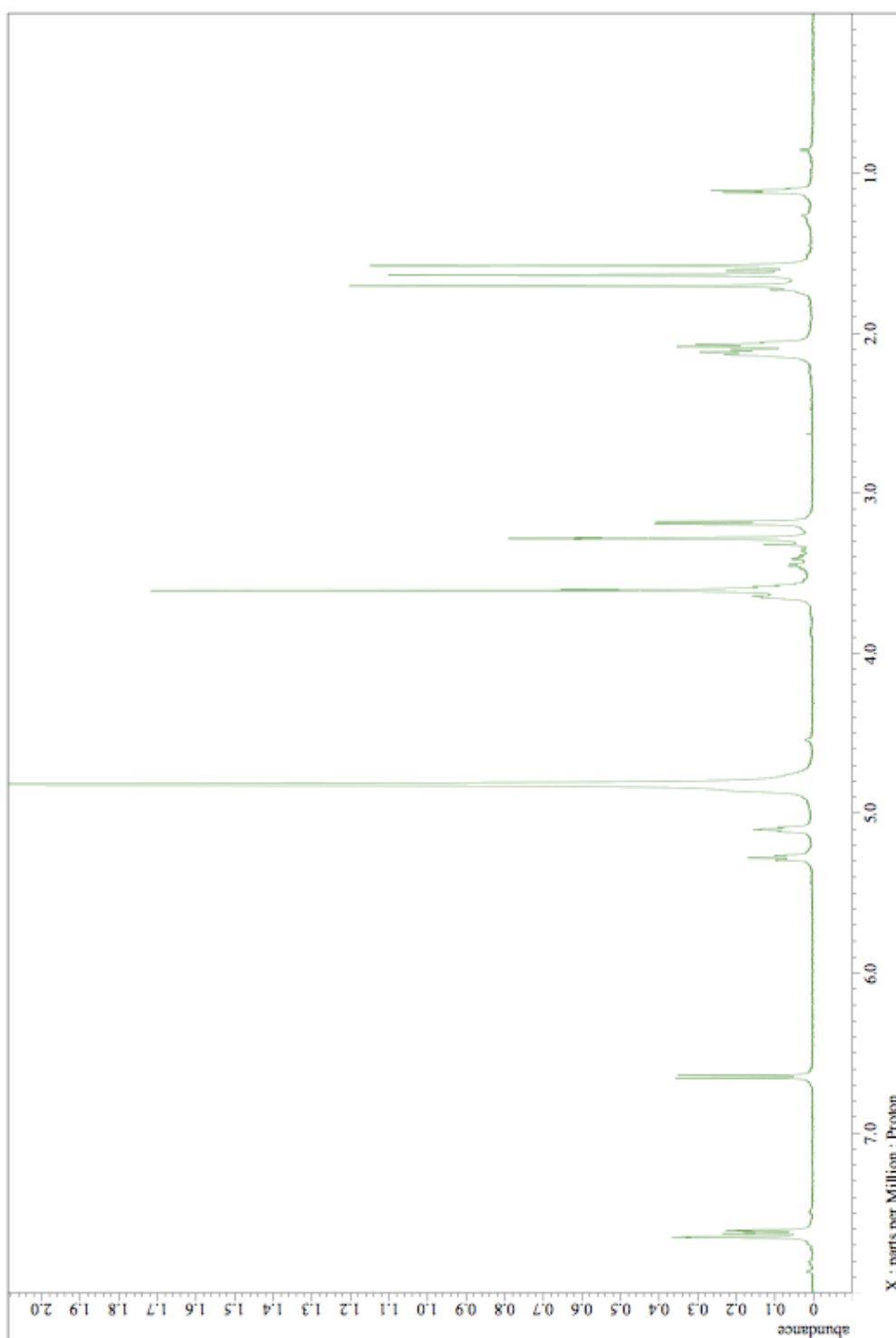


[illegible]

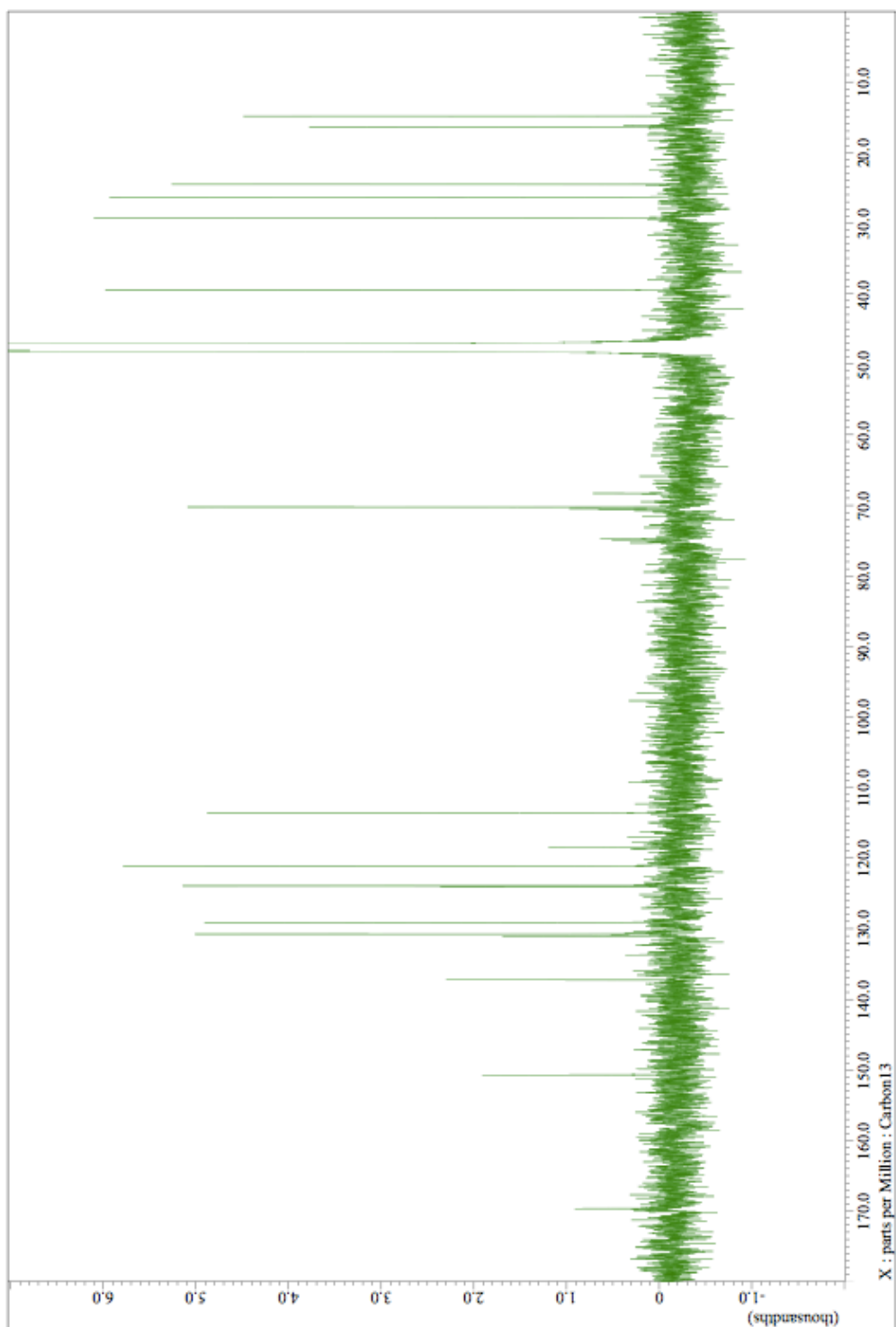
**Supplementary Figure 16. Sequence alignment (a) and phylogenetic analysis (b) of BezE and other P450s.** The heme-binding motif and a clade containing BezE are highlighted in (a) and (b), respectively. The sequence alignment was constructed with the Geneious alignment. The phylogenetic tree was constructed with the Geneious tree builder using the neighbor-joining method. BLOSUM62 was used to obtain the distance from the global alignment of all sequence pairs. The amino acid sequences used for the construction of the phylogenetic tree are as follows. AcnG8, CCO61879, *Streptomyces iakyrus*; AknT, AAF73456, *Streptomyces galilaeus*; AmphL, AAK73504, *Streptomyces nodosus*; AmphN, AAK73509, *Streptomyces nodosus*; AurH, AJ575648, *Streptomyces thioluteus*; AveE, BAC68651, *Streptomyces avermitilis* MA-4680 = NBRC 14893; BezE, LC177364, *Streptomyces* sp. RI18; BioI, POD88223, *Bacillus subtilis*; ChryOIII, CBH32091, *Streptomyces albaduncus*; CYP105A1, 2ZBX, *Streptomyces griseolus*; CYP105N1, 4FXB, *Streptomyces coelicolor* A3(2); CYP105P1, 3ABA, *S. avermitilis*; CYP107BR1, 5GNM, *Pseudonocardia autotrophica*; CYP107W1, 4WPZ, *S. avermitilis*; CYP154A1, 1ODO, *S. coelicolor* A3(2); CYP158A2, 1SE6, *S. coelicolor* A3(2); EryCII, AAB84066, *Saccharopolyspora erythraea* NRRL 2338; EryF, AAA26496, *S. erythraea* NRRL 2338; EryK, 2JJN, *S. erythraea* NRRL 2338; GdmP, ABI93790, *Streptomyces hygroscopicus*; GerPI, ABB52529, *Streptomyces* sp. KCTC 0041BP; GfsF, BAJ16472, *Streptomyces graminofaciens*; HmtS, CBZ42153, *Streptomyces himastatinicus* ATCC 53653; HmtT, CBZ42154, *S. himastatinicus* ATCC 53653; LnmA, AAN85514, *Streptomyces atroolivaceus*; LtmK, ACY01404, *Streptomyces amphibiosporus*; MeiE, AAM97314, *Streptomyces nanchangensis*; MycG, Q59523, *Micromonospora griseorubida*; NysL, AAF71769, *Streptomyces noursei* ATCC 11455; OleP, 4XE3, *Streptomyces antibioticus*; OxyB, CAE53361, *Actinoplanes teichomyceticus*; OxyE, 3O1A, *A. teichomyceticus*; P450BM3, ADA57059, *Bacillus megaterium*; P450-mel, BAG23448, *Streptomyces griseus* subsp. *griseus* NBRC 13350; P450nor, P23295, *Fusarium oxysporum*; P450revI, BAK64643, *Streptomyces* sp. SN-593; P450sky, AEA30275, *Streptomyces* sp. Acta 2897; PenM, ADO85587, *Streptomyces exfoliatus*; PikC, AAC68886, *Streptomyces venezuelae*; PimD, CAC20932, *Streptomyces natalensis*; PksS, KIX82980, *B. subtilis*; PntM, ADO85571, *Streptomyces arenae*; RufO, BBA20962, *Streptomyces atratus*; SaBezE, WP\_029184464, *Streptomyces acidiscabies*; SgvP, AGN74891, *Streptomyces griseoviridis*; SiBezE, WP\_009339637, *Streptomyces ipomoeae*; SnBezE, WP\_031228687, *Streptomyces niveus*; SoBezE, WP\_031048156, *Streptomyces olivaceus*; StaH, AAM80533, *Streptomyces toyocaensis*; StaP, ABI94389, *Streptomyces longisporoflavus*; TbtJ1, 5VWS, *Thermobispora bispora* DSM 43833; ThnC, AMR44303, *Streptomyces* sp. FXJ1.172; TxtE, WP\_037694808, *Streptomyces scabiei*; WP\_040025446.1, WP\_040025446, *Streptomyces* sp. 150FB; WP\_046088441.1, WP\_046088441, *Streptomyces antioxidans*; WP\_052855320.1, WP\_052855320, *Streptomyces celluloflavus*; WP\_062724467.1, WP\_062724467, *Streptomyces caeruleatus*.



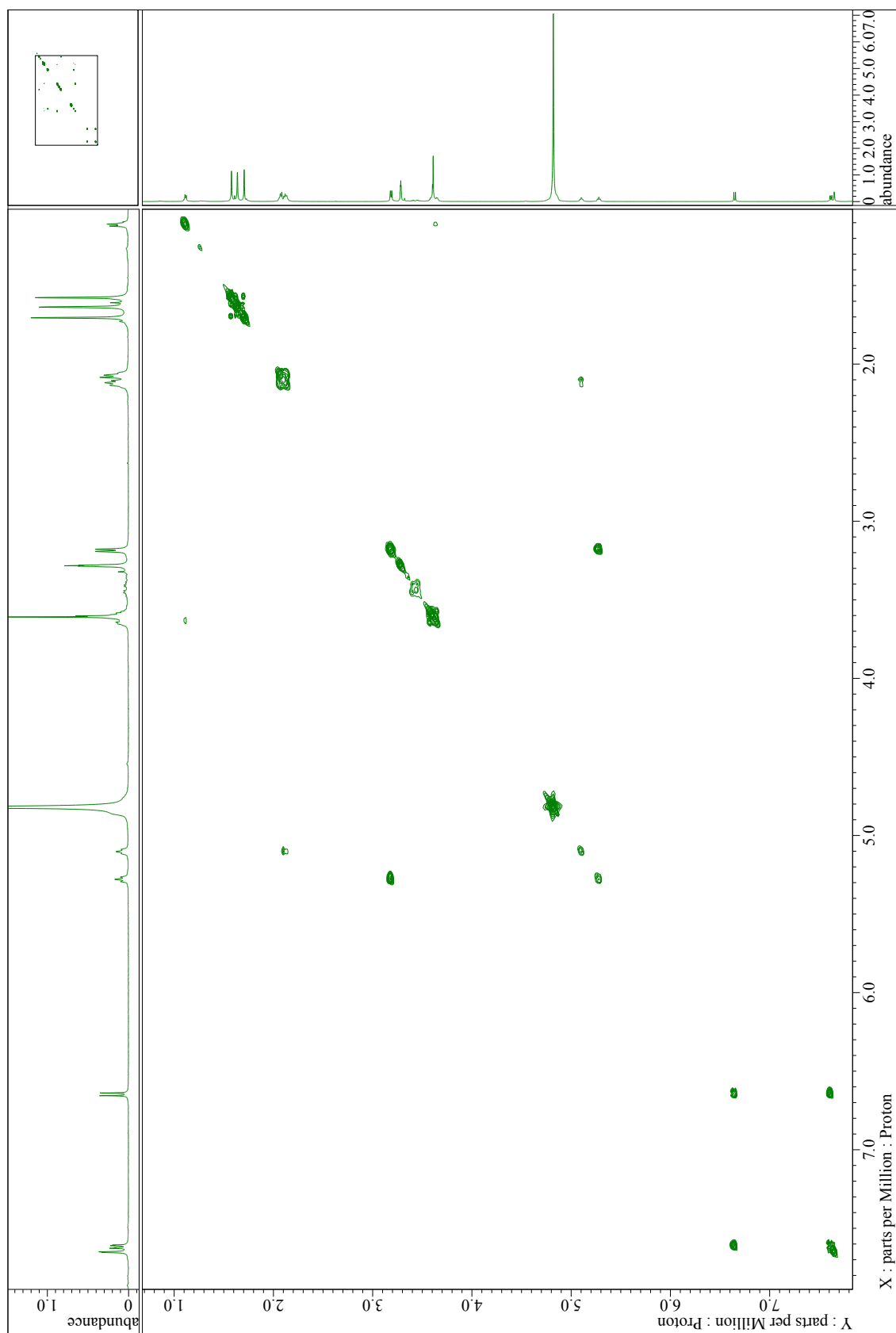
**Supplementary Figure 17. Schematic representation of aziridine ring opening.** Two isomers, (9*R*,10*R*) in (a) and (9*S*,10*S*) in (b) are possible for the putative biosynthetic intermediate with an aziridine ring. Compounds **5a**, **5b**, and **6c** with the correct absolute stereochemistry are produced only from the aziridine intermediate with (9*S*,10*S*) stereochemistry by S<sub>N</sub>2 reaction as depicted in (b).



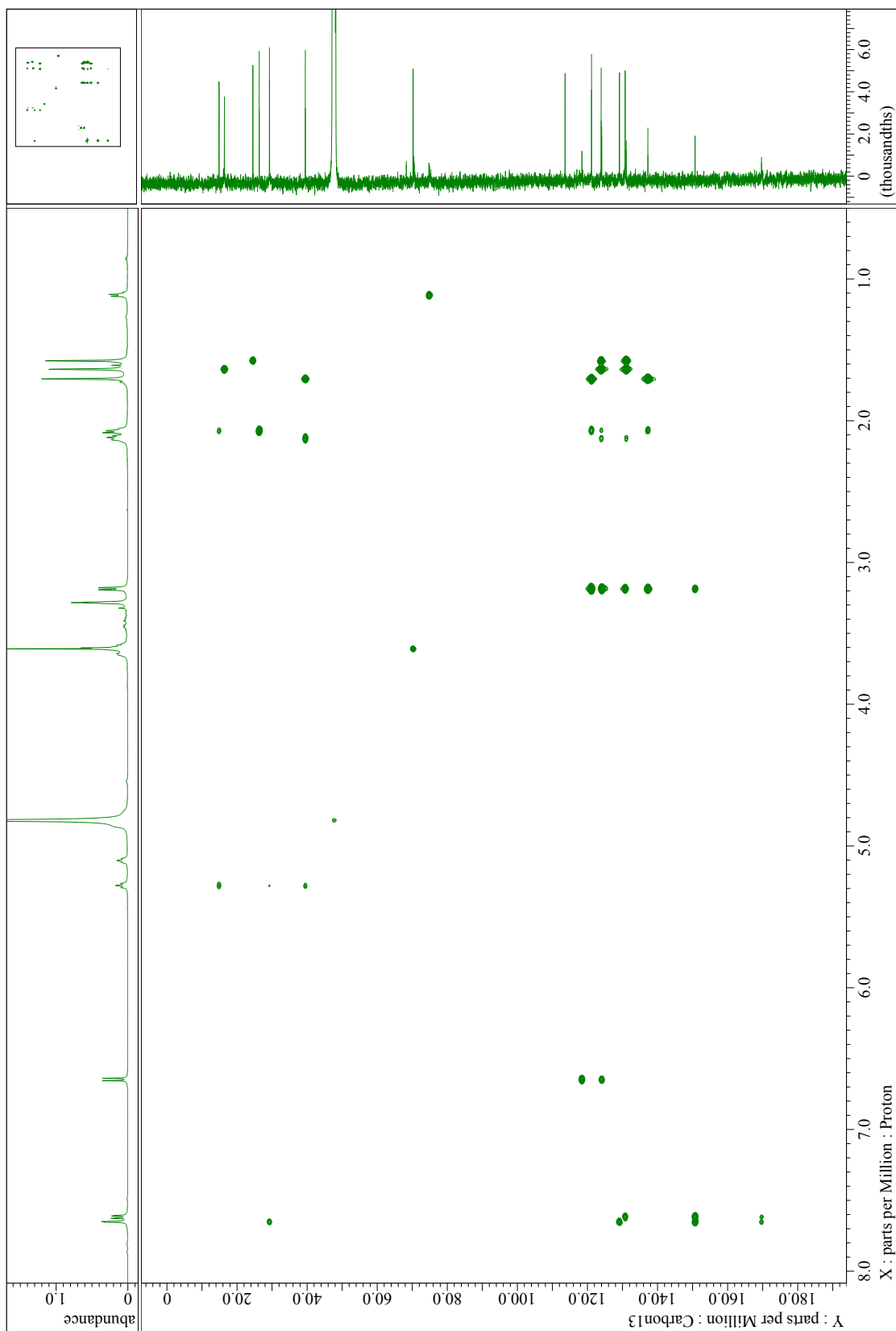
Supplementary Figure 18.  $^1\text{H}$  NMR ( $\text{CD}_3\text{OD}$ ) spectrum for **2a**.



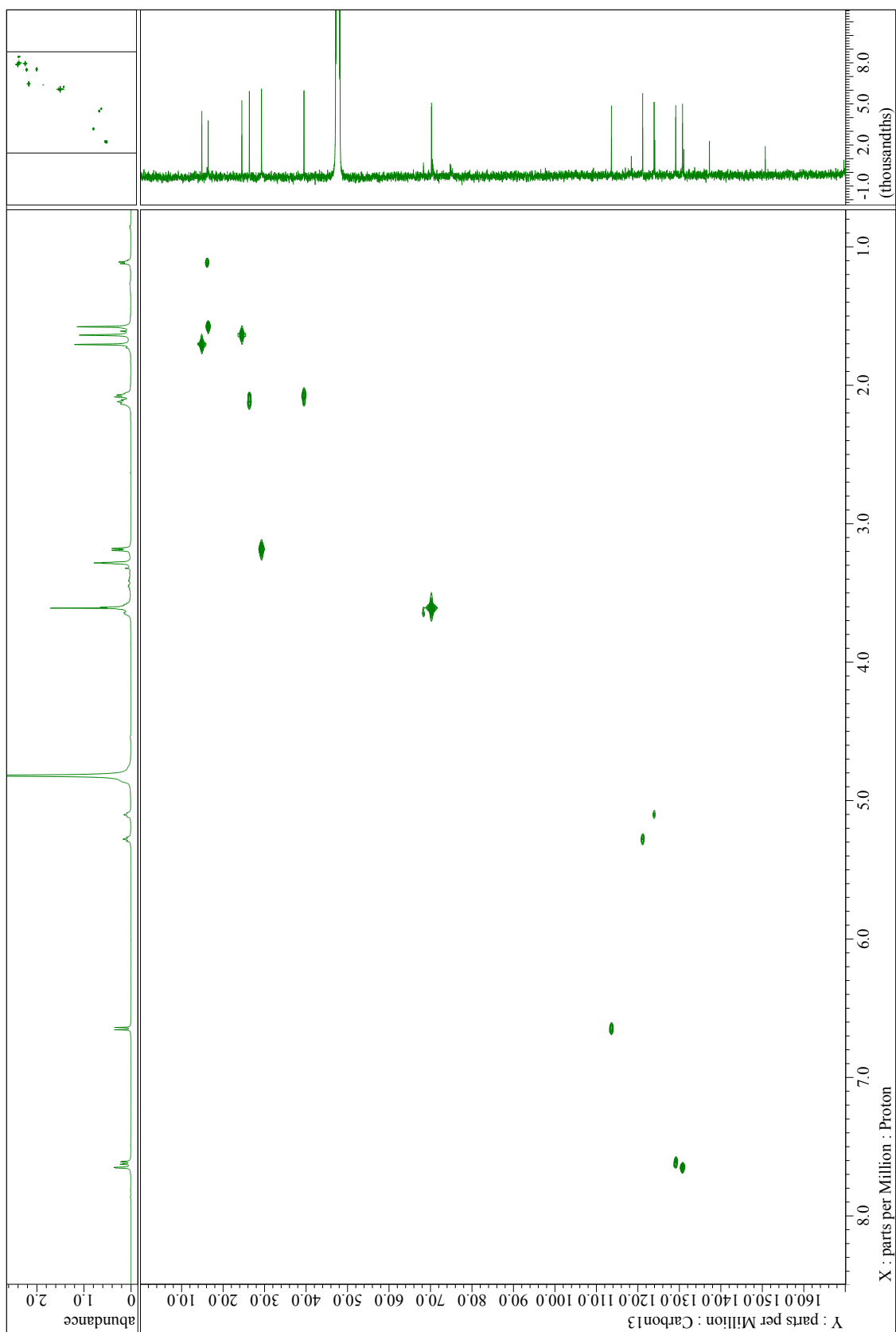
Supplementary Figure 19.  $^{13}\text{C}$  NMR ( $\text{CD}_3\text{OD}$ ) spectrum for **2a**.



Supplementary Figure 20. COSY spectrum for **2a**.

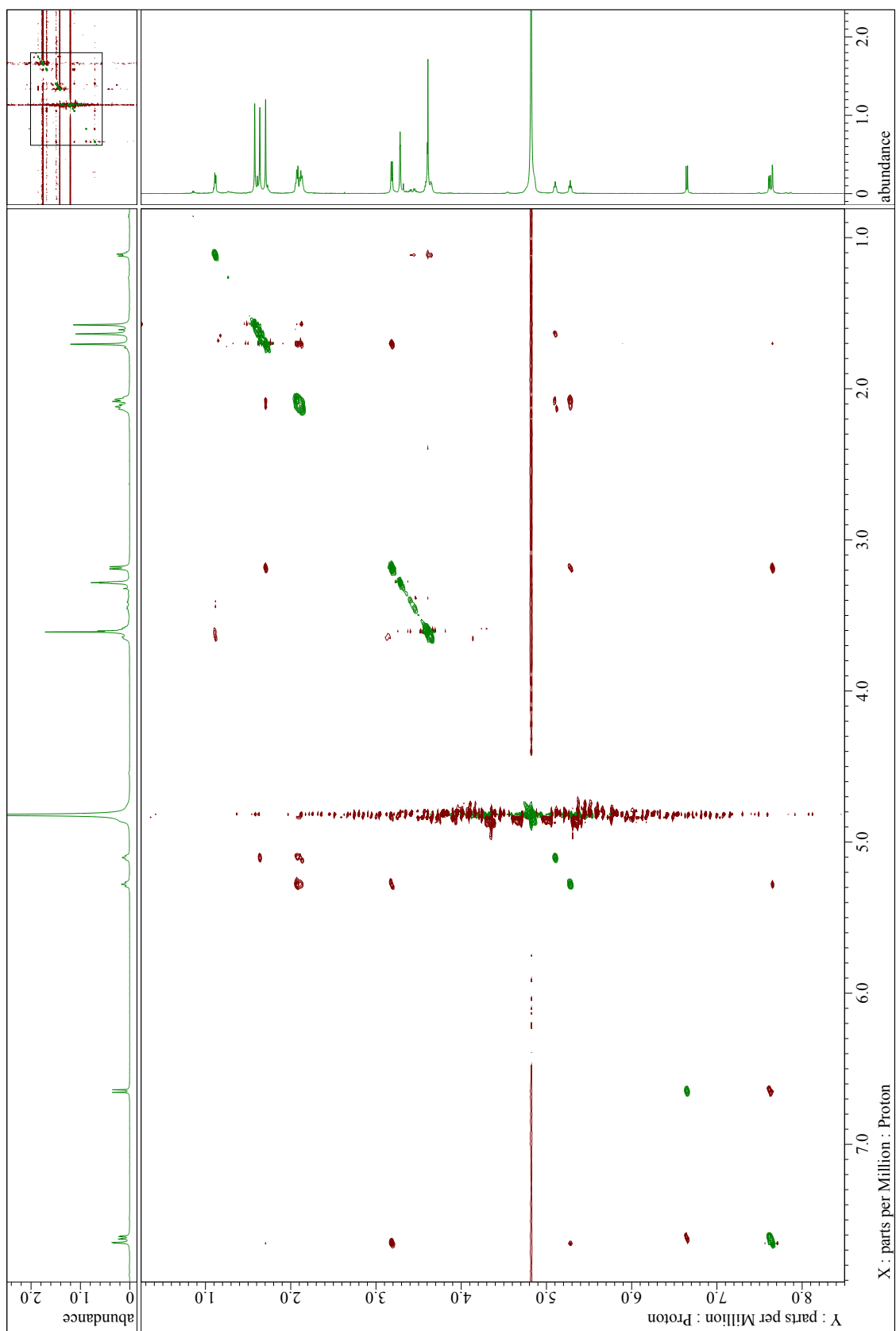


Supplementary Figure 21. HMBC spectrum for **2a**.

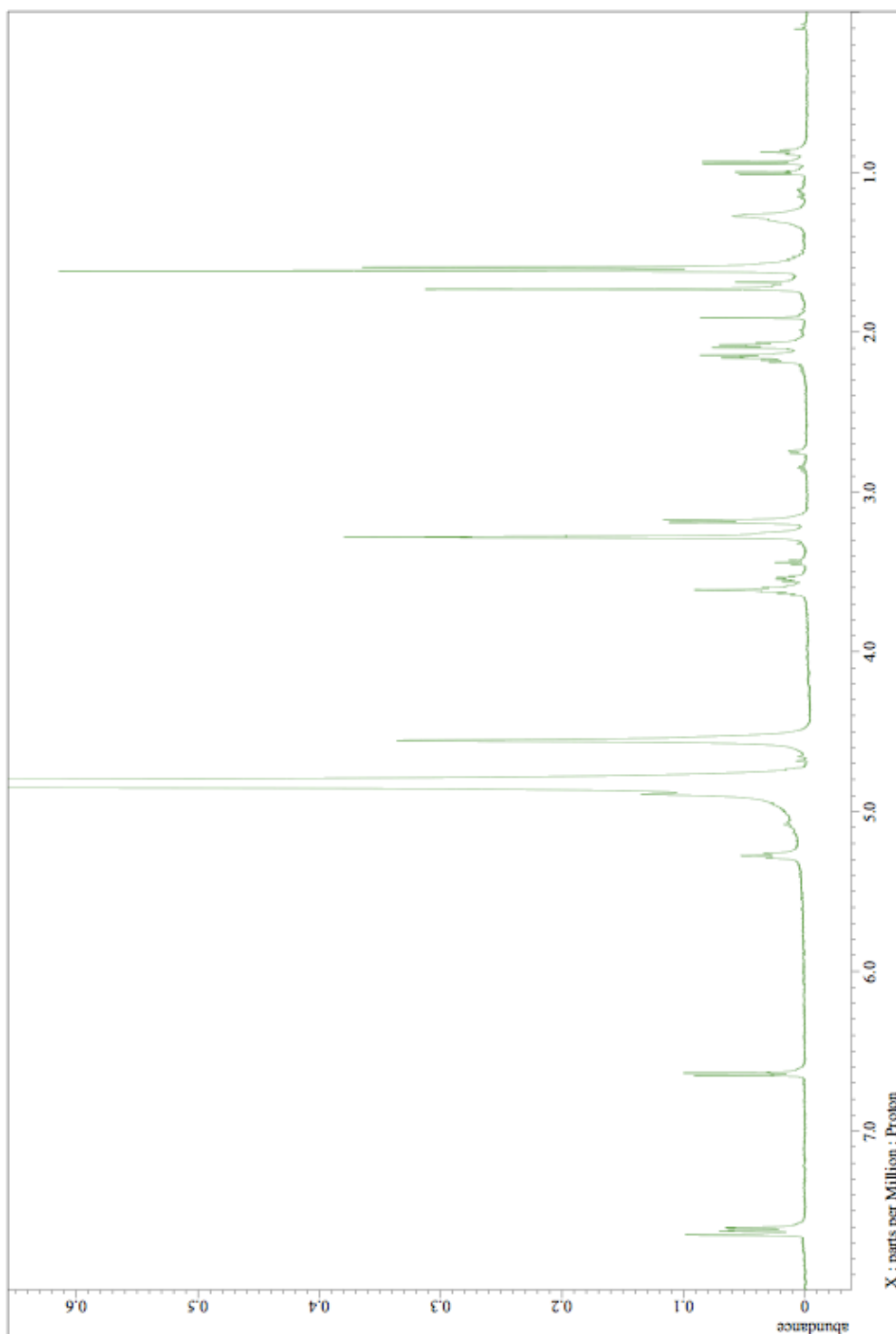


Supplementary Figure 22. HMQC spectrum for **2a**.

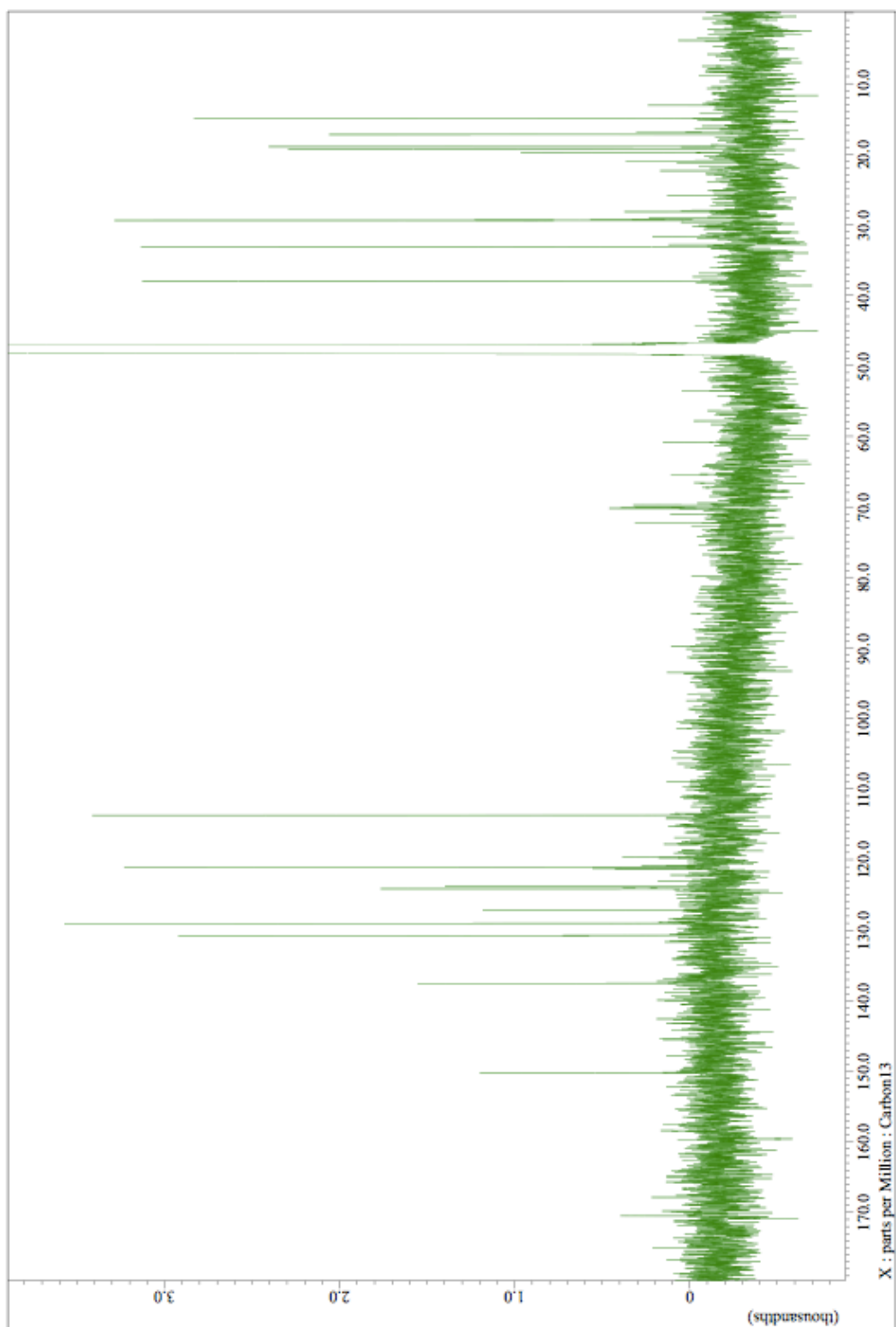




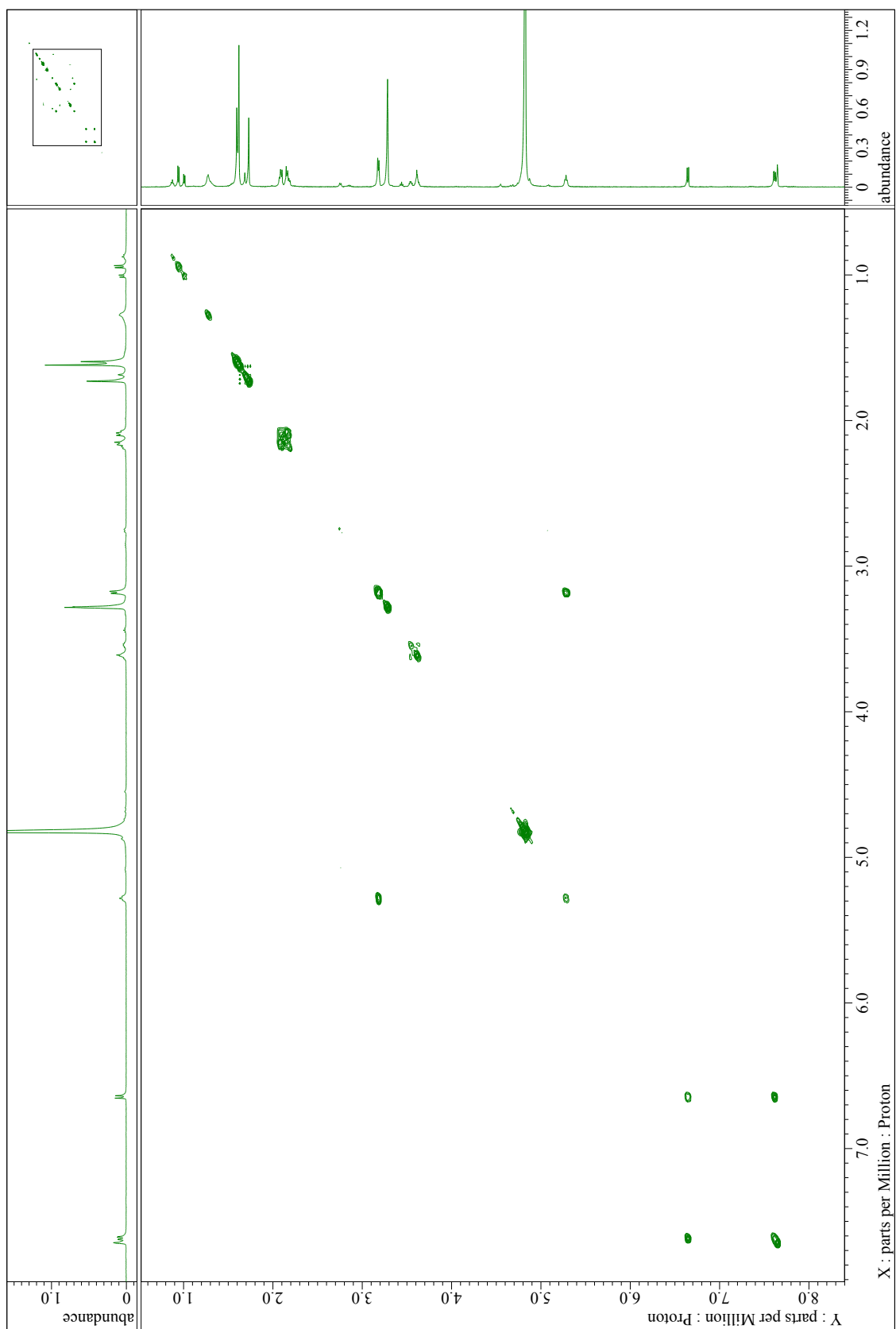
Supplementary Figure 23. NOESY spectrum for **2a**.

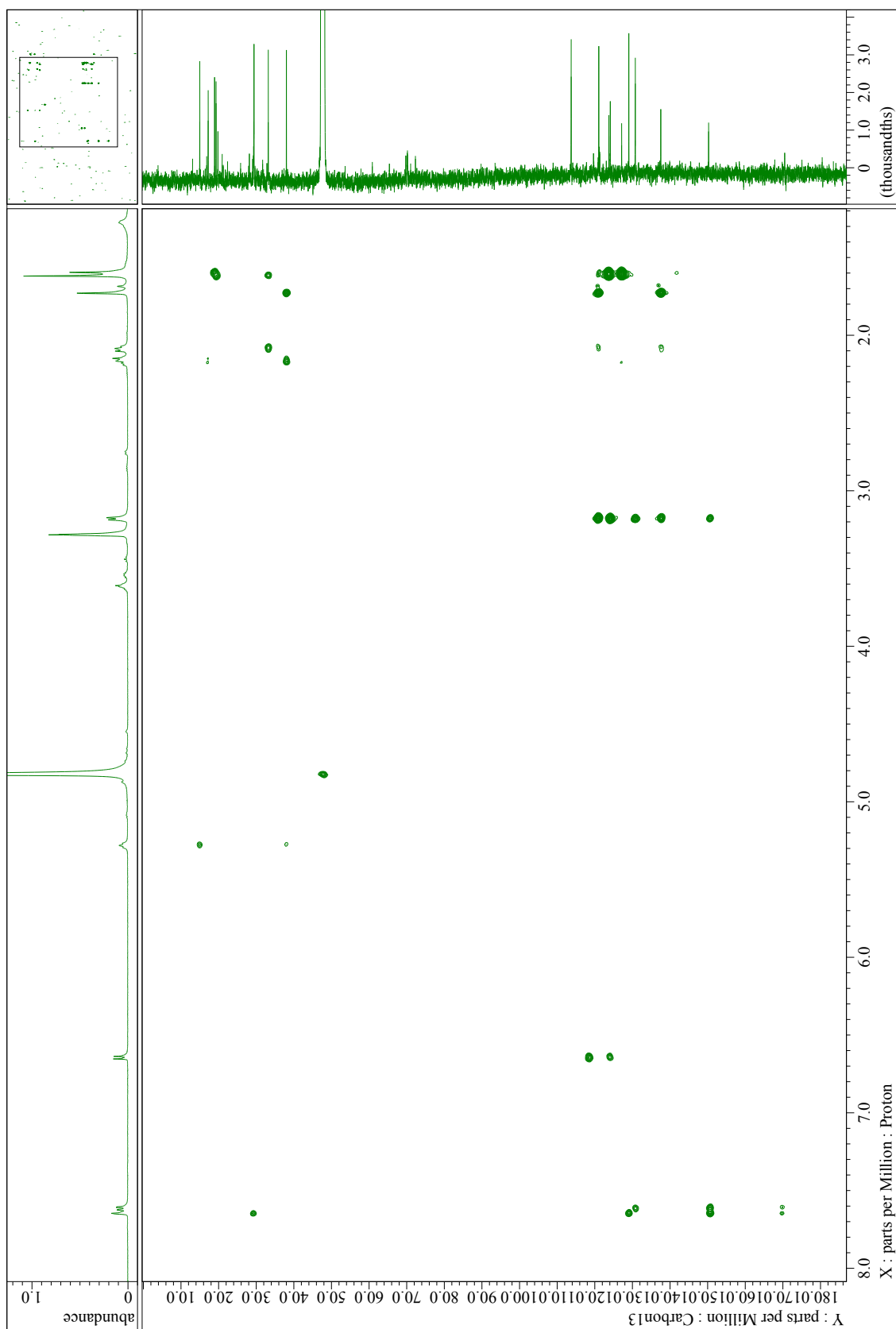


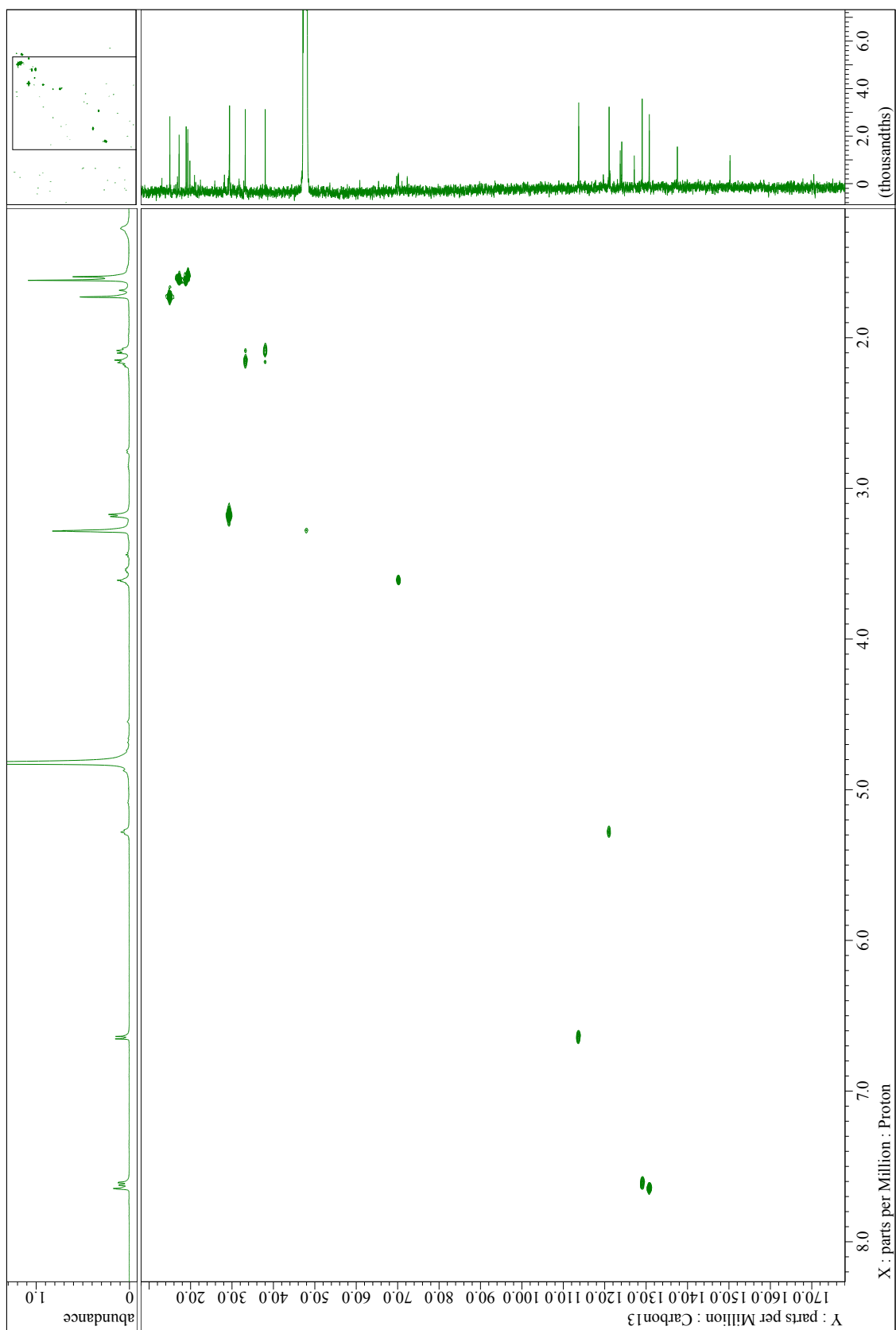
Supplementary Figure 24.  $^1\text{H}$  NMR ( $\text{CD}_3\text{OD}$ ) spectrum for **2b**.



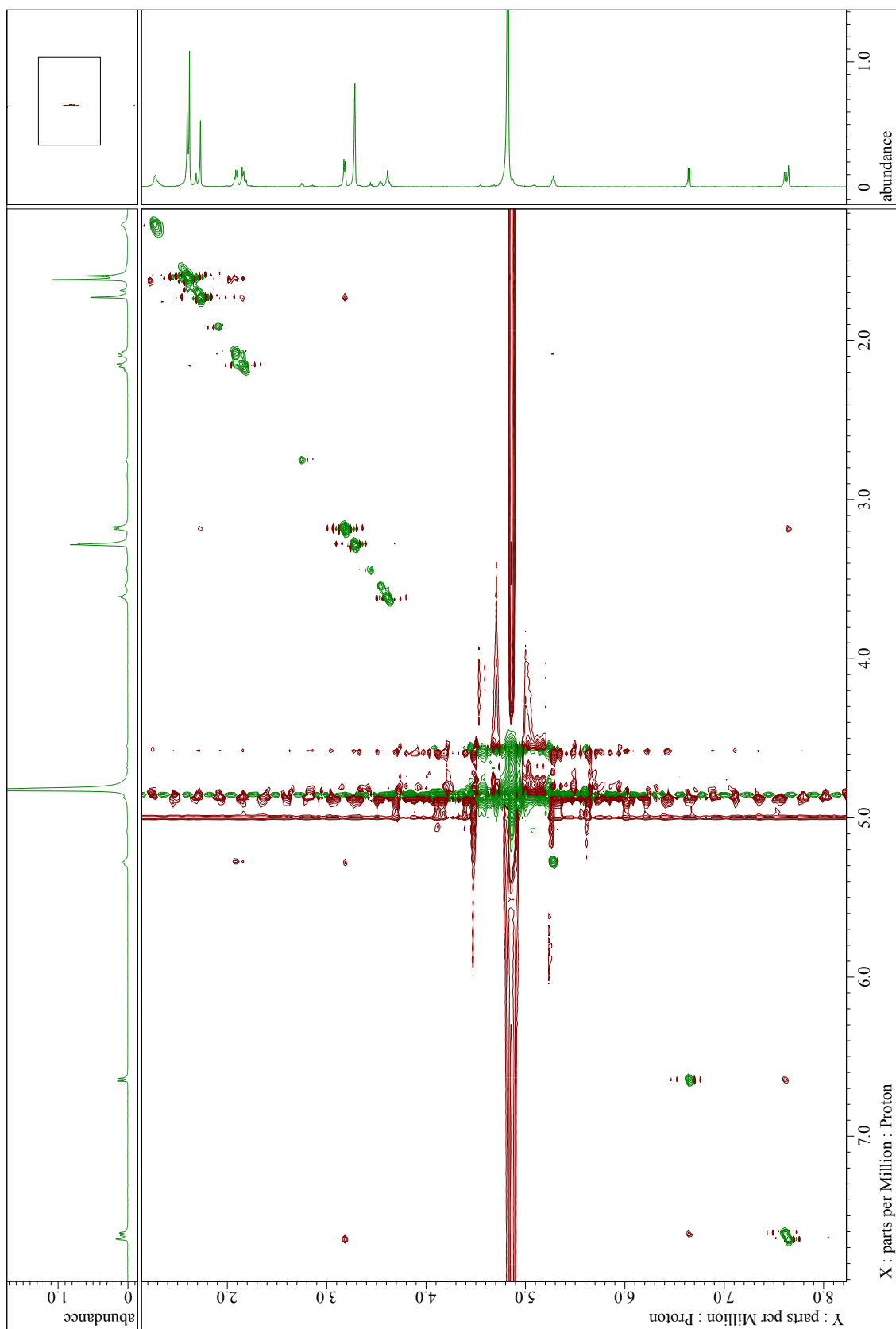
Supplementary Figure 25.  $^{13}\text{C}$  NMR ( $\text{CD}_3\text{OD}$ ) spectrum for **2b**.



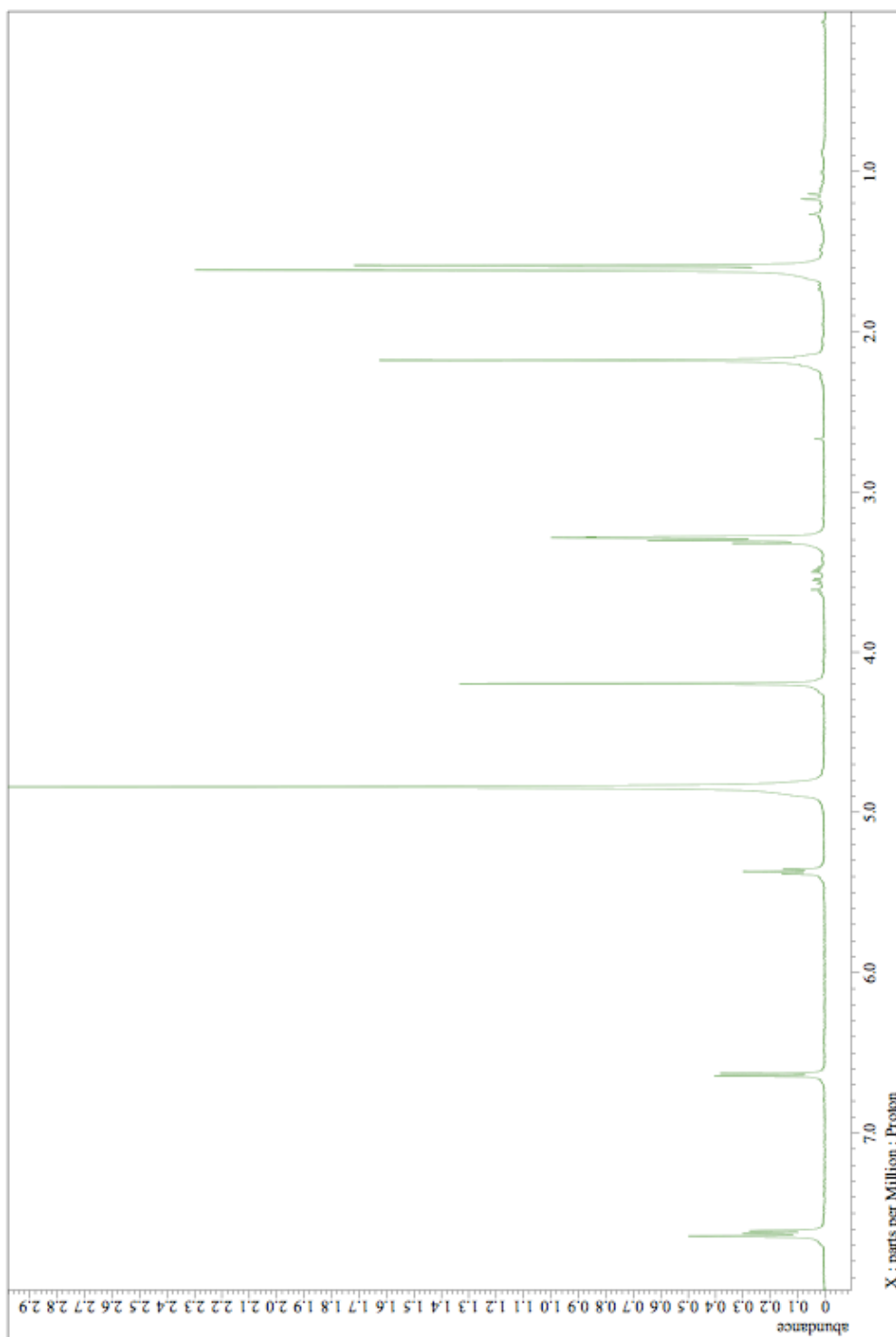




Supplementary Figure 28. HMQC spectrum for **2b**.

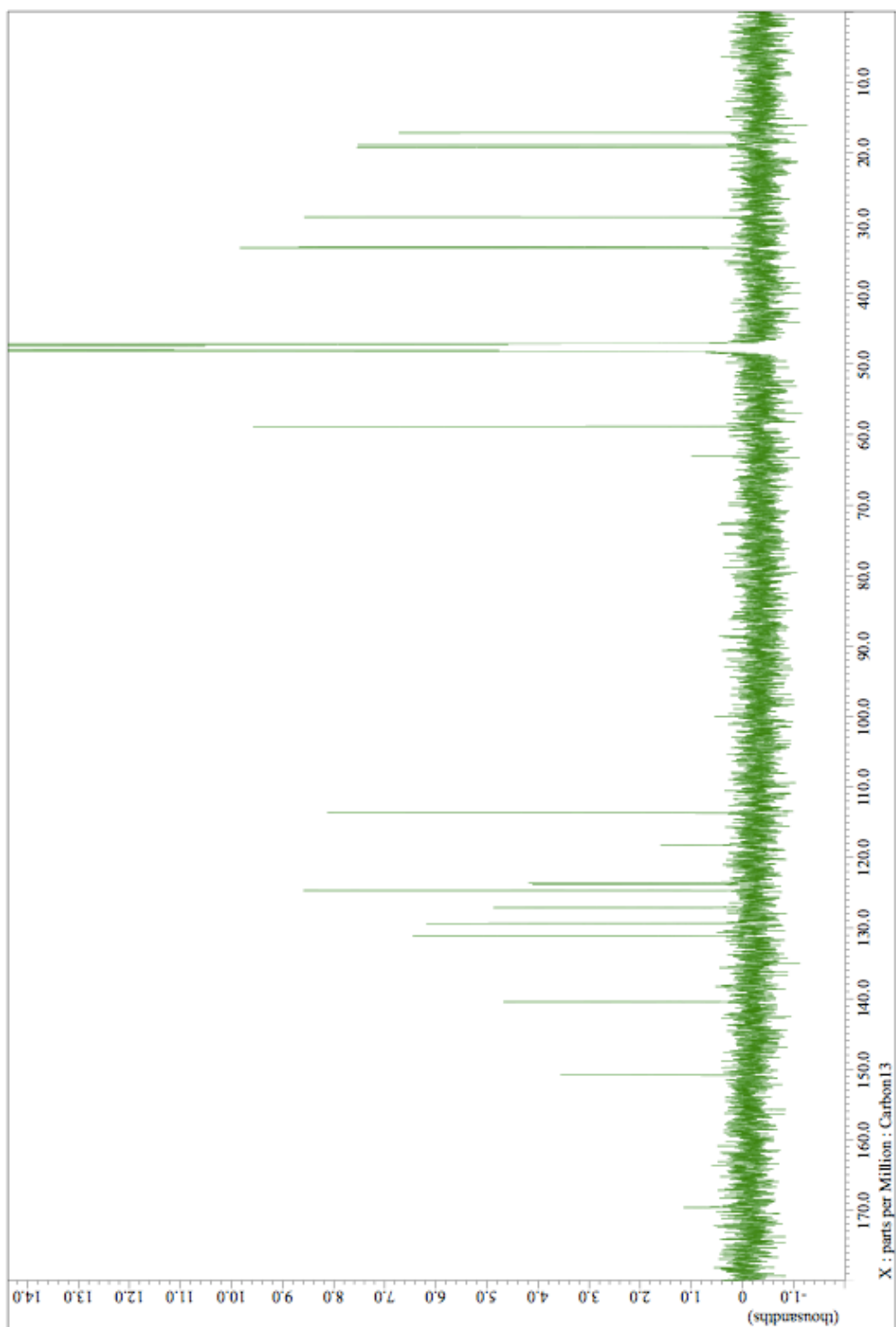


Supplementary Figure 29. NOESY spectrum for **2b**.

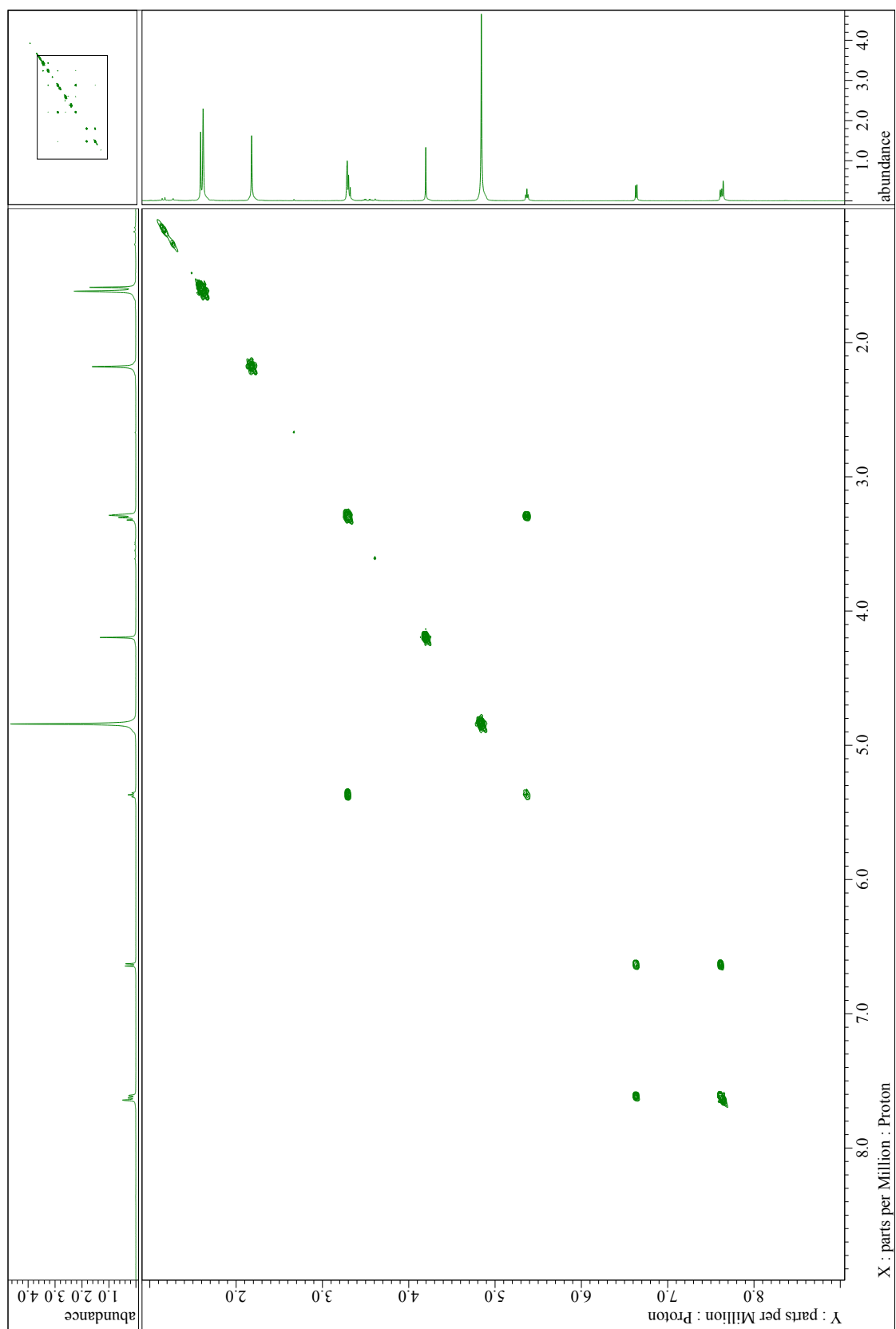


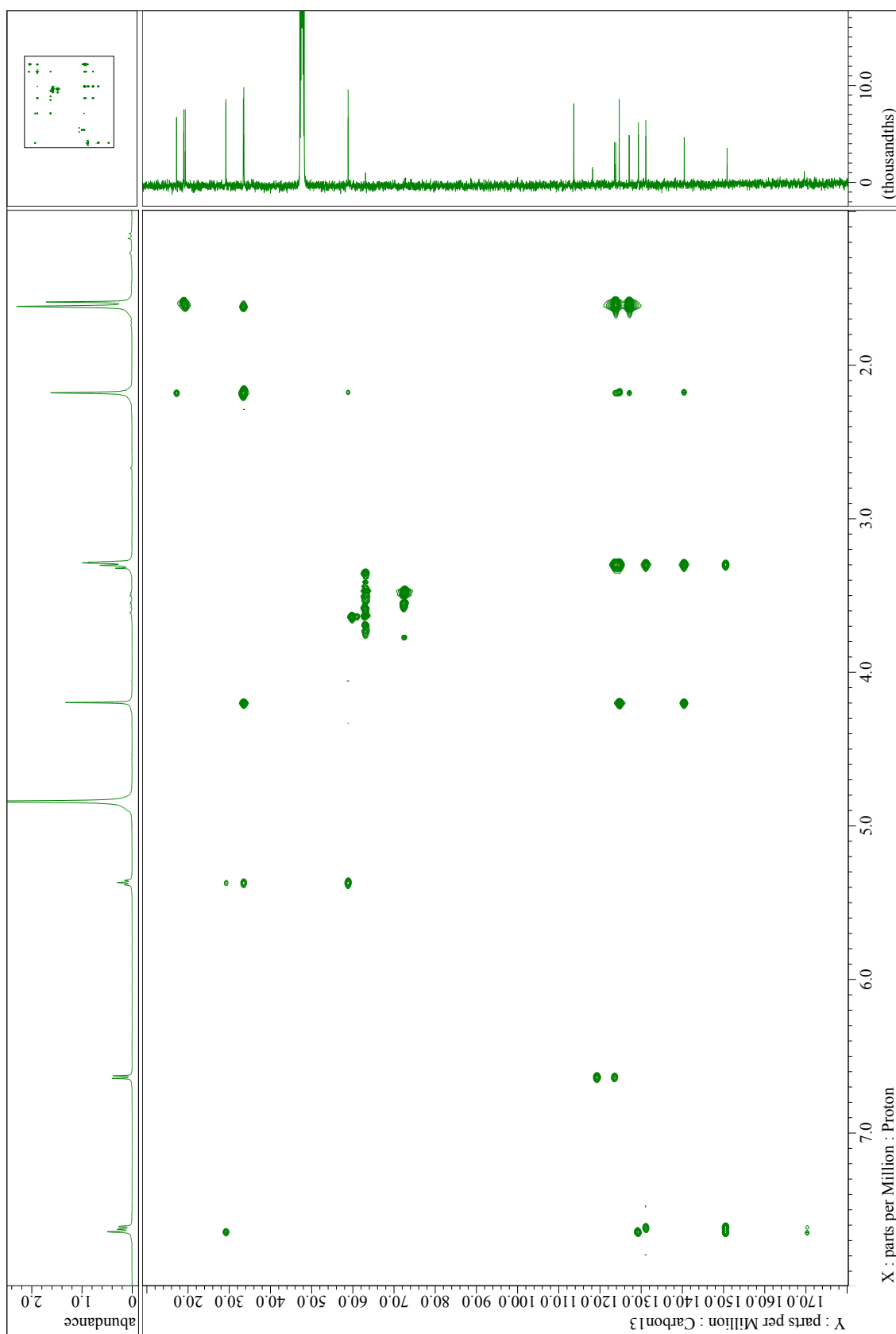
Supplementary Figure 30.  $^1\text{H}$  NMR ( $\text{CD}_3\text{OD}$ ) spectrum for **2c**.



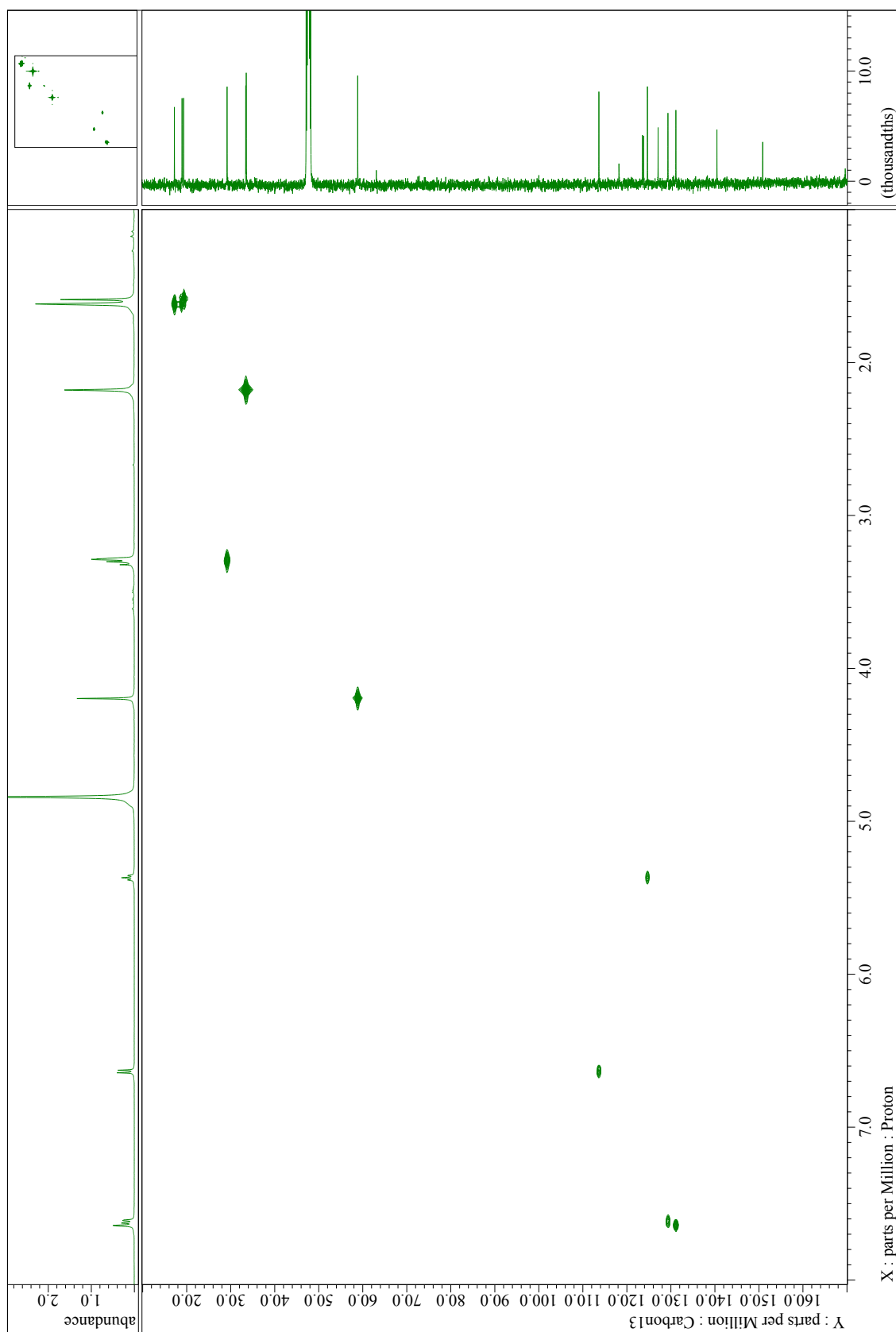


Supplementary Figure 31.  $^{13}\text{C}$  NMR ( $\text{CD}_3\text{OD}$ ) spectrum for **2c**.

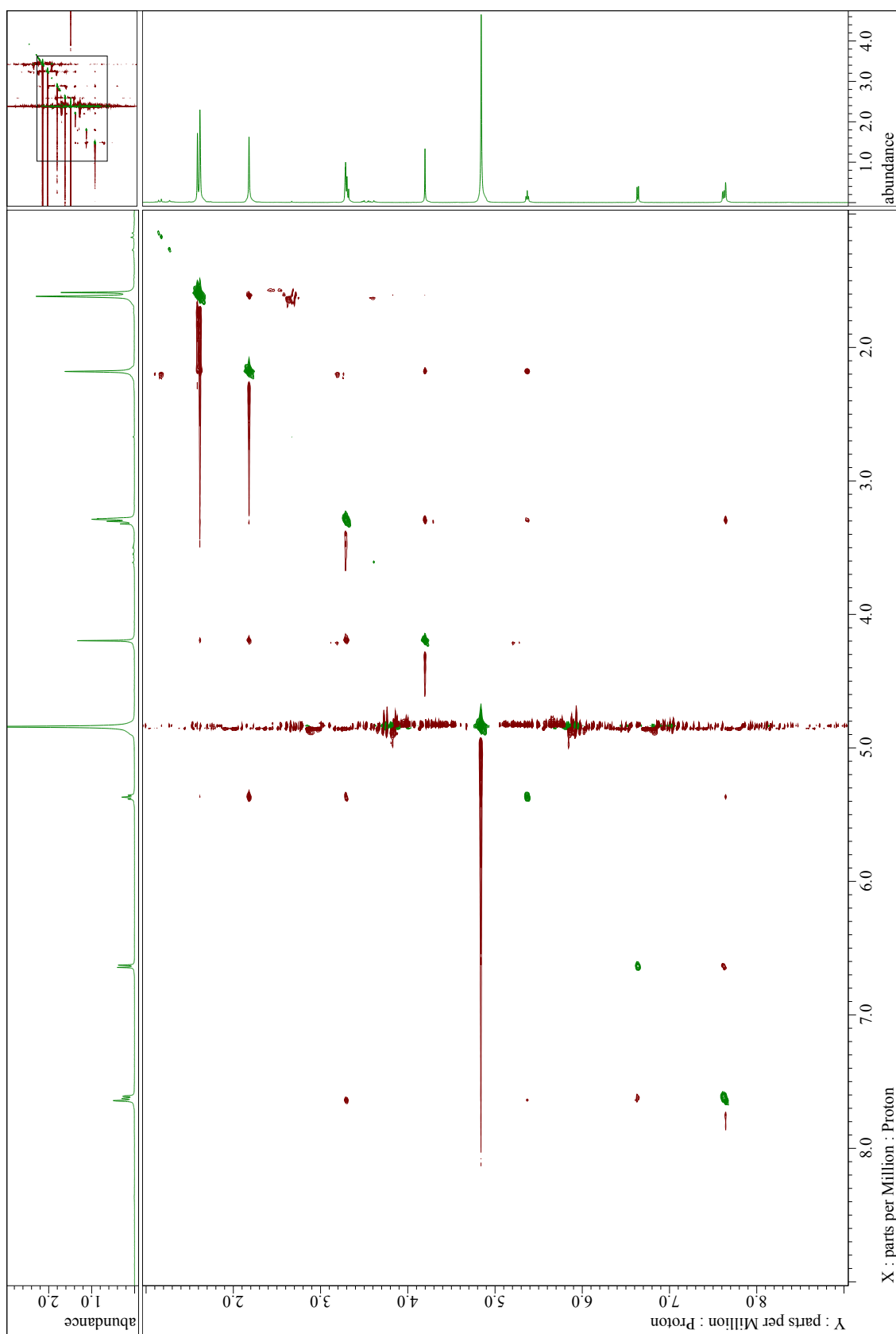


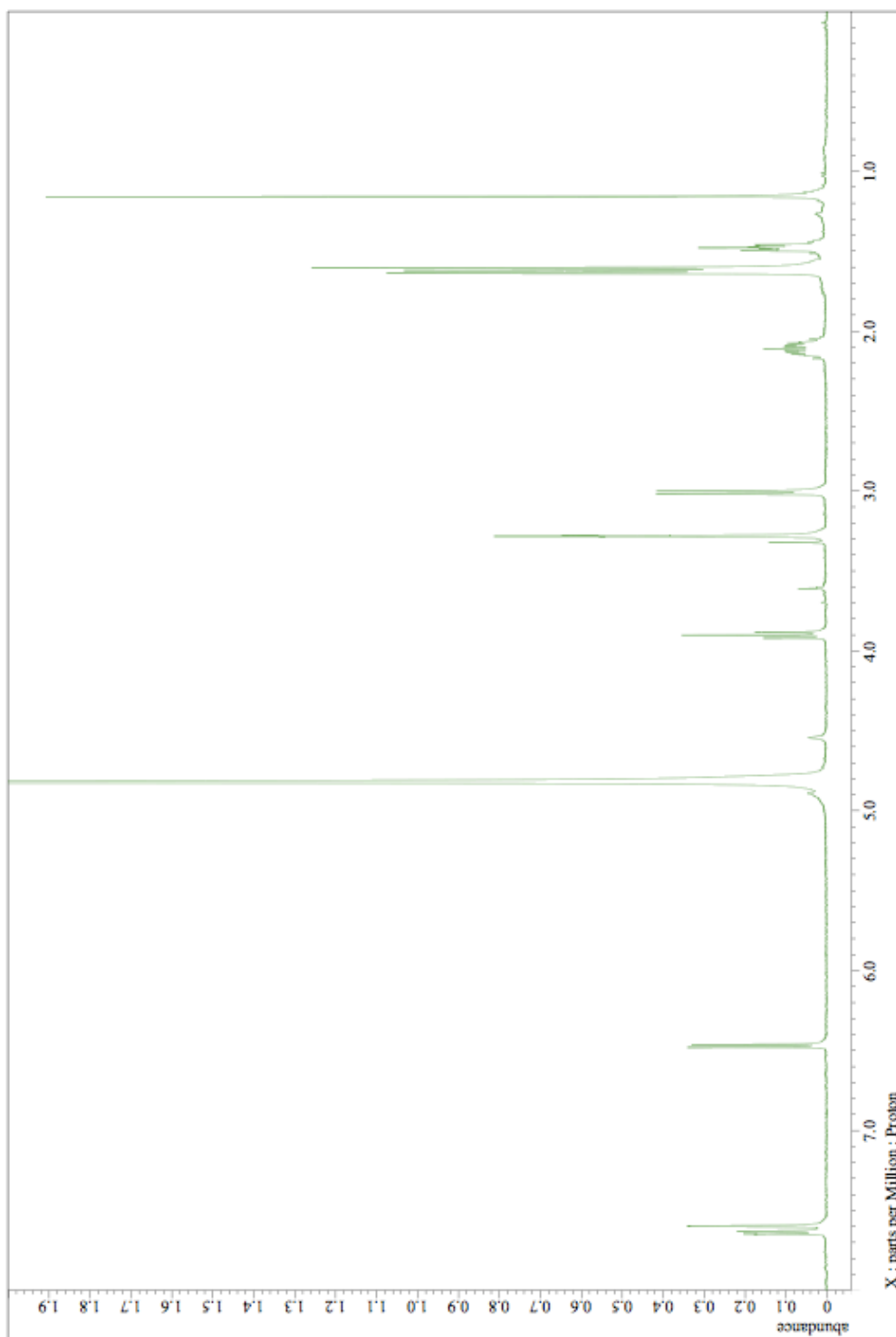


Supplementary Figure 33. HMBC spectrum for **2c**.

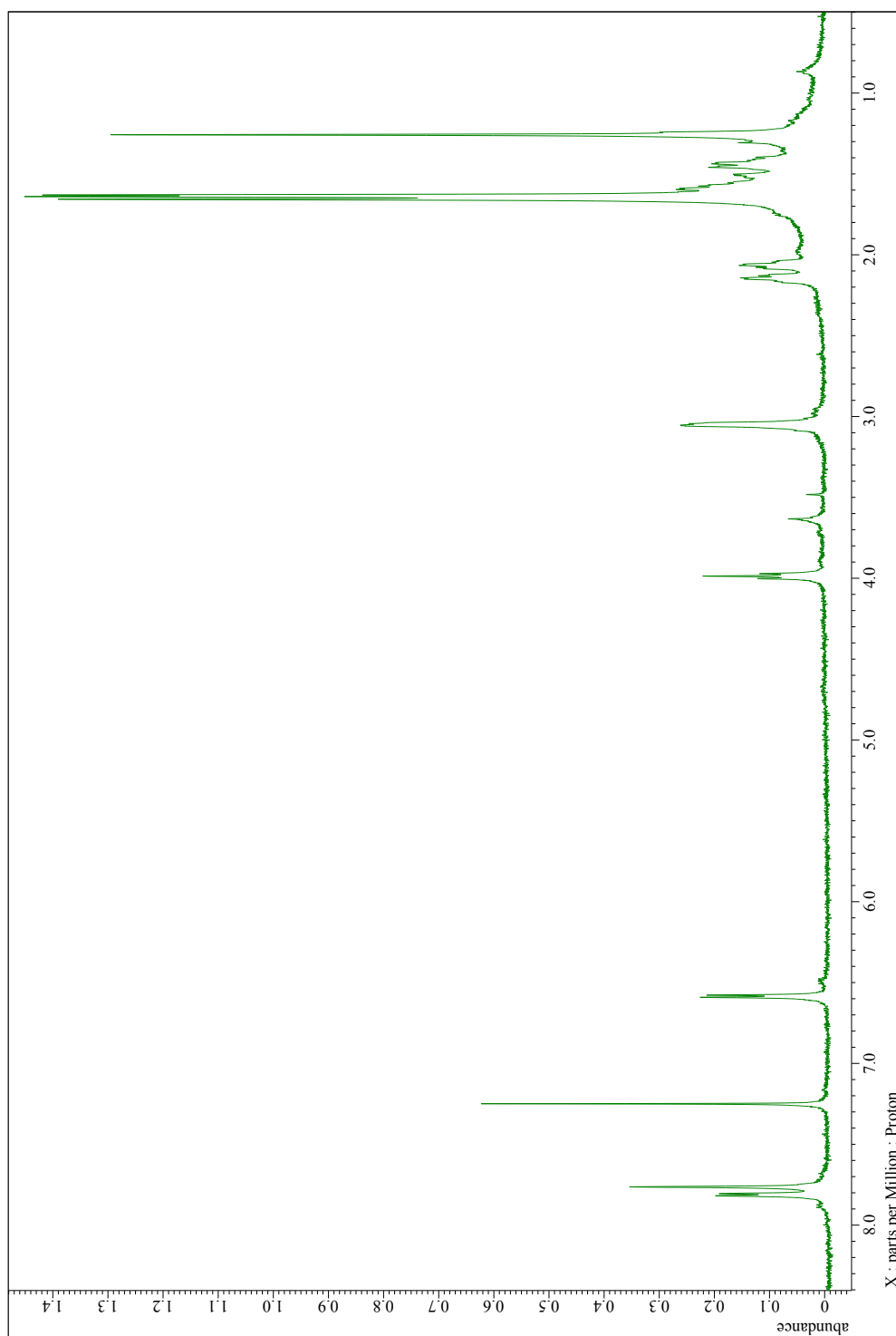


Supplementary Figure 34. HMPC spectrum for **2c**.

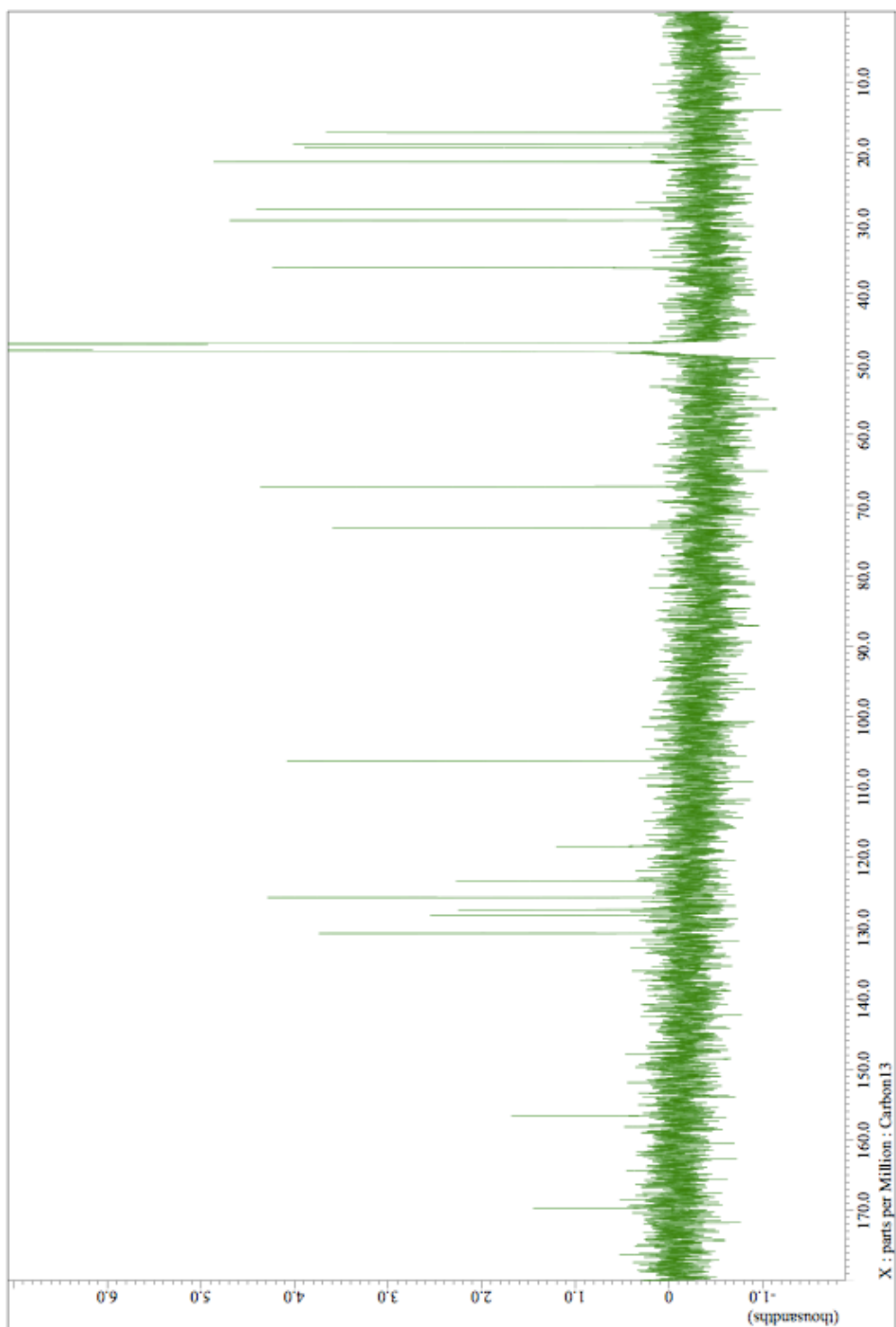




Supplementary Figure 36.  $^1\text{H}$  NMR ( $\text{CD}_3\text{OD}$ ) spectrum for **5b**.

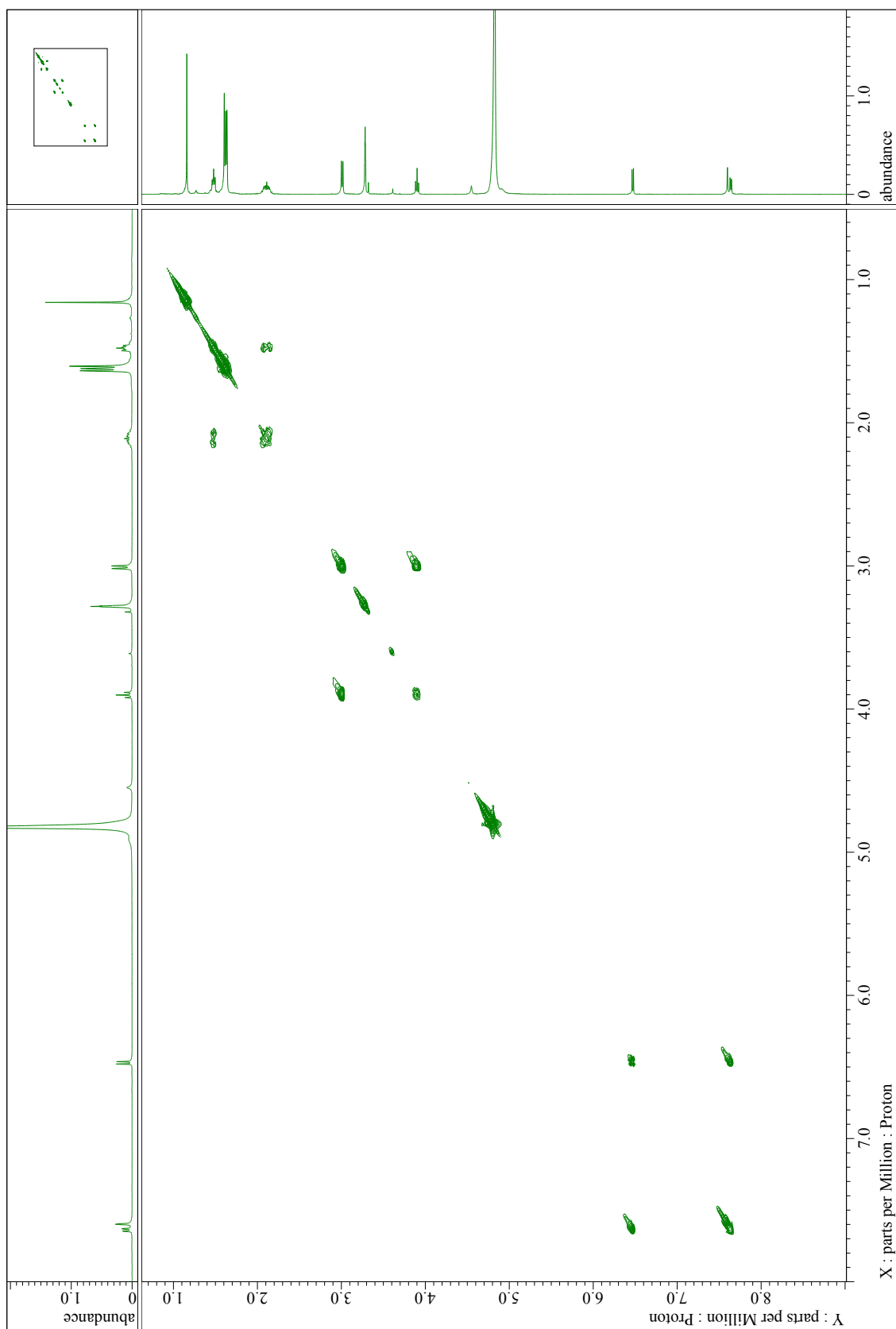


Supplementary Figure 37.  $^1\text{H}$  NMR ( $\text{CD}_3\text{Cl}$ ) spectrum for **5b**.

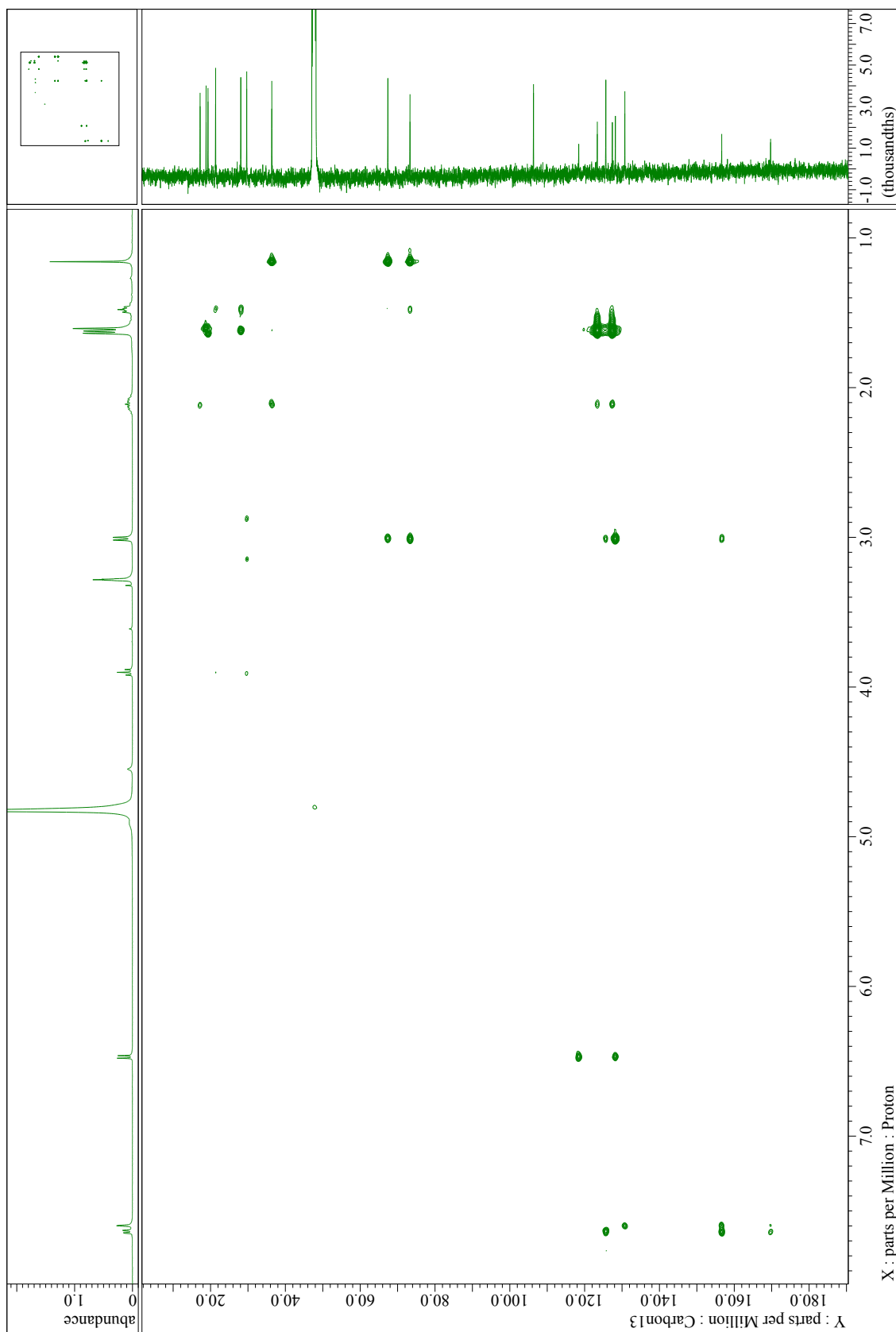


Supplementary Figure 38.  $^{13}\text{C}$  NMR ( $\text{CD}_3\text{OD}$ ) spectrum for **5b**.

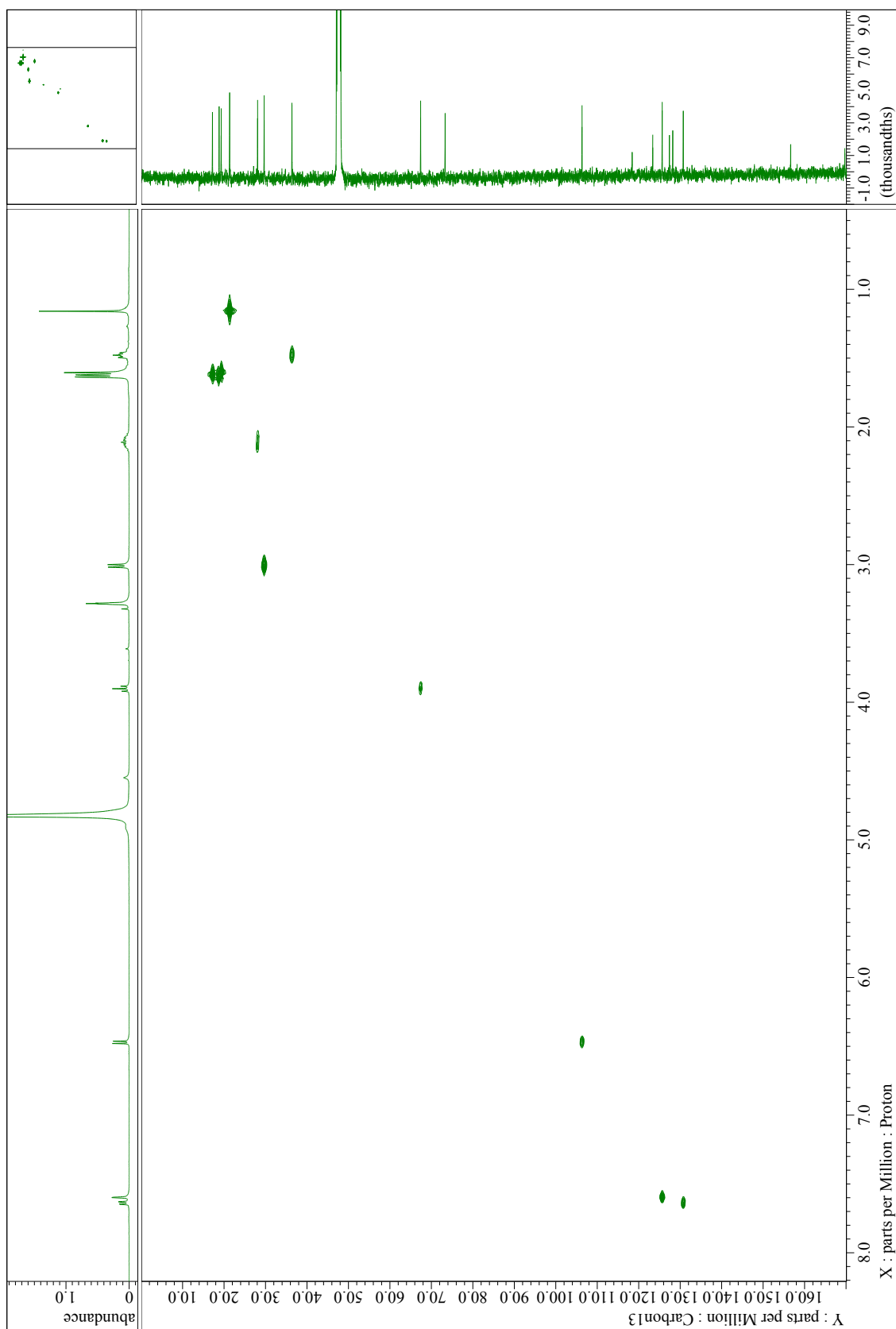




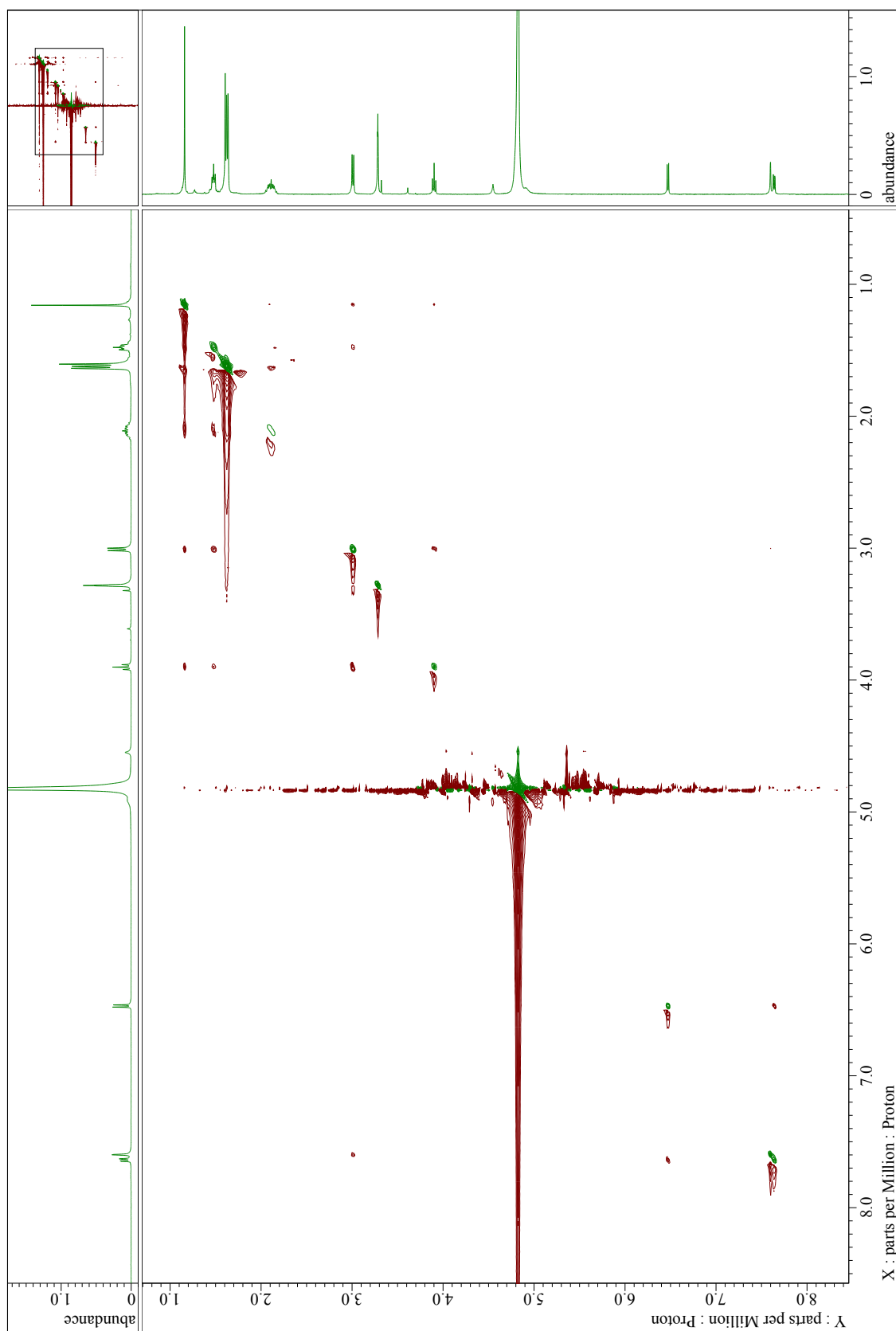
Supplementary Figure 39. COSY spectrum for **5b**.

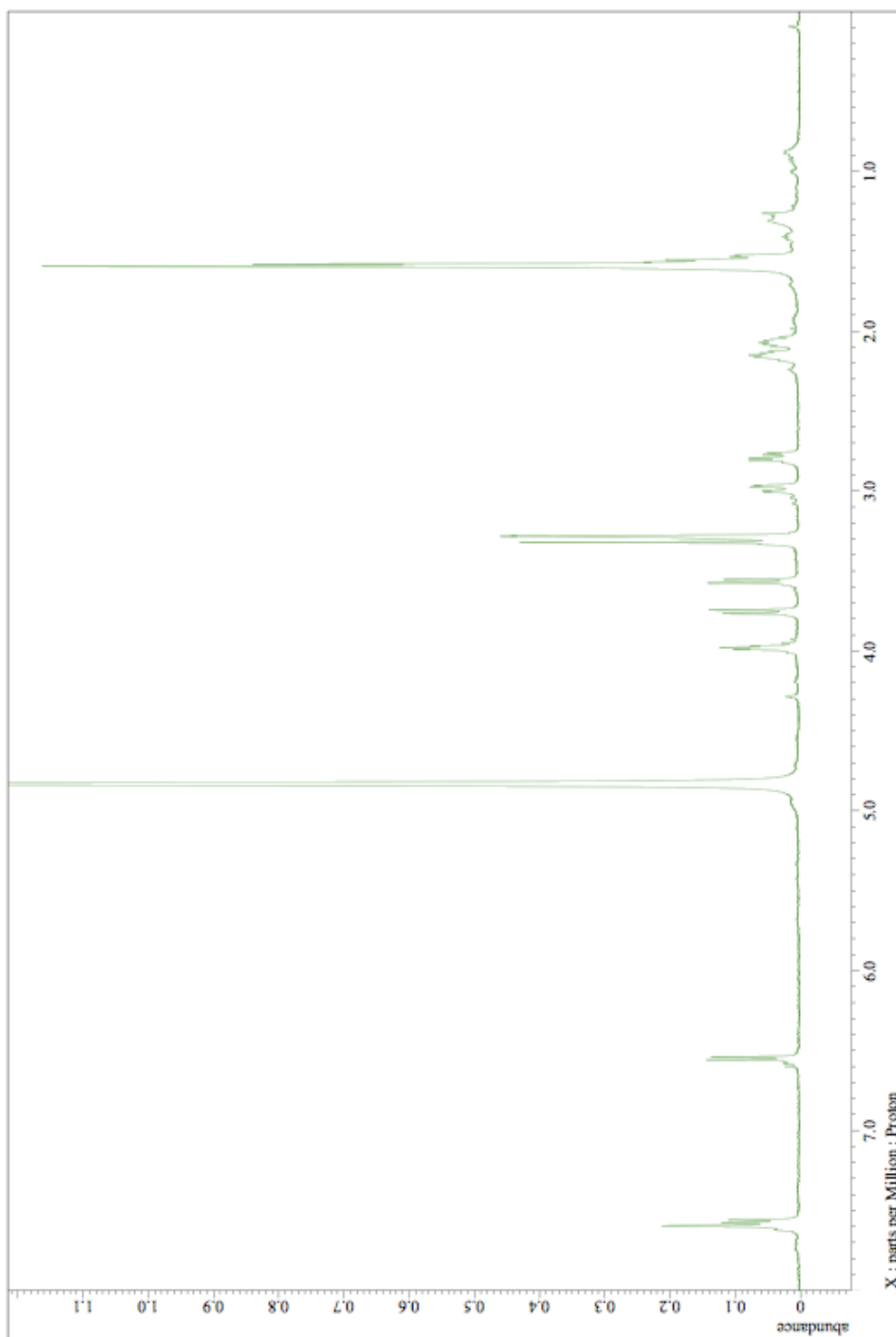


Supplementary Figure 40. HMBC spectrum for **5b**.

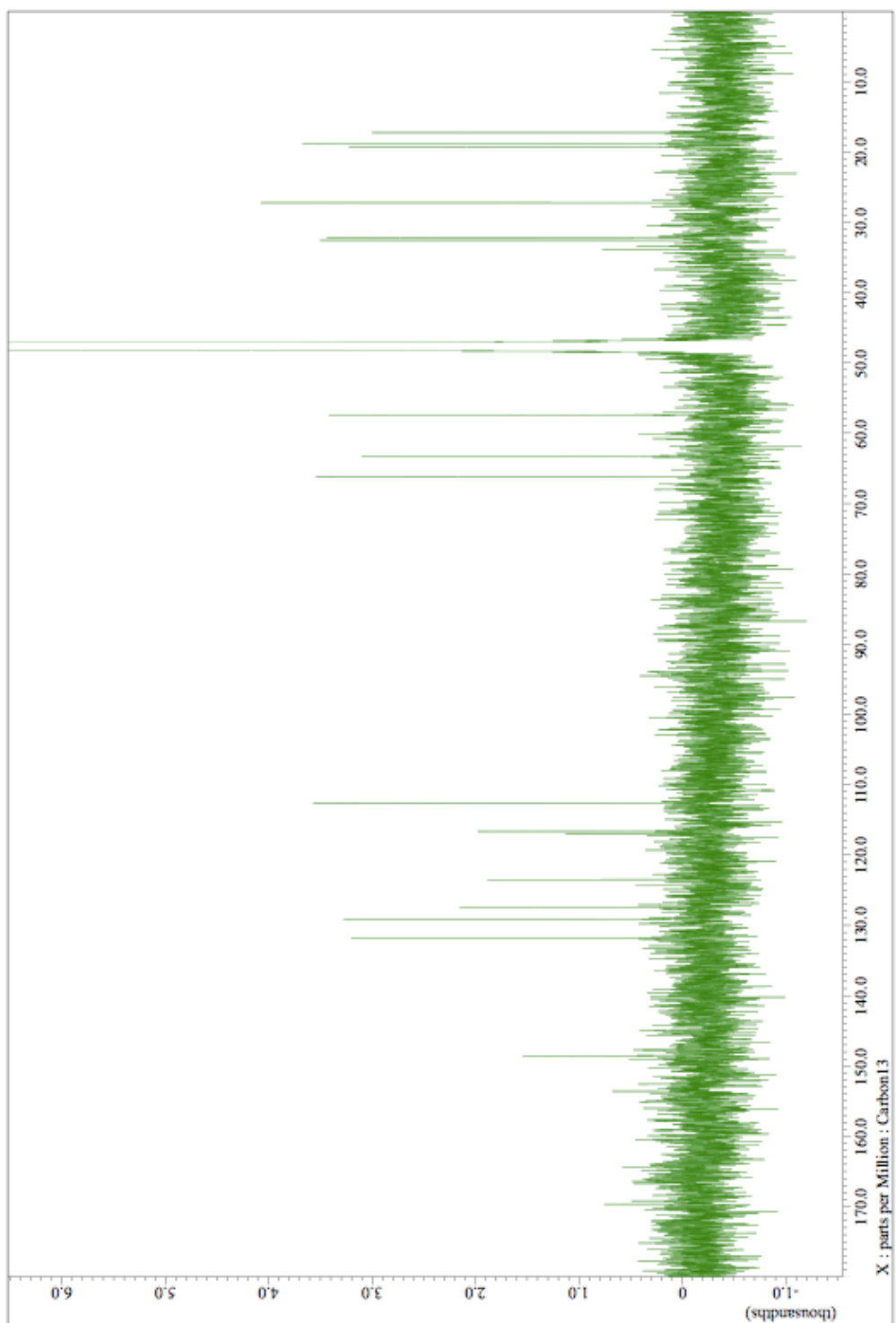


Supplementary Figure 41. HMPC spectrum for **5b**.

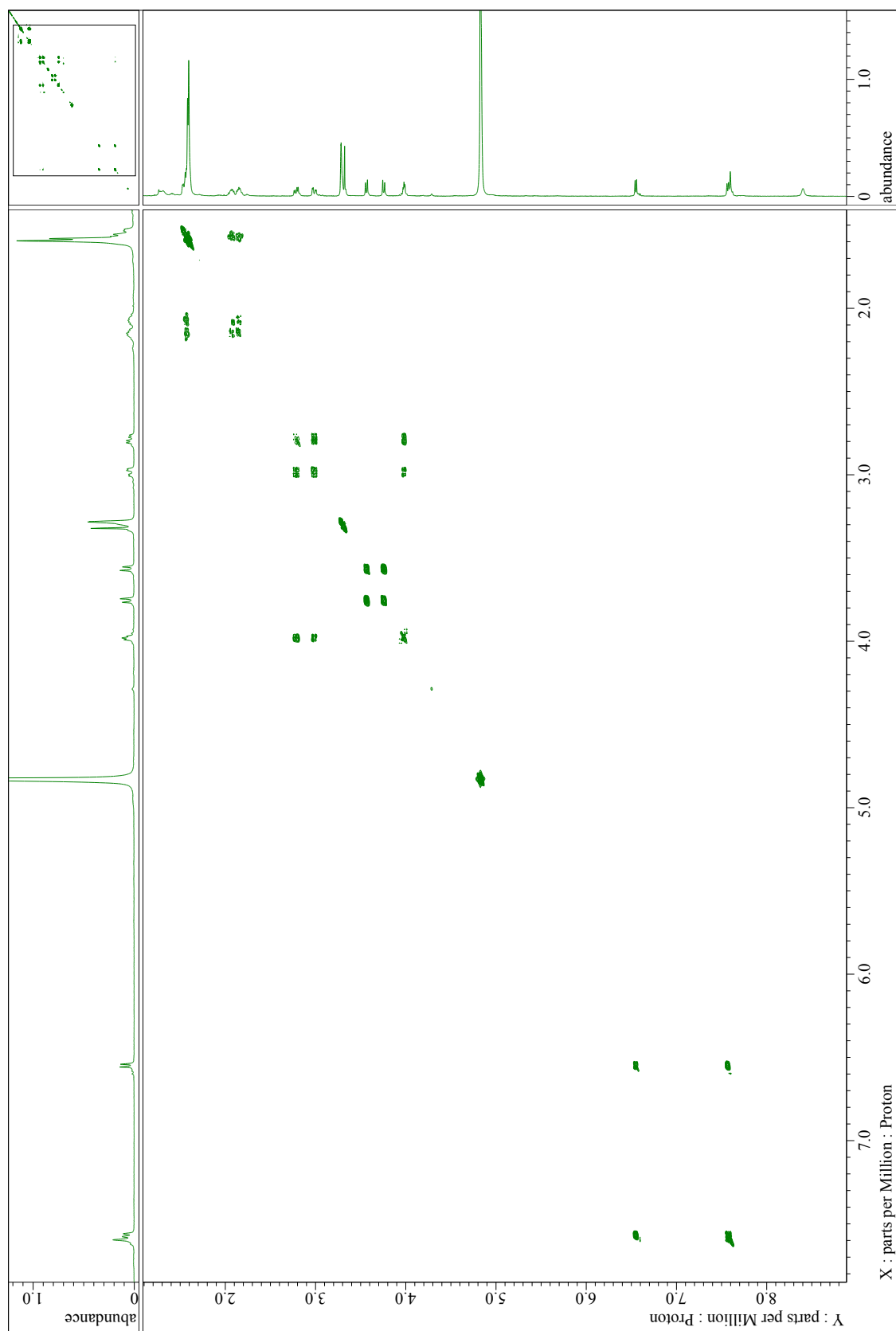


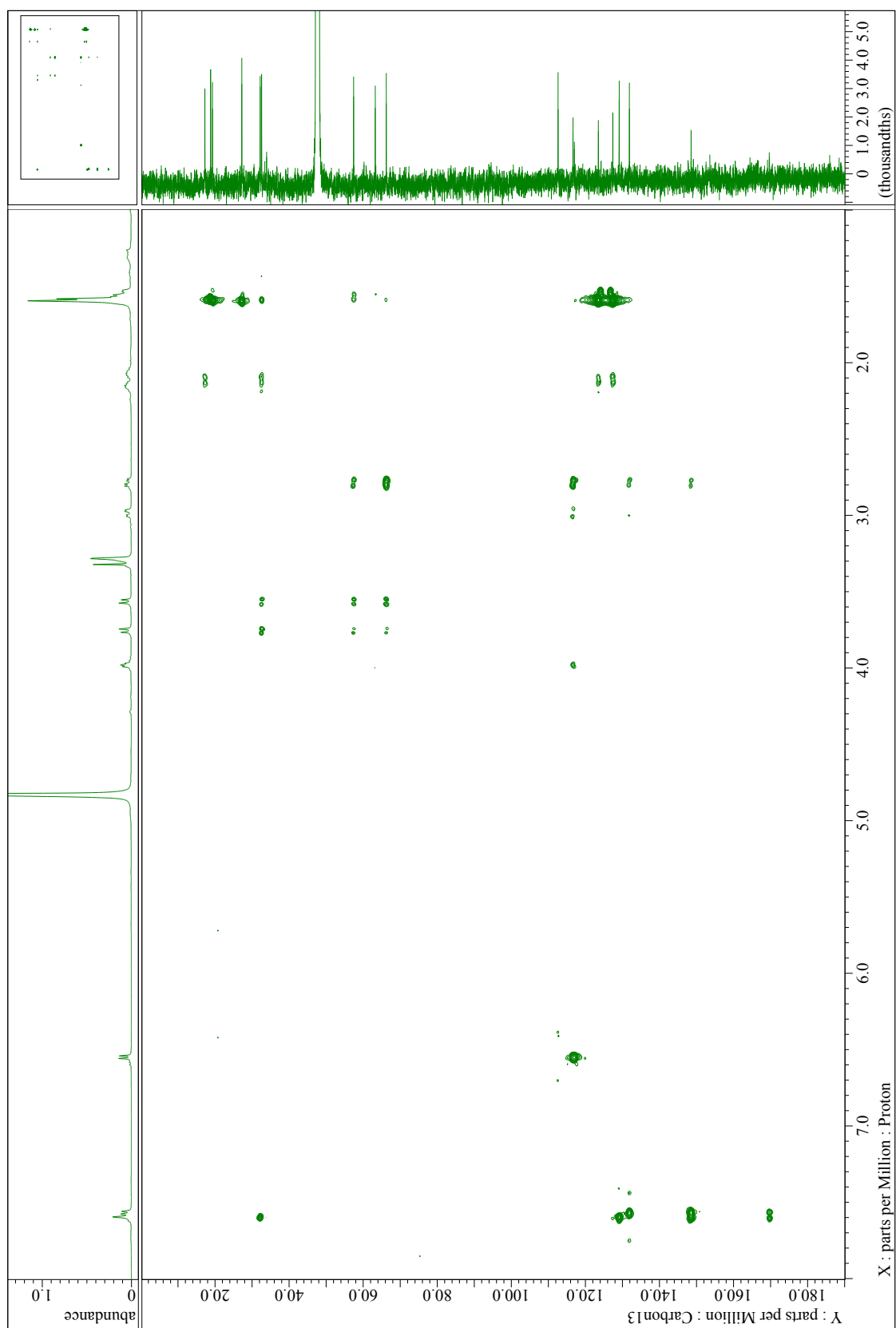


Supplementary Figure 43.  $^1\text{H}$  NMR ( $\text{CD}_3\text{OD}$ ) spectrum for **6'c**.



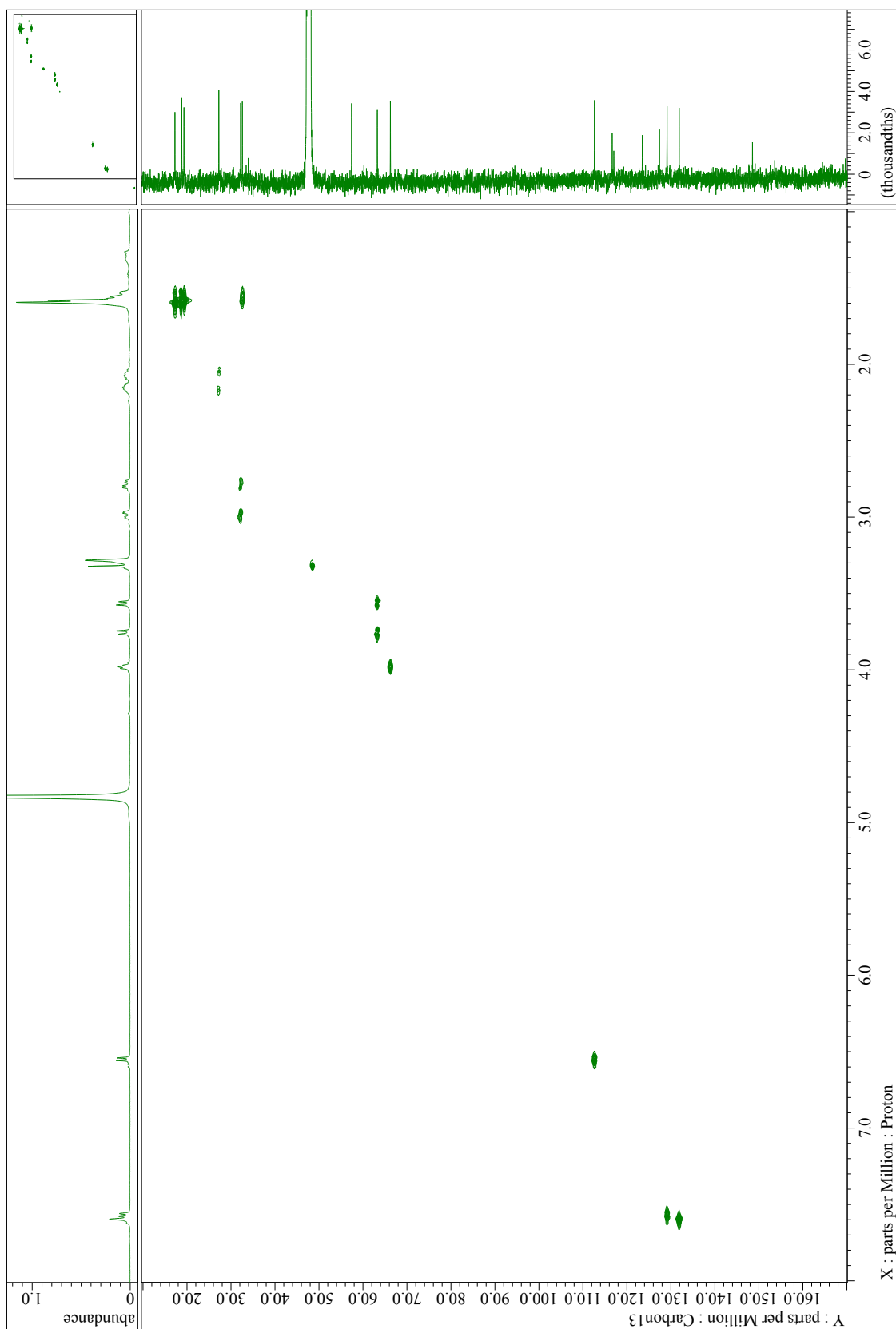
Supplementary Figure 44.  $^{13}\text{C}$  NMR ( $\text{CD}_3\text{OD}$ ) spectrum for **6'c**.



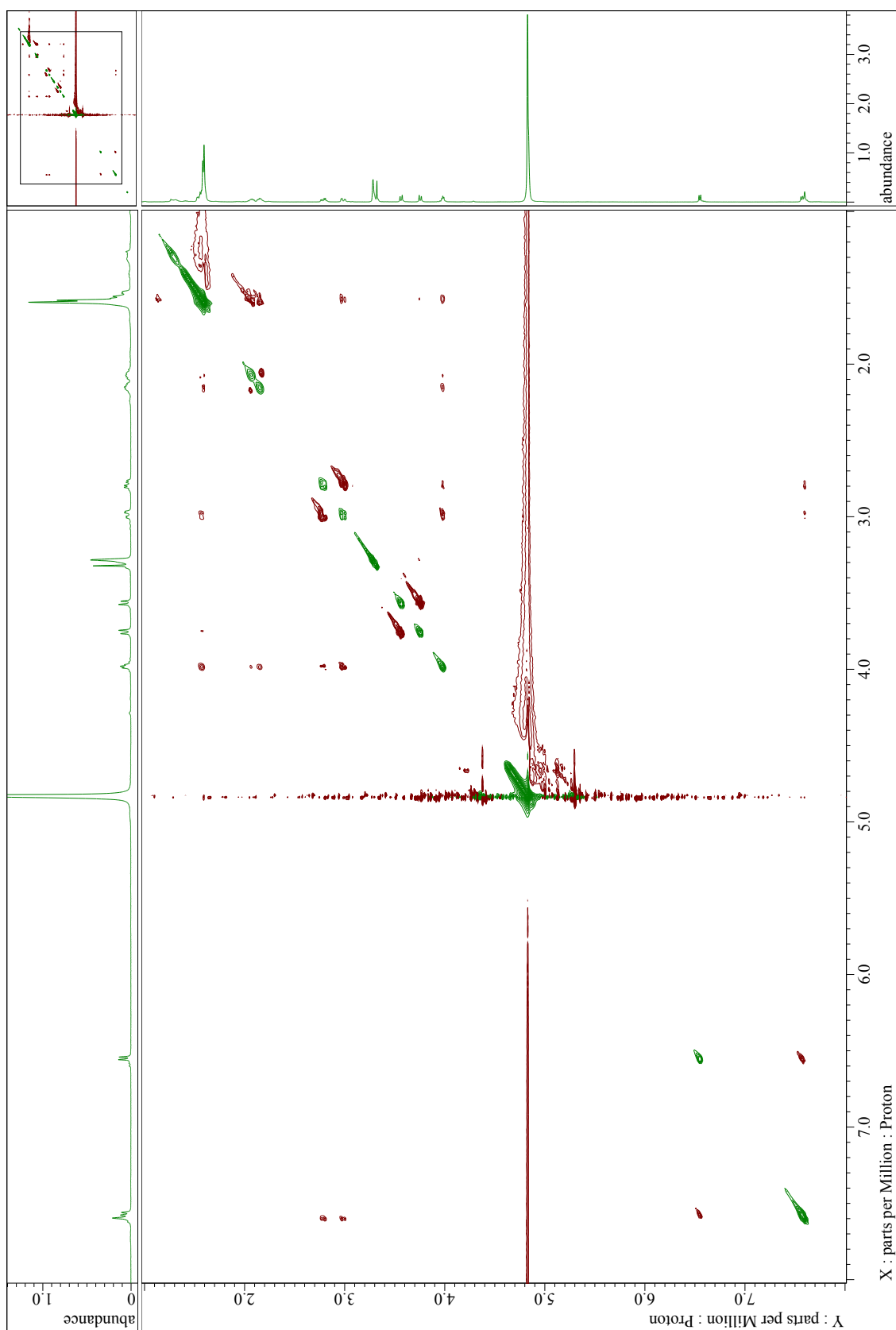


Supplementary Figure 46. HMBC spectrum for 6'c.

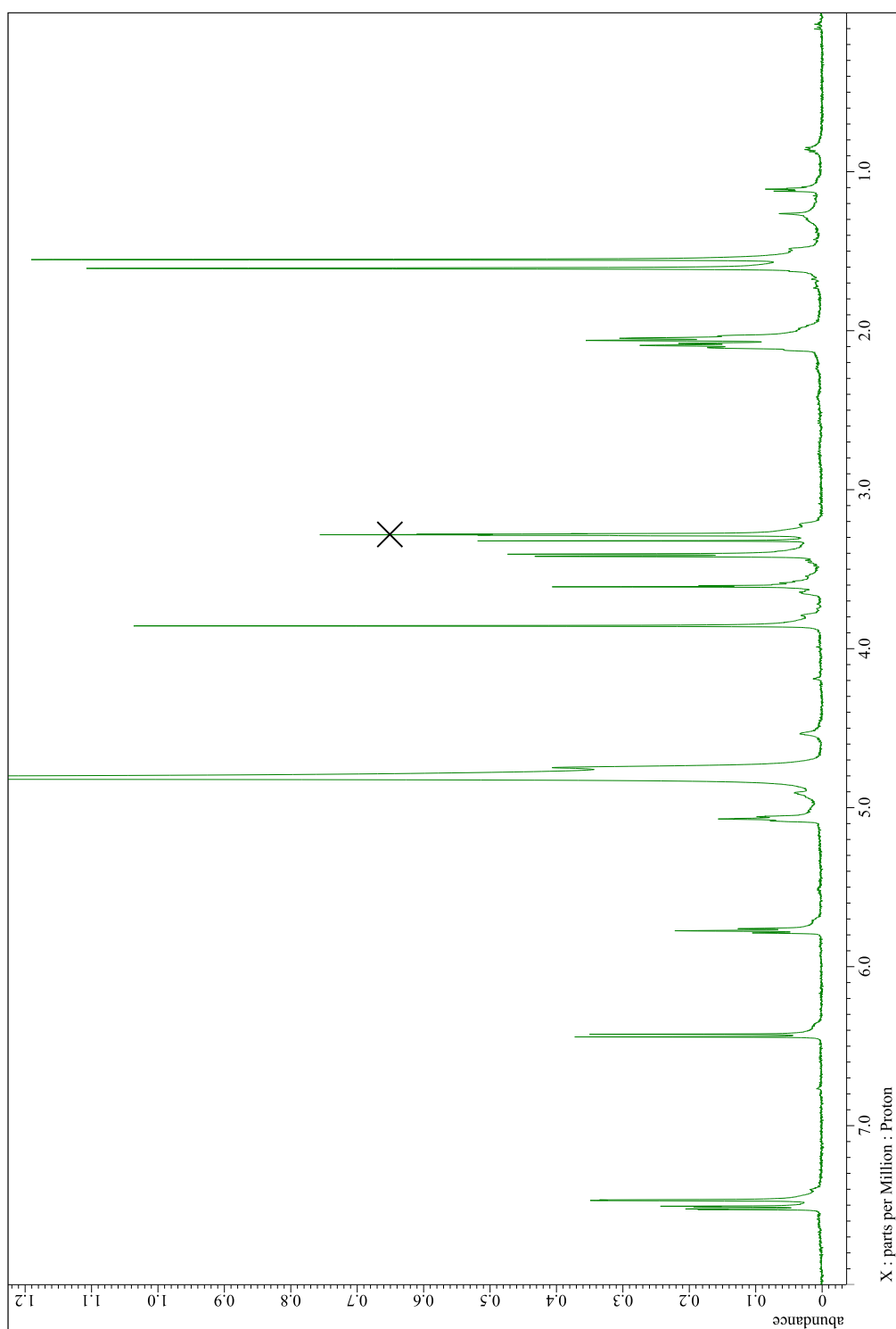




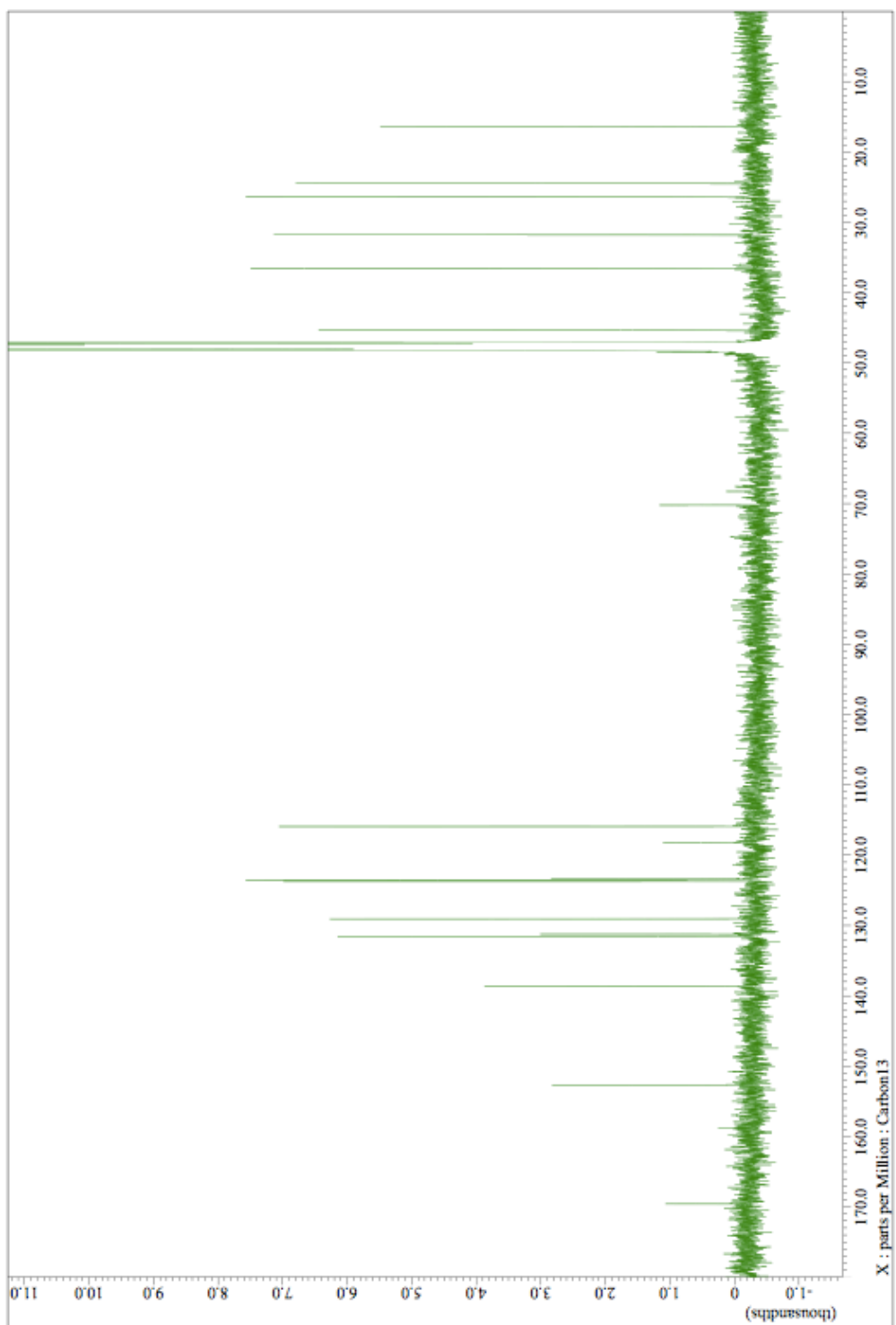
Supplementary Figure 47. HMQC spectrum for **6'c**.



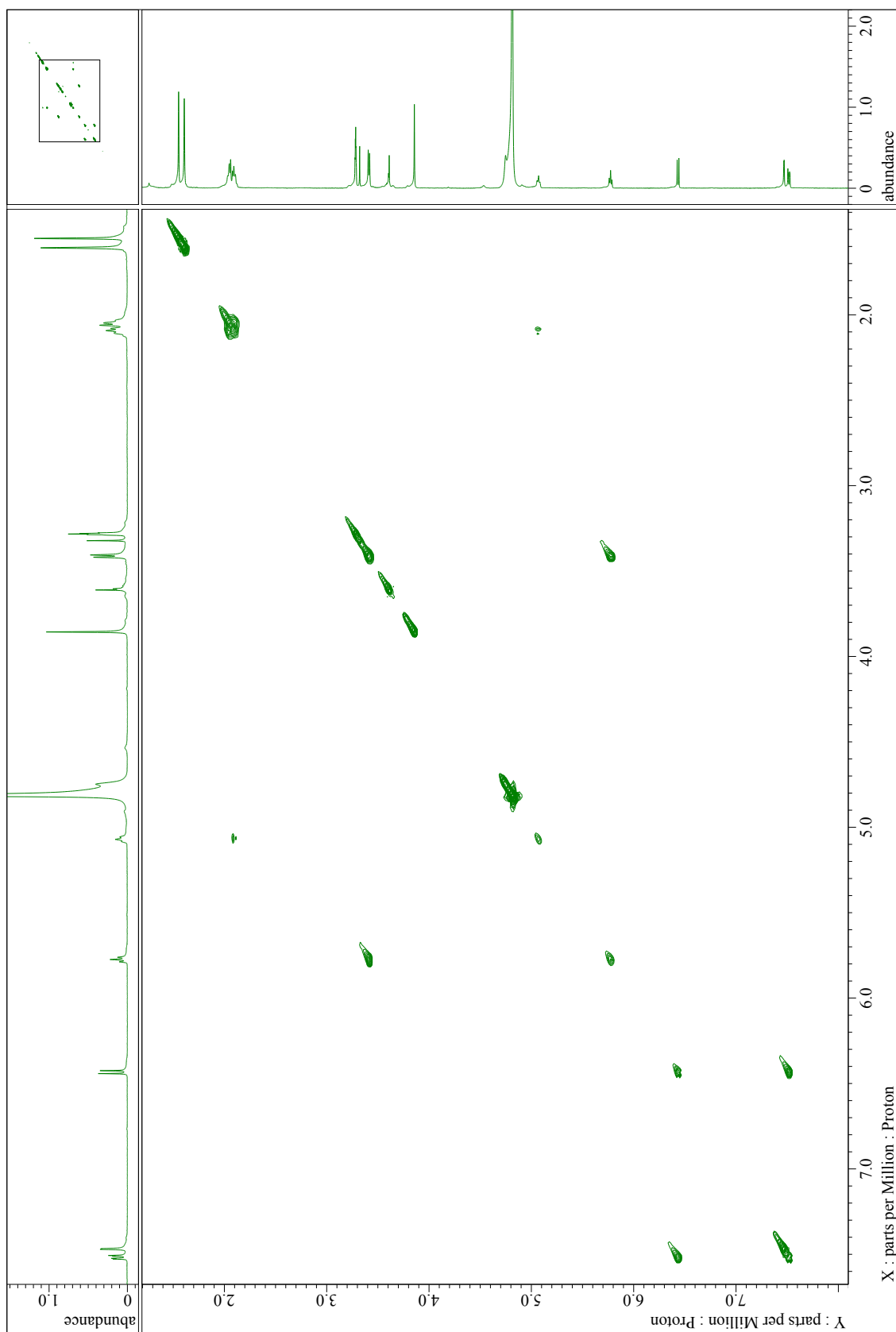
Supplementary Figure 48. NOESY spectrum for 6'c.

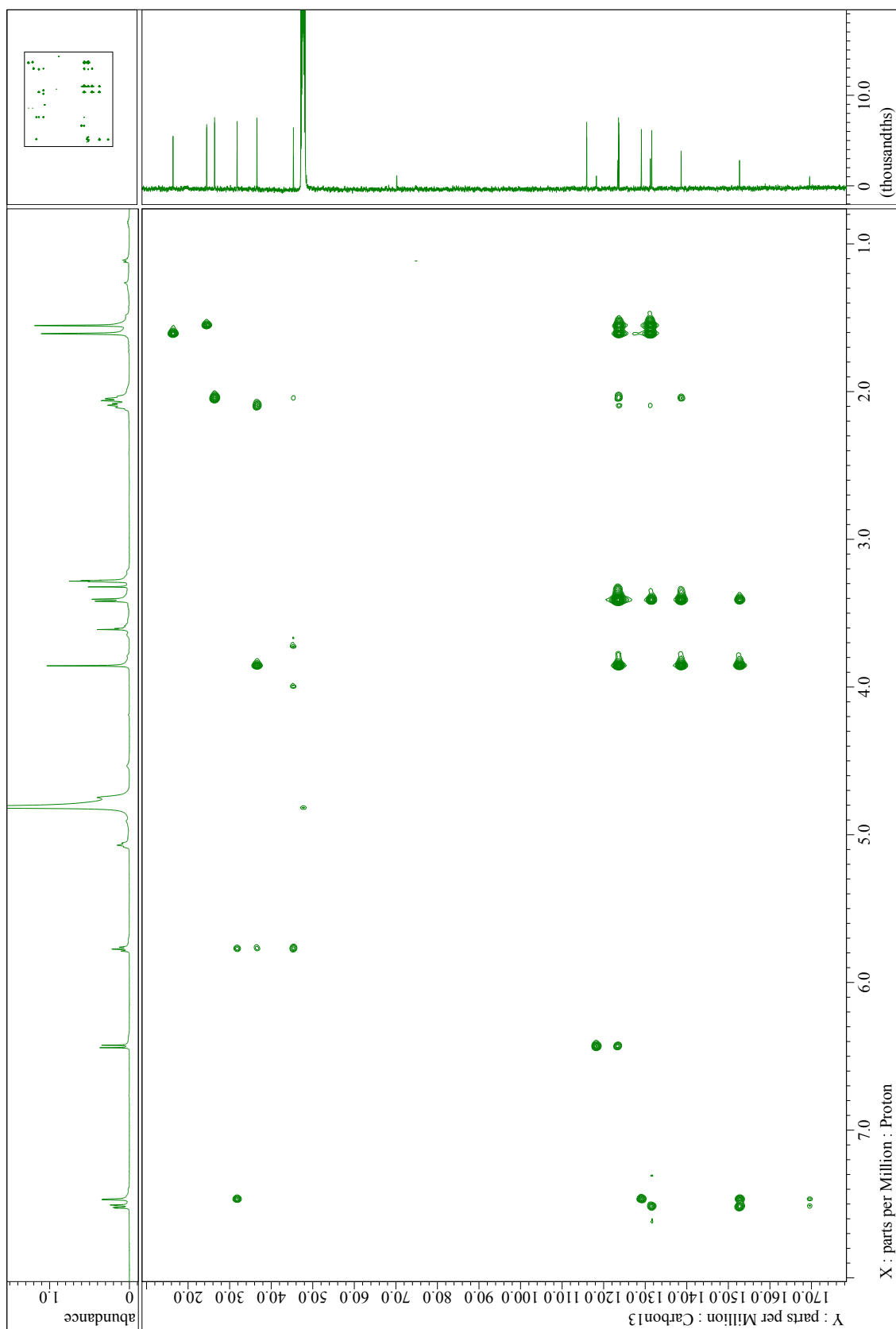


**Supplementary Figure 49.**  $^1\text{H}$  NMR ( $\text{CD}_3\text{OD}$ ) spectrum for **7a**. A noise peak is indicated by X.

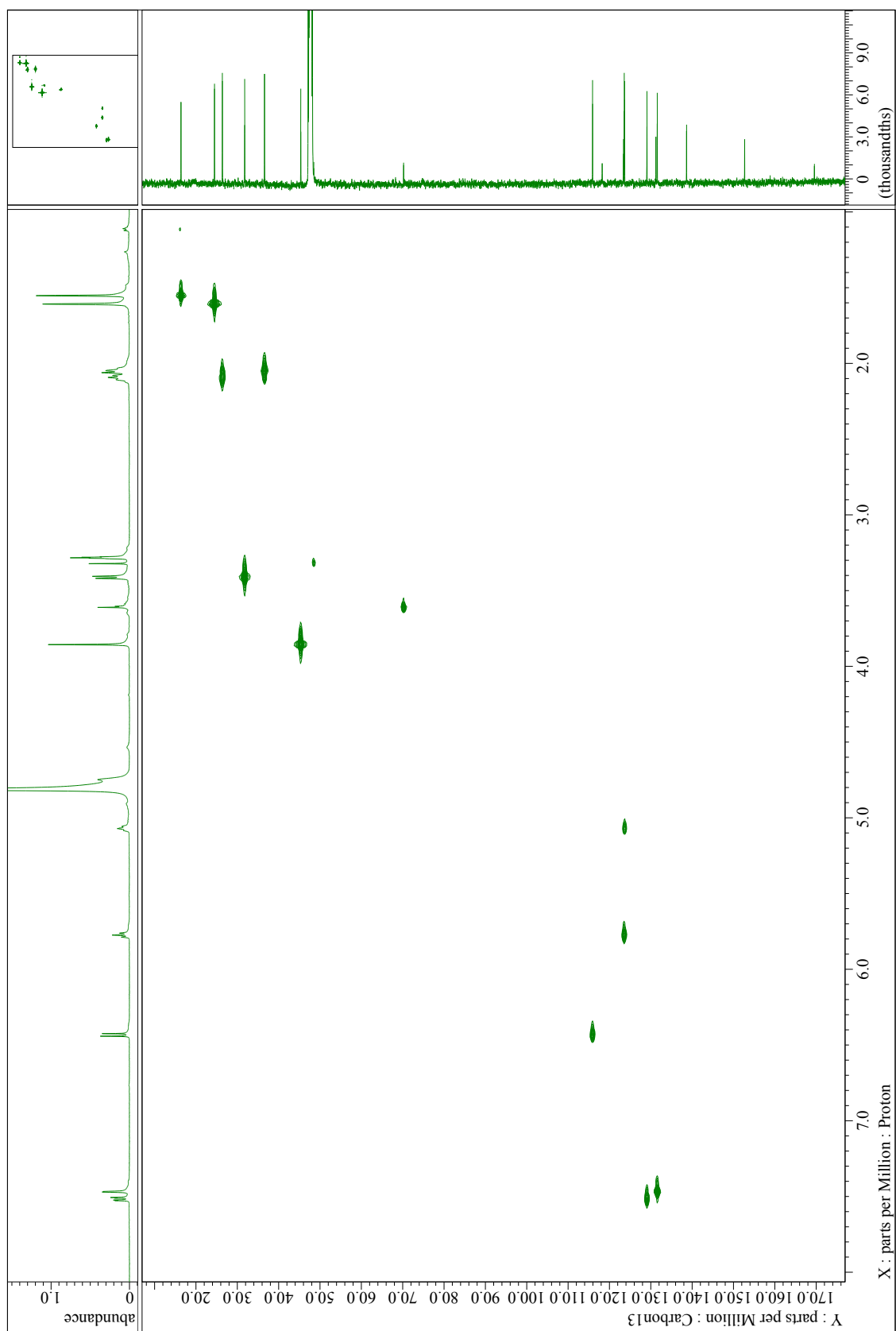


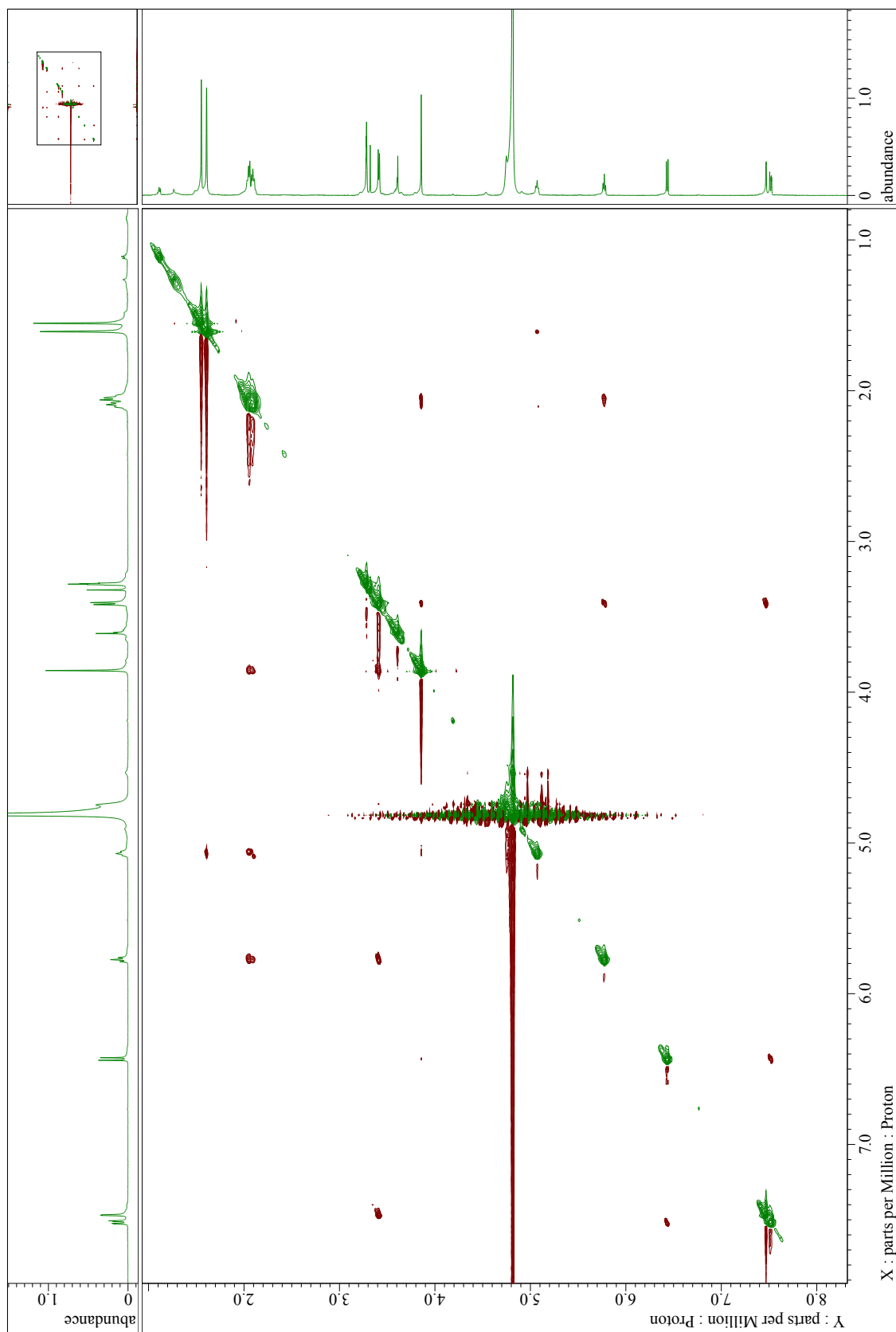
Supplementary Figure 50.  $^{13}\text{C}$  NMR ( $\text{CD}_3\text{OD}$ ) spectrum for **7a**.





Supplementary Figure 52. HMBC spectrum for **7a**.





Supplementary Figure 54. NOESY spectrum for **7a**.



## SUPPLEMENTARY REFERENCES

- [1] Takano, E.; White, J.; Thompson, C. J.; Bibb, M. J. *Gene*, **1995**, *166*, 133.
- [2] Hatanaka, T.; Onaka, H.; Arima, J.; Uraji, M.; Uesugi, Y.; Usuki, H.; Nishimoto, Y.; Iwabuchi, M. *Protein Expr. Purif.* **2008**, *62*, 244.
- [3] Hayashi, T. Study on the biosynthesis of benzastatin derivatives from *Streptomyces*. Ph. D. Thesis. The University of Tokyo, Tokyo, Japan, March, **2013**.
- [4] Hayashi, S.; Ozaki, T.; Asamizu, S.; Ikeda, H.; Ōmura, S.; Oku, N.; Igarashi, Y.; Tomoda, H.; Onaka, H. *Chem. Biol.* **2014**, *21*, 679.
- [5] Fu, J.; Bian, X.; Hu, S.; Wang, H.; Huang, F.; Seibert, P. M.; Plaza, A.; Xia, L.; Müller, R.; Stewart, A. F.; Zhang, Y. *Nat. Biotechnol.* **2012**, *30*, 440.
- [6] Fahey, R. C.; Newton, G. L. *Methods Enzymol.* **1987**, *143*, 85.
- [7] Ren, P. D.; Pan, X. W.; Jin, Q. H.; Yao, Z. P. *Synthetic commun.* **1997**, *27*, 3497.